SLOW INTERMUSCULAR OSCILLATIONS AND STRATEGIES TO TANGO WITH A ROBOT

A Thesis Proposal
Presented to
The Academic Faculty

by

Nayef Elian Ahmar

In Partial Fulfillment
of the Requirements for the Degree
Doctor of Philosophy in the
School of Electrical and Computer Engineering

Georgia Institute of Technology

December 2018

Copyright © 2018 by Nayef Elian Ahmar

SLOW INTERMUSCULAR OSCILLATIONS AND

STRATEGIES TO TANGO WITH A ROBOT

Approved by:

Dr. Minoru Shinohara, Advisor
School of Biological Sciences
Georgia Institute of Technology

Dr. Mark A. Clements, Co-Advisor
School of Electrical and Computer Engineering
Georgia Institute of Technology

Dr. David V. Anderson
School of Electrical and Computer Engineering
Georgia Institute of Technology

Dr. Jun Ueda
School of Mechanical Engineering
Georgia Institute of Technology

Dr. Omer T. Inan
School of Electrical and Computer Engineering
Georgia Institute of Technology

Dr. Frank L. Hammond III
School of Mechanical Engineering
Georgia Institute of Technology

Date approved: November 5, 2018

Dedicated to

Elian, Nouhad, Angele, Hani, May,

Bea, Jad, Mourched, and Elian J.

♥ ☺ ♫

ACKNOWLEDGEMENTS

I am indebted to my committee members, their time, guidance, and efforts to make me a better researcher. I feel privileged to be guided and advised by Mark Clements, an icon in signal processing. I am thankful to Shino Shinohara for sharing his scientific intellectual insights. I am also grateful to Jun Ueda for putting all the needed resources in front of me especially for second experiment that was entirely run in his lab. Many thanks go to David Anderson for his generosity and feedback mainly in preparation for proposal. I am also thankful to Omer Inan and Frank Hammond III for gracefully serving on my committee.

Countless members of the Georgia Institute of Technology professors from Biological Sciences, Electrical and Computer Engineering, College of Computing and other departments inspired me. Your generosity in sharing knowledge and opportunities is unique. Many thanks to Lena Ting, Boris Prilutsky, Teresa Snow, Justin Romberg, Erik I Verriest, Ghassan AlRegib, Christopher Rozell, Maysam Ghovanloo, Thad Starner, Melody Moore Jackson, Bruce Walker, Wassim Haddad, and many more.

Many thanks to the people who made the process of pursuing a PhD more enjoyable with a big smile and can do attitude, especially George Riley, Magnus Egerstedt, Richard Nichols, Daniela Staiculescu, Adrienne Durham, Luis Ocasio, and Tasha Torrence.

I am deeply appreciative to Antonio Moualeu for his assistance with robotic device SW modification. Cole Simpson and his initial work on the project and EMG acquisition. Thanks to Kent Osborn for introducing me to tensegrity field and our discussion about

physiology. Rosana Ginart, your mentorship and friendship is memorable. I am grateful as well to many colleagues I met throughout the years at GT, Elma Kajtaz, Kyunggeune Oh (Ted), John Johnson, Mark Lyle, Atul Shekhar, Tracy Norman Giest, Ellenor Brown, Westin Williams, Euisun Kim, and Waiman Meinhold. Not to forget the undergraduate students and human subject volunteers for gracefully being part of experiments for pilot and test.

Outside the lab and classrooms, I was fortunate to learn from many great dance instructors while diving into the practice of human to human interaction through partner dancing. Amazing people put me in the right direction, Robert Tolentino, "there are only two dances, Rhythm and Smooth"; Buddy Stotts, "project your energy"; Jorge Morales, "posture more important than beat"; Angel Montero and April Parker, "Argentine Tango is about being in the now"; Gabriela Lopez, "On every collection there is room for a new idea". Many thanks as well to Kate Bennett, Matthew Boguslawski, Marie Lou, and to GT various dance clubs and members.

To my father, Elian (the thinker), who taught me to love learning and read between the lines, to my mother, Nouhad (the doer), who trained me to learn from mistakes and never give up, thank you for your sacrifices, flexibility, and unrelenting attitude toward challenges. To my siblings and loved ones, I am very grateful for the unconditional love, sacrifices and support; little would have mattered without you.

Finally, I am grateful to the National Science Foundation for the partial support of this work through the National Robotics Initiative grant.

TABLE OF CONTENTS

LIST OF TABLES

LIST OF FIGURES

LIST OF SYMBOLS

μ	Mean
σ	Standard Deviation
f	Frequency
F	Fourier Transform
r	Pearson correlation coefficient
t	Time

LIST OF ABBREVIATIONS

ACC	Acceleration
AEMG	Amplitude Electromyography
BB	Biceps Brachii
BR	Brachioradialis
CL	Constant Level
DOF	Degree Of Freedom
ECU	Extensor Carpi Ulnaris
EMG	Electromyogram
ERLCOH	Event Related Linear Coherence
ERPCOH	Event Related Phase Coherence
ERSP	Event Related Spectral Perturbation
FCU	Flexor Carpi Ulnaris
FRC	Force
HRI	Human Robot Interaction
ITC	Inter Trial coherence
MSE	Mean Square Error
MECH	Mechanical Output / Kinetic + Kinematic
MUAP	Motor Unit Action Potential
MVC	Maximum Voluntary Contraction
PDF	Probability Density Function
POS	Position
RMSE	Root Mean Square Error

SD	Standard Deviation
STF	Stiffness
SVM	Support Vector Machine
TGT	Target
TB	Triceps Brachii
VL	Varying Level
VEL	Velocity

QUICK TERMS LOOK UP TABLE

Agonist muscle	Main force generator muscle during movement.
Alternating co/contraction	Static fast co/contraction alternation (3.5s) of activation.
Antagonist muscle	Muscle that opposes the agonist.
Coactivation	Concurrent (un/intentional) activation of agonist and antagonist muscles around a joint.
Cocontraction	Intentional concurrent activation of agonist and antagonist muscles around a joint.
Contraction	Intentional activation of a single muscle.
Common drive	< 5 Hz common command signal from CNS that regulates the net sum of excitatory and inhibitory inputs (most effect below 3 Hz).
Dynamic co/contraction	Isotonic co/contractions of muscles when the joint angle and muscle length change, with or without contraction strength change.
Fast coactivation	Fast dynamic moving robotic arm (~3s) during square-wave trajectory.
Maximum Voluntary Contraction	Maximal isometric force that a subject can generate per muscle.
Relationship (in this text)	Association or correlation.
Reverse direction coactivation	Slow dynamic change of direction coactivation during sine-wave trajectory.
Slow coactivation	Quasi-constant velocity dynamic coactivation during sine-wave trajectory.
Slow oscillations	< 3 Hz correlated oscillations.
Static co/contraction	Isometric co/contractions of muscles when the joint angle and muscle length do not change although contraction strength may vary.

Steady coactivation	Static involuntary coactivation during square-wave trajectory.
Steady-state coactivation	Steady coactivation (square-wave) or slow coactivation (sine-wave)
Steady co/contraction	Static voluntary co/contraction.
Synchrony (muscles)	Correlation in amplitude or phase between muscles.
Synergist muscle	Muscle that stabilizes a joint around which movement is occurring and assist the agonist along the way.
Transient cocontraction	Static fast alternation (3.5s) of activation.
Varying Level cocontraction	Static fast alternation (3.5s) of activation.

SUMMARY

Steadiness and stiffness control failures are recurring problems in many fields. They are both, at least in part, the byproduct of "common drive", a nervous system process that activates or relaxes all muscles in synchrony (or harmony), even the opposing ones. The objective of the proposed research is to investigate these common neural oscillations for improving concurrent activation control around elbow joint muscles with direct application to Human-Robot Interaction (HRI). It is divided into two tracks: 1) study the association between neuromuscular adaptations and system performance for human movement control and 2) develop methods to assess and influence an operator's skill level and task-dependent physical states from physiological measures during interaction with an external object in a closed loop system.

A framework with a three-step approach has been implemented: 1) Two experiments (basic controlled research, and a real-life engineering application of HRI) were designed, and data were collected from 80 subjects completing various tasks under different constraints. 2) The relationship between system performance (neural or mechanical) and muscle correlated neural oscillations was explored in different settings (static, dynamic, and transient coactivation). 3) Multiple methods to influence or modulate intermuscular correlated oscillations were investigated in order to enhance system performance results.

The primary finding suggests that individuals with less correlated neural oscillations (decoupled muscles), as measured by surface Electromyography (EMG), tend to perform steady static cocontraction more skillfully (assessed by amplitude EMG or AEMG). As subjects became more familiar with the task during the steady test or transient practice,

their performance improved while either intermuscular amplitude or in-phase coherence or both decreased, depending on the task, muscle, and muscle pair. These associations during steady cocontraction test were more prevalent for the subject group whose muscles had been habituated in a single muscle contraction practice task than they were in other groups. On the other hand, these positive linear correlations were more significant for the Cocontraction group (that practiced out-of-phase cocontraction) during the more difficult faster alternating target matching practice than the target matching test, especially for mean square error. There was also a linear association between correlated oscillations of a select few muscle pairs and both the neural (mean AEMG, steady coactivation) and mechanical (position error and stiffness, slow coactivation) outputs during static or dynamic tasks with vibration across subjects. Nevertheless, such associations during static and dynamic coactivation tasks were different from the static cocontraction case. Subjects who had higher muscle coherence pair tended to be those who maintained lower mean AEMG, lower position error and lower muscle stiffness possibly as a countermeasure to the vibration that was added to the robotic device to ensure muscle coactivation. Finally, the following methods to influence or modulate these newly discovered relationships or their underlying correlated oscillations were identified: repetition, out-of-phase cocontraction practice, and a single muscle contraction habituation.

The common drive is embedded in the nervous system; it is predictable in its degrading impact on performance; nevertheless, this study was able to influence its potential effect to some extent through practice and repetition. On the other hand, the current results confirm that the physiological neural system is not necessarily hard-wired,

but adapts to the requirements of completing a task and thus cannot be studied in isolation of the robotic system properties. As such, a proper HRI framework would benefit from a good grasp of task-specific demands as well as system hardware properties in addition to models of neural and mechanical output (MECH) as a function of internal processes such as correlated oscillations.

CHAPTER 1. INTRODUCTION

When two athletes engage in a contact sport such as wrestling, usually each one coactivates his muscles: simultaneously activating antagonist and agonist muscle groups of the same joint and in the same plane of movement. Each player can sense his opponent's muscle activations in real time. There is symmetrical (i.e., reciprocal) flow of information between parties that enables each player to build a template of his opponent strategies, weaknesses, and strengths. Likewise, haptic devices in a Human-Robot Interaction (HRI) setting, such as human-assisted powerlifting, necessitate physical contact between the operator and the machine. Force feedback creates a coupled dynamic system between the two. Nevertheless, the flow of signaling between the two is generally absent, more specifically–the robot is entirely unaware of operator physiology, skills, or intent. When instabilities are encountered, the coupled system suffers due to inefficient adjustments of the human operator's stiffness. The operator usually attempts to control oscillations by stiffening more, potentially causing the system to break down.

Such asymmetry could be the cause of many problems. Primarily, the non-reciprocity leads to the ineffective handling of operator's coactivation control resulting in system failure. Nonetheless, if one wants to sense and channel the operator's physiological state to a robot, there is a wealth of data that needs to be optimized first into simple, meaningful bits.

Stiffness control and coactivation are not limited to HRI. They touch people's lives in many everyday activities. As such, it is beneficial to identify potential people with a

compromised ability for steady or slow coactivation and develop effective training or rehabilitation strategies for improvement. Hence, it is essential to understand fundamental neural characteristics that are related to the ability of individuals to control unbalanced coactivation of antagonistic muscles under different constraints.

Henceforth, a multi-step approach is proposed to identify crucial coactivation features: First, relationships are uncovered between correlated oscillations and performance metrics (neural and mechanical output) under various constraints of movement in humans. Then an attempt will be made to modulate or interfere with such relationships. What follows is a brief description of different chapters of the thesis.

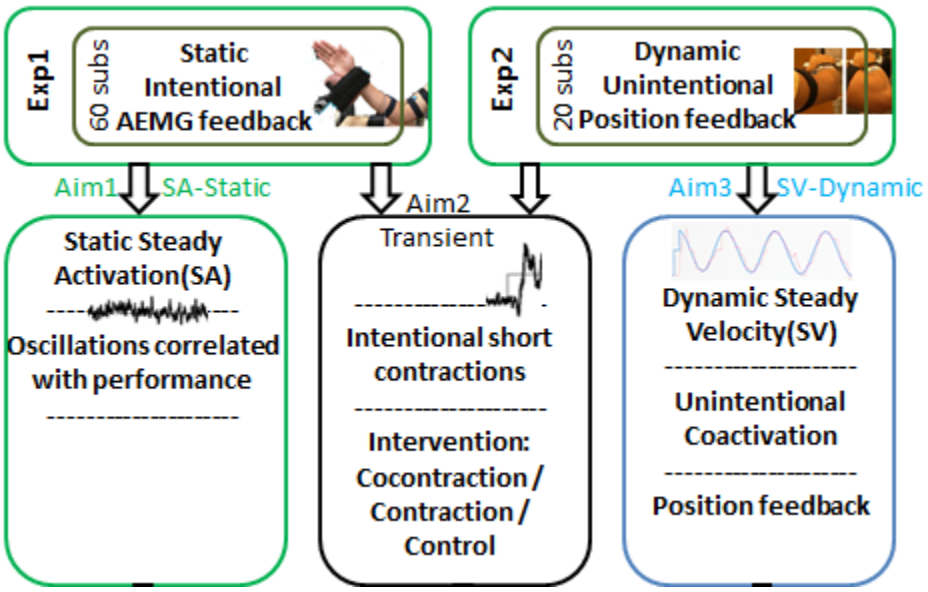

Figure 1 Roadmap of experimental design and specific aims

1.1 Definitions and review

The discussion starts (CHAPTER 2) with a list of definitions and a brief review of some important concepts for this current multidisciplinary work: From physiology, neuro-muscular cocontraction, surface EMG, to signal processing and data analysis.

1.2 Experimental design

Two experiments were designed and conducted: 1) Static contraction, with AEMG feedback (section 3.1); 2) Dynamic contraction, with position feedback (section 4.1). Temporal and spectral features for both experiments were extracted, correlated, and statistically investigated.

1.3 Specific Aims

Hypotheses and predictions are outlined (sections 3.2, 3.3, and 4.2) while charting three specific aims (Figure 1) under different constraints that form an anchor point for answering the research questions.

1.3.1 Aim-I static: Slow oscillations are associated with steady cocontraction performance.

Aim-I builds a foundation by addressing the relationship between intermuscular neural oscillations and performance metrics. Two objectives:

1- Determine whether there is an underlying association between the low-frequency correlated neural oscillations between muscles and the performance of steady unbalanced cocontraction across individuals.

2- Determine whether a bout of out-of-phase cocontraction practice reduces the in-phase low-frequency correlated neural oscillations and improves the performance of steady unbalanced cocontraction of antagonistic muscles in healthy young adults.

1.3.2 Aim-II transient-intervention: Modulation or influence of neuromuscular oscillations through interventions

The transient stage is potentially more susceptible to problems due to its brisk transitory nature such as alternating muscle contraction levels abruptly. There is more chance of stiffening muscles inefficiently, leading to potential hazards. Therefore, uncovering neural processes during fast-changing activations is of no less importance than steady-state. However, studying the non-stationary transient stage poses more challenges than the steady-state because of the complex interaction between many variables in a short duration. Regardless, the possible association between correlated oscillations between muscles and performance measures during non-steady activations had been studied. On the other hand, the role of intervention in influencing the outcomes had been explored. More specifically, investigations were made on whether one could modulate such correlated oscillations through intervention.

Two objectives,

1- Determine whether a bout of out-of-phase cocontraction practice reduces the in-phase low-frequency correlated neural oscillations in steady and transient unbalanced cocontraction of antagonistic muscles across individuals.

2- Determine whether there is an underlying association between the low-frequency correlated neural oscillations between muscles and the performance of transient static unbalanced cocontraction during practice across individuals

1.3.3 Aim-III dynamic: Slow oscillations are associated with mechanical output during dynamic coactivation while controlling a vibrating object.

Designing and studying a well-controlled static experiment uncovered many insights; however, it was not clear whether the uncovered linear relationships between correlated oscillations and neural output performance would replicate in a dynamic world. Dynamic activities might not necessarily have the same physiological properties of static ones, and the world outside the lab is a dynamic chaotic environment. It was unknown if such relationships existed for mechanical output performance as well. The end goal was to extract the physiological parameters most useful for a better HRI output performance, both neural and mechanical.

Two objectives,

1- Determine whether there is an underlying association between the low-frequency correlated neural oscillations between muscles and the mean activation level and variability of AEMG during steady coactivation task across individuals,
2- Determine whether there is an underlying association between the low-frequency correlated neural oscillations between muscles and the mechanical output

performance and characteristics (a- position accuracy, and b- endpoint stiffness) during slow coactivation task across individuals.

1.4 Overview

Finally, findings and recommendations for an improved HRI were summarized in CHAPTER 5. Neural and mechanical output and their physiological significance were clarified. A list of questions to address when building an HRI impedance controller algorithm was suggested. The added value in the new tools utilized to extract and quantify the physiological processes in play and their relationships were highlighted. The importance of modulating such relationships through various means was emphasized. Then the thesis concludes after a brief expansion on potential applications in HRI and beyond.

CHAPTER 2. DEFINITIONS AND LITERATURE SURVEY

This study will lay the groundwork with some definitions, standard practices, and a review of some key literature findings for the following investigation.

2.1 Background definitions

2.1.1 Static and dynamic muscle contractions

Static or isometric contractions of a muscle refer to when the joint angle and muscle length do not change although contraction strength may vary. Such contraction is referred to as 'static' throughout the text. On the other hand, isotonic contractions of a muscle refer to when joint angle and muscle length change, but the contraction strength does not vary. In other cases, contraction strength could vary together with muscle length. The term "dynamic" contraction is used to refer to such cases.

2.1.2 Agonist, antagonist, and synergist muscles

An agonist muscle is the main force generator during movement. For instance, if one activate his biceps brachii (BB) lifting an object, BB is the agonist. However, if one is activating triceps brachii (TB) by pushing down against an object, then TB is the agonist muscle during the contraction.

An antagonist muscle is the one that opposes the agonist. During lifting an object in this example, TB is the antagonist muscle. It is inhibited as BB contracts.

A synergist muscle, on the other hand, is the one that helps to create movement by helping the agonist function. For instance, in the object lifting example, brachioradialis (BR) is a synergist muscle. It assists BB muscle.

2.1.3 Coactivation vs. Cocontraction

For this proposal, muscle coactivation is referred to as the concurrent activation of agonist and antagonist muscles around a joint. When the simultaneous contractions are intentional (ex. maintain a given contraction level consciously), the coactivation subclass is referred to as cocontraction.

2.1.4 Common drive

When controlling a certain level of motor output as steady as possible using agonistic muscle(s), steadiness in motor output is primarily influenced by low-frequency oscillations (<5 Hz) of discharges of motor units (38, 46). Such neural oscillations are associated with the generation of muscle force (17, 18). In this frequency range, correlated modulation of motor unit discharges are observed within and across muscles, and they are believed to be produced by a ‘‘common drive’’ (9). The common drive is the net drive signaling that all motor neuron from same pool receive that originates from the Central Nervous System (CNS) as it regulates the net sum of excitatory and inhibitory inputs.

2.1.5 Stiffness control

The human body effectively interacts with its surrounding by modulating its limb stiffness through three primary mechanisms: muscle coactivation (23), stretch reflexes

(23) and posture choice (47). Stretch reflex commands are not sent from the brain; this study does not address them. Posture selection plays a significant role, especially in 3D settings. Hence, subjects' posture is outside the scope and focus of this study. Muscle coactivation, on the other hand, is the main culprit of stiffening arm muscles. It changes the stiffness of a joint through antagonistic muscles acting on the joint. The higher the forces of the antagonistic muscles on the joint are, the stiffer the joint becomes (50). The collective coactivation of different muscle pairs, in turn, can control and orient the limb endpoint impedance (23).

2.1.6 Unbalanced concurrent activation

Concurrent activation of antagonistic muscles about a joint (coactivation) is involved in a wide array of daily activities. People coactivate when performing an unfamiliar motor task, standing on an unstable surface (e.g., surfing, train), operating an industrial robotic arm such as a powerlifting device, and reaching for, holding, or moving an object with accuracy, and steadiness. In individuals with various movement disorders such as cerebral palsy and Parkinson's disease, the coactivation of antagonist muscles is often different from that of healthy individuals regarding timing and magnitude (21, 48). In sports and other physical activities, the ability to control accurate and steady coactivation would influence motor performance that requires joint stabilization such as gymnastics, tai chi, yoga, dancing, sumo wrestling, archery, biathlon, and car racing. In producing comparable magnitudes of torque in opposite directions for stabilizing a joint with coactivation, the activation level can be different (i.e., unbalanced) between antagonistic muscles (51) because the capability for force generation can be disproportionate across muscles due to variable muscle architecture and moment arm (35).

2.1.7 Tremor and vibration

There have been many observations of 10, 20, and 40 Hz tremor effects under the influence of different frequencies of vibration (28, 29, 49). For instance, the three oscillation frequencies were modulated with different spectral amplitude under various contraction levels (in % maximum voluntary contraction of rectified EMG) during human finger muscle contraction (29). Such a phenomenon may reflect the rhythmicity of central neural firing. It is possible that peak frequencies are invariant to the mechanical properties of the system. Instead, they are a persistent feature at different levels of recruitment of motor units.

2.2 Signal and noise

2.2.1 Electromyography (EMG) signal

Human muscles are a collection of fibers attached to the bones through tendons. Each muscle fiber is innervated by one motoneuron that transmits command signals from the central nervous system (CNS) through a train of neural pulses. One motoneuron can innervate multiple muscle fibers, forming a motor unit (MU). CNS generated signals travel through nerve fiber into neuromuscular junction (NMJ) where they target and excite the membranes of all innervated fibers. Every motoneuron pulse induces a local depolarization of the transmembrane potential of each muscle fiber, called single-fiber action potential (SFAP). AP travel through muscle fiber to the end of tendon causing contraction. The sum of multiple SFAP from all fibers in a motor unit is called motor unit

action potential (MUAP). The firing rate of MUs shapes the magnitude and density of the observed signal, and adjusts the contraction process, and modulates the force output of the muscle.

Multiple MU are concurrently active, and their APs superimpose temporally and spatially to form a complex additive interference pattern that is called EMG (Figure 2). This interference can be detected within the muscle itself invasively or on the surface.

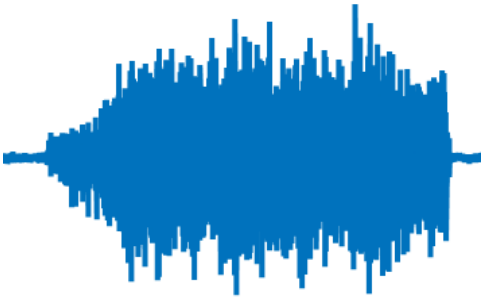

Figure 2 Multiple overlapping action potentials of many simultaneous firing of motor units recorded at surface EMG.

2.2.2 Maximum Voluntary Contraction (MVC)

For comparison across trials, muscles, and subjects, the force (or torque) is usually normalized with respect to the maximal isometric force that a subject can generate at the monitored joint for each muscle. The tasks consist of a gradual increase in activation from zero to maximum over 3 s with the maximum held for 2–3 s. The highest measure is chosen of at least three consecutive MVCs per each muscle ensuring all measures are within 5% or less from each other. Subjects maintain a similar posture to the actual test.

2.2.3 Noise, crosstalk, and other factors affecting EMG signal

EMG signal suffers from additive noise (exogenous effect) such as inherent (equipment noise), ambient (electromagnetic radiation on our bodies) noise, and motion

artifact (electrode interface and cables). Additionally, the signal is affected by inherent instability due to the randomness of the firing rate of motor units.

EMG can also be corrupted by activation from nearby muscles due to crosstalk (endogenous effect). When signals travel far from neighboring muscles to reach surface electrodes, it is equivalent to applying a low pass filter to incoming interference which adds low-frequency energy to the signal, hence skewing median frequency toward zero. Crosstalk is most disturbing when both agonist and antagonist muscles alter their contribution to the torque when changing their corresponding contraction levels (8). Reducing the outcome of such interference includes taking special care of the type and positioning of electrodes, studying large muscles, and for validation purposes, adding a control muscle for paired comparison. Besides, crosstalk interference can be decreased using blind source separation algorithms (16).

The EMG is low pass filtered by the skin and tissue; hence, the measured amplitude and frequency of firing are a transformed version of the original signal. As a result, interpretation of surface EMG source separation creates many challenges (3, 32). For instance, the amount of fat tissue between source and electrodes can act as a low pass filter altering the median frequency and other properties of the signal across subjects or locations. Such an effect is amplified as the thickness of tissue grows (8).

2.2.4 Stationarity of signal

In a dynamic contraction, many mechanical, physiological, anatomical and electrical changes occur and affect the relationship between the EMG signal strength and the force produced by the muscle. For example, the force-length relationship of the muscle fibers

varies non-linearly, and the shapes of the MUAPs are altered because the distance between the surface electrode and the contracting muscle fibers is not constant anymore. These effects are further intensified if the displacement occurs at a fast pace as a result of varying time delay between the signal and force (8). Consequently, it is preferred to investigate with isometric tasks before tackling dynamic conditions. Static contractions would more likely preserve the stationarity of the signal due to the stability of electrode position with respect to active muscle fibers. For dynamic contractions, many of the classical spectral techniques will fail. There are however some promising methods such as Cohen's class of time-frequency distributions or Wavelets (25) for such nonstationary cases.

2.3 Analysis

There are a wide variety of techniques and algorithms that can be used to analyze EMG signal. They range from Classical techniques (ex. smoothing, rectification, and measuring fatigue) to the less exploited Time-frequency representations (ex. Wavelet and Chirplet Transforms), to feature extraction and classification.

2.3.1 Smoothing

AEMG signal is usually derived from the raw signal by computing mean power through a moving average (MA) window, or more preferably a Root mean square (RMS) window that accounts better for fast transition such as contractions. However, larger window size increases the risk of phase shift.

2.3.2 Fatigue

When a single motor unit is firing continuously to the level of fatigue, it leads to MUAP slowing down. In the frequency domain, this corresponds to spectral compression (32). Fatigue, hence, is measured by computing the shift in mean or median of power in the frequency spectrum of the EMG signal (45). Mean or median power is preferred to taking the peak of the spectral waveform of the EMG signal as the latter has little significance in the presence of multiple motor units firing together.

2.3.3 Stimulus-locked vs. Response-locked

Some subjects have an earlier reaction time to stimulus; hence they can better match the target position. Others have higher reaction variability across trials. Since the aim is physiological, data reliability could be improved by attending to subject response-locked time stamps in segmenting windows. In other words, one way is to separate traces based on the target position (stimulus-locked). An alternative method with some potential advantages is to divide segments based on subject's response, not target (response-locked).

2.3.4 Envelope detection: Rectification and Hilbert Transform

Rectification, a conventional process in preprocessing EMG signal, is a non-linear operator that changes the frequency components of the signal to which it is applied (19). Some argue that EMG rectification is a necessary step as it enhances the EMG power spectrum around the mean motor unit firing rate while suppressing power in the higher frequency range which is mainly reflective of MUAP shape (22). Others have shown

through simulation that massive distortion is possible due to rectification, and they argue against applying it (30, 31). A new study (39) has revealed that rectification is beneficial when evaluating the strength of common synaptic inputs to the motor neurons for low-frequency (< 15 Hz), short duration of action potentials, and low cancellation level of MUAP, i.e., low MVC. Nevertheless, because of the novelty and physical demand of the cocontraction target used in this experiment, Hilbert transform was relied on to validate the results (36). Hilbert Transform was used to extract envelope information instead of rectification under similar constraints: Both techniques gave similar results.

2.3.5 Time-frequency representation

Based on the Heisenberg-Gabor limit, referred to as uncertainty principle, one cannot simultaneously finely localize a signal both in time and frequency domains. Wavelet Transforms are attractive because they contain similar information to short time Fourier Transform as seen in Figure 3-A, with additional unique properties of higher resolution in time at high frequencies of the basis function. Wavelet Transforms are the representation of an integral function by a specific orthonormal series generated by Wavelet, for performing signal analysis when frequency information varies over time. The coiflet-4 Wavelet has been used successfully for EMG preferably after dimensionality reduction (15).

Sinusoidal Wavelet, on the other hand, is a short-time Discrete Fourier Transform (DFT) for each time and frequency resolution with a number of cycles in each data window that increases slowly with frequency. This is ideal for obtaining a superior

resolution at higher frequencies. It has been shown (26) that this method is quantitatively comparable to using Hilbert Transform.

Chirplet Transform (Figure 3-B) initially reported in (27) presents some advantages compared to short time Fourier Transform (STFT) since the latter uses a windowed sine wave not capable of capturing fast changes in the frequency domain. Chirplet time-frequency transform has been applied to study transient and steady-state visual evoked potential (SSVEP) (7, 37), similar to this study purpose.

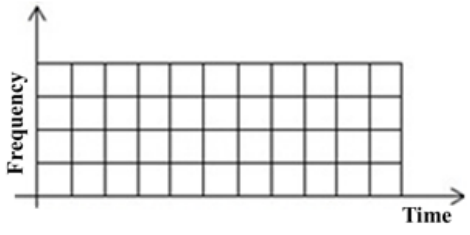

A1, STFT (Short time Fourier Transform)

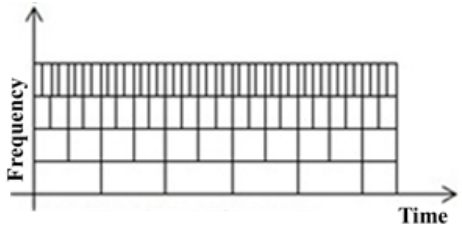

A2, WT (Wavelet Transform)

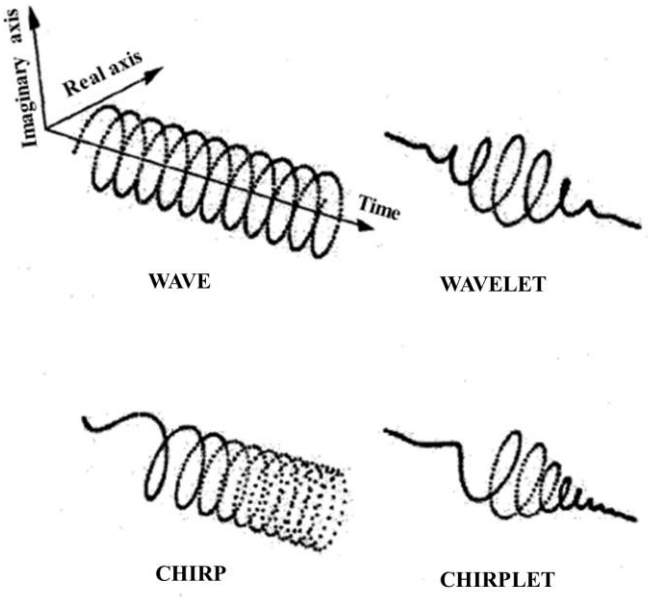

B, Wave / Wavelet, Chirp / Chirplet

Figure 3 A, Difference in time resolution at ascending frequencies (6) for Fourier (A1) and Wavelet Transforms (A2). B, Comparison of Chirplet and Wavelet. WAVE: 3D helix. The angle of rotation between each sample and the next is constant; hence the frequency is constant. WAVELET: Windowed wave with amplitude reduction in time. CHIRP: Linearly increasing angle of rotation between

one sample and the next. Frequency change as well. CHIRPLET: Same linearly increasing angle of rotation starts with a growing amplitude and then a decreasing one.

Wigner-Ville distribution has been used successfully for nonstationary signals for its balance between temporal and frequency resolution. It is like a Fourier Transform acting on the delay variable of a mirrored covariance function (44). Its joint density spectrum delivers strong localization characteristics usually concentrated around signal instantaneous frequency (1). However, such superior performance comes at the expense of introducing noise artifact (43) and negative energy with no physical significance.

$$W_x(t,w) = \int_{-\infty}^{\infty} x\left(t+\frac{\tau}{2}\right) x^*\left(t-\frac{\tau}{2}\right) e^{-iw\tau} d\tau \qquad \textbf{(1)}$$

2.3.6 Classification

When drawing inferences from uncertain noisy sensory signals, conflicting or even inaccurate information from different processes, it is preferable to use a set of tools that can handle such fuzziness in the data. Some of the specific soft computing methods are fuzzy logic, neural and adaptive networks, probabilistic networks, chaos, learning, and others. Each method is complementing to others, illuminating one aspect of the problem. Other nonparametric classification methods include Statistical learning theory such as Support Vector Machine (SVM) that transform data into a linearly separable space. Bayes classifier that introduces a decision strategy to minimize the expected value of the total classification cost (14). Cluster analysis, a set of unsupervised methodologies that

automatically group samples, or cases, into classes of similar objects. Such methods could be tested for classifying EMG signals for a better HRI although they were not integrated into this thesis. They are listed for future direction.

2.3.7 Features

A summary of some classical or novel algorithms and features (1, 12, 32, 37) is presented in Table 1. This study will test a select few appropriate for the analysis of EMG.

Table 1 List of algorithms and features with potential application to EMG

Feature Type	Feature Name	Feature Name
Temporal	• Mean, • Mean absolute value slope, • Willison amplitude, • Slope sign changes, • Standard deviation,	• Waveform length, • Kurtosis, • Complexity, • Zero-crossing, • Moving standard deviation,
Spectral	• Frequency ratio, • Coherence,	• Power spectral density,
Time-frequency Representation	• Wigner-Ville distribution, • Event-related spectral perturbation,	• Wavelet Transform, • Event-related amplitude and phase coherence,
Information Theory	• Shannon entropy, • Sample entropy,	• Mutual information,
Nonlinear	• Katz fractal dimension,	• Nonlinear energy,
ASR	• Real Cepstrum,	• Mel-frequency Cepstrum,

CHAPTER 3. STATIC COCONTRACTION

A well-controlled static experiment to identify and possibly influence the relationship between correlated oscillations and cocontraction performance is presented first. Findings and discussions are addressed in two separate sections: Steady cocontractions (aim-I), and transient contractions and the role of the intervention period (aim-II).

3.1 Experiment I, Static intermuscular contractions with AEMG feedback

3.1.1 Experimental setup and protocol

3.1.1.1 Subjects

Sixty right-handed healthy young adults (22.5 ± 3.0 years old, 30 men) without any history of neurological disorder participated in the study. Handedness was confirmed with the Edinburgh Handedness Inventory (41). They all gave their written informed consent in accordance with the Institutional Review Board at Georgia Institute of Technology. Subjects were divided into three groups that received different intervention: Cocontraction, Contraction, and Control.

3.1.1.2 Experimental setup

Subjects were seated on a chair with a backrest, seat belts attached (Figure 4-A). The right shoulder was flexed to 20^{o} from the anatomical position, i.e., the upper arm was placed forward from the trunk by 20^{o}. The elbow was rested on a table, and the forearm was constrained to a padded attachment at the wrist in the neutral position, using a Velcro

strap. With their fingers fully extended, the elbow joint was kept at 80^{o} from the anatomical position during the tasks.

Surface EMG signal was recorded from two elbow flexor muscles, biceps brachii (BB) and brachioradialis (BR), and one elbow extensor muscle, triceps brachii (TB), (Figure 4-B). EMG of the BB–TB pair was used as the antagonistic muscle pair for the cocontraction tasks. Because EMG from this muscle pair could be influenced by potential crosstalk because of their anatomical proximity, EMG recording of BR allowed for an additional antagonistic muscle pair (BR–TB) for analysis, which is less susceptible to crosstalk. Before bipolar electrodes were attached to these muscles, the skin surface was prepared by shaving the hair, gently exfoliating the skin, and cleaning with alcohol.

The electrodes had a differential amplifier (× 300) and a band-pass filter (15-2,000 Hz) with the inter-electrode distance of 18 mm (Motion Lab Systems, Baton Rouge, LA). EMG signals were acquired at 1,000 samples/s using an analog-to-digital converter (NI USB-6216, National Instruments, Austin, TX) and Matlab (Mathworks, Natick, MA).

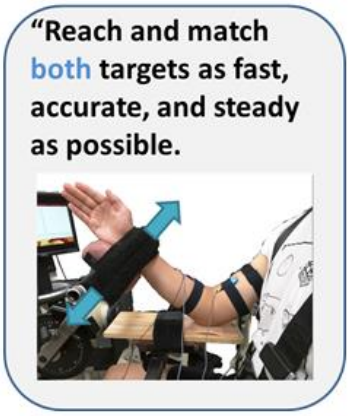

A

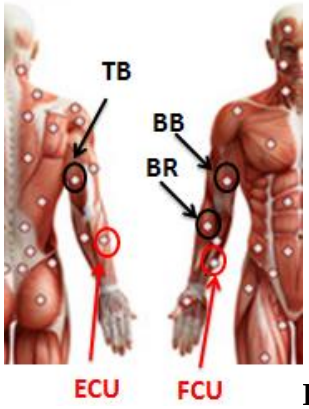

B

Figure 4 A, Experiment I setup; B, Electrodes placement for experiment I (BB, TB, and BR) and experiment II (BB, TB, BR, FCU, and ECU).

3.1.1.3 Experimental protocol

All participants performed a target-matching test using rectified and smoothed EMG amplitude (AEMG) of BB and TB before and after a bout of intervention. For normalizing AEMG, maximal voluntary contraction (MVC) was performed at the beginning of the experiment as described in 2.2.2. MVC was performed as the maximal contraction of each muscle group independently, and not concurrently. Each subject then performed the steady cocontraction test before and after an intervention to assess cocontraction performance and neural oscillations. In addition, steady contractions were performed before and after the intervention to assess potential neuromuscular fatigue.

3.1.2 Steady cocontraction Test

All subjects were tested on their ability to control steady cocontraction of BB and TB by matching their AEMGs to two pairs of target templates before and after an intervention. In all templates, the baseline was a resting level for both muscles, followed by different levels of AEMG between the muscles (Figure 5). In one pair, the target template for BB started with 4% MVC for 3.5 s followed by 12% MVC (HIGH target) for 24.5 s while the template for TB started with 12% MVC for 3.5 s followed by 4% MVC (LOW target) for 24.5 s (Figure 5). This target pair was termed as TB-LOW / BB-HIGH target. In another pair of templates, the roles of BB and TB were swapped and termed as BB-LOW / TB-HIGH target. Subjects were instructed to "reach and match

both targets as fast, accurate, and steady as possible." The order of the pair of templates was pseudo-randomized, and there was a 32 s rest in between trials.

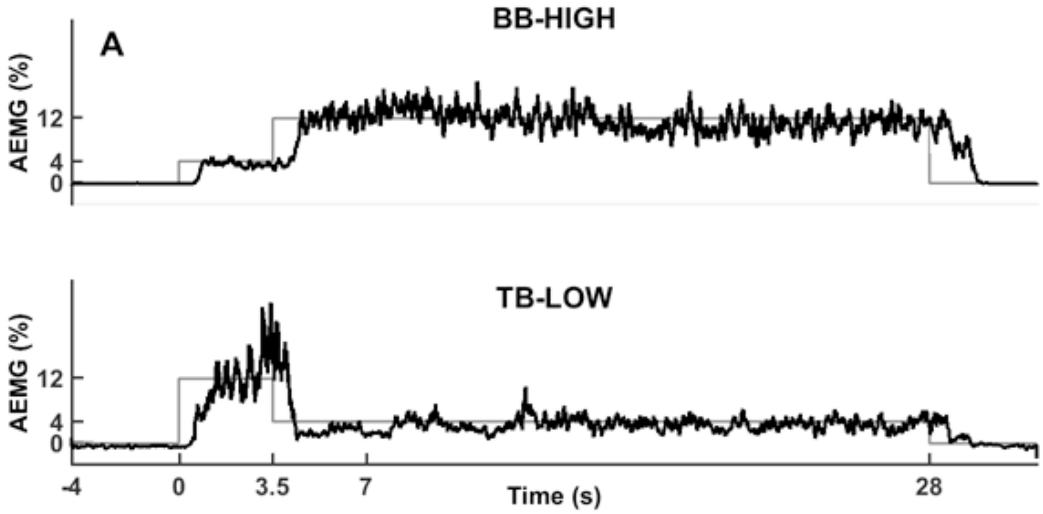

Figure 5 Representative rectified and smoothed EMG (AEMG) signals of the biceps brachii (BB) and triceps brachii (TB) for visual feedback during the steady cocontraction test. Signals are overlaid to the targets in gray. Subjects contracted BB and TB muscles for two target pairs. Only one target pair is displayed.

3.1.3 Intervention

After the completion of the initial steady cocontraction test, subjects received about 52 min (including 37 min of rest) of one of three types of interventions depending on their assigned group. In the Control group, subjects did not perform practice but rested while reading. In the Cocontraction group, subjects performed out-of-phase cocontraction practice of BB and TB concurrently. In contrast to the steady test, cocontraction practice trials were alternating unbalanced activation of BB and TB muscles in a shorter duration with the purpose of forcing the phase between the two muscles to desynchronize. In the

Contraction group, subjects performed practice of repeatedly adjusting contraction levels of BB or TB independently. In other words, the Contraction group practiced similar targets as Cocontraction group except using a single muscle at a time. Such a practice might have a habituation effect later in the test state. In both Cocontraction and Contraction groups, there were 32 practice trials, with a 32 s rest in between. The protocol was designed in order for subjects to voluntarily produce out-of-phase low-frequency correlated oscillations between BB and TB repeatedly (Figure 6).

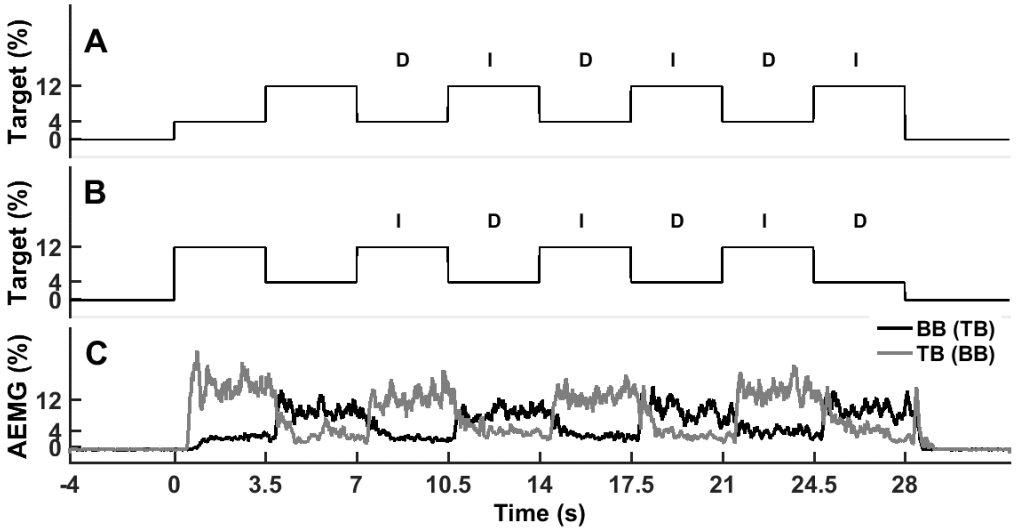

Figure 6 Target sequences for BB and TB in practice trials. In Cocontraction group, subjects activated one muscle for sequence A and another muscle for sequence B simultaneously. Assignment of muscles to the sequences was alternated. In Contraction group, subjects contracted one muscle for sequence A or sequence B separately. Assignment of muscle and sequence was varied. C, Representative recording of AEMGs during practice in Cocontraction group.

3.1.4 Steady contraction

To obtain EMG signals for determining the median frequency as an indirect measure of neuromuscular fatigue, steady contractions were performed immediately before the steady cocontraction test, immediately before the intervention, and after the steady cocontraction retest post-intervention. In each trial, subjects were asked to contract either the elbow flexor or the extensor muscles independently to match the AEMG of BB or TB, respectively, to the target of 12% MVC for 28 s. This trial was repeated three times for each muscle.

A summary map of experimental design including test and intervention is displayed in Figure 7. All 60 subjects completed the cocontraction test before and after the intervention. Only one out of two randomized target level conditions is displayed with BB transitioning from LOW (4% MVC) to HIGH (12% MVC) / TB HIGH to LOW; the other being BB HIGH to LOW / TB LOW to HIGH. During cocontraction intervention (top middle column), 20 subjects practiced with two target level conditions being randomized. Twenty subjects practiced single muscle contraction with four target level conditions randomized (center) during contraction intervention. Twenty control subjects were not involved in muscle activation practice; instead, they read while resting for an equivalent duration as other tasks (bottom middle column).

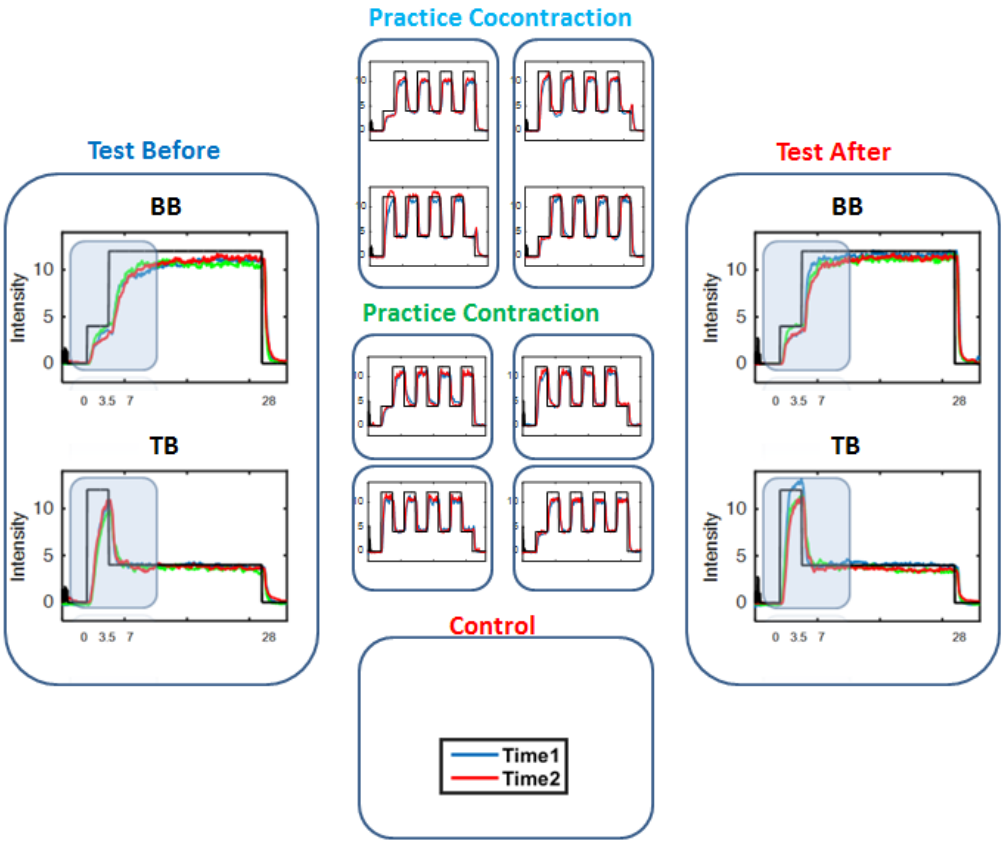

Figure 7 Experimental design, test and intervention: Cocontraction test before (left column) and after (right column) intervention. Three traces are for averages across trials and subjects of AEMG of each group (cocontraction, contraction, and control). As for intervention (middle column), cocontraction practice with two target level conditions randomized (top); Single muscle contraction practice with four target level conditions randomized (middle); Control with no activation involved for the same duration (bottom). For intervention, Time1 and Time2 correspond to 1st and 2nd half of trials respectively. Transparent rectangles in test denote transient segment.

3.1.5 Data analysis

The amplitude of EMG signal was computed through a series of steps. After the mean value of the raw EMG signal was subtracted, it was full-wave rectified and smoothed using a moving average window of 125 samples (125 ms). Resting background noise at

the beginning of the experiment was subtracted. The signal was then normalized by the maximal value during MVC for each muscle (AEMG). Thus processed AEMG was used for providing visual feedback to the subjects. To assess the variability in maintaining steady cocontraction, the variance of AEMG was calculated across the last 21 s (from time 7 s to 28 s) before going back to the baseline. To assess the accuracy in matching the cocontraction level about the steady target (i.e., slow deviations from the target), the mean squared error (MSE) between AEMG and target was calculated for the same period after applying a 1-s moving average.

For assessing the oscillatory characteristics of EMG signals, the following processing was performed. An 8^{th} order Butterworth high-pass filter of 15 Hz cutoff was applied, using a zero-phase forward and reverse digital IIR filter. After removing the mean value, the signal was full-wave rectified. Resting background noise was subtracted. The last 21 s of the constant target (steady-state) was extracted, and the mean value was subtracted. All six trials were concatenated together to form a 126-s long segment. To assess the power content of oscillations, estimates of the event-related spectral perturbation (ERSP) (12) or shifts in the power spectrum of each muscle in time and frequency were derived using a Hanning window with the size of 2,048 samples (2.048 s) with 512 samples (0.512 s) overlap (2).

$$ERSP(f,t) = \frac{1}{n}\sum |F(f,t)|^2 \quad \textbf{(2)}$$

For phase and amplitude coherence between muscles for test (Figure 8), cocontraction practice (Figure 9), contraction practice when BB is active (Figure 10), or

contraction practice when TB is active (Figure 11), the event-related phase coherence (ERPCOH) and event-related linear coherence (ERLCOH) (12) between each pair of muscles (BB-TB, BB-BR, BR-TB) were estimated using the window size of 2,048 samples (2.048 s) with 512 samples (0.512 s) overlap (equations **(3)** and **(4)**).

$$ERPCOH^{a,b}(f,t) = \frac{1}{n}\sum \frac{F^a(f,t)F^b(f,t)^*}{|F^a(f,t)F^b(f,t)|} \quad \textbf{(3)}$$

$$ERLCOH^{a,b}(f,t) = \frac{\sum F^a(f,t)\,F^b(f,t)^*}{\sqrt{\sum |F^a(f,t)|^2}\sqrt{\sum |F^b(f,t)|^2}} \quad \textbf{(4)}$$

Although common drive frequency can be in the 0 to 5 Hz range, relatively high coherence amplitude was observed below 3 Hz; therefore the focus was on the 0 to 3 Hz range instead. For spectral power (EMG power), amplitude coherence (EMG coherence) and phase coherence (EMG phase), mean value in the 0-3 Hz range was computed across the 21 s. Correlated oscillations were computed using both FFT and sinusoidal Wavelet methods. Finally, Inter-trial coherence (ITC) (12), a measure that shows the event-related phase-locking across trials in time and frequency (Figure 34, bottom plot) was computed in the 0-3 Hz range and across the 21 s.

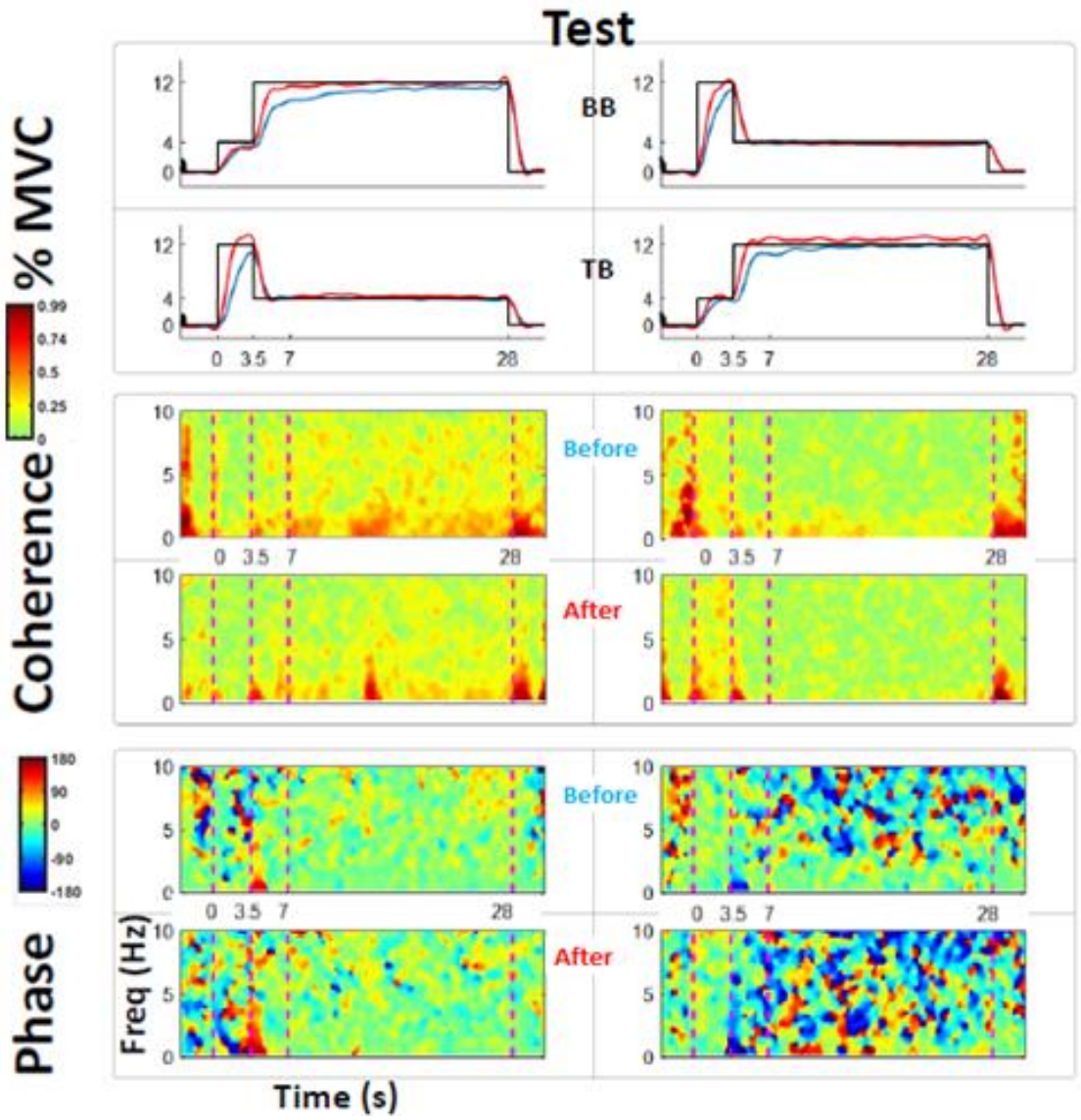

Figure 8 Signals grand average during the cocontraction test. BB-HIGH (left column), and BB-LOW (right column) average across trials in 20 subjects: Top 2 rows, time series data (top: BB, bottom: TB; before and after practice); Rows 3&4, amplitude coherence between BB and TB before and after practice; similarly, rows 5&6 show phase coherence corresponding to rows 3&4. The x-axis is a measure of time between -4 and 32 s.

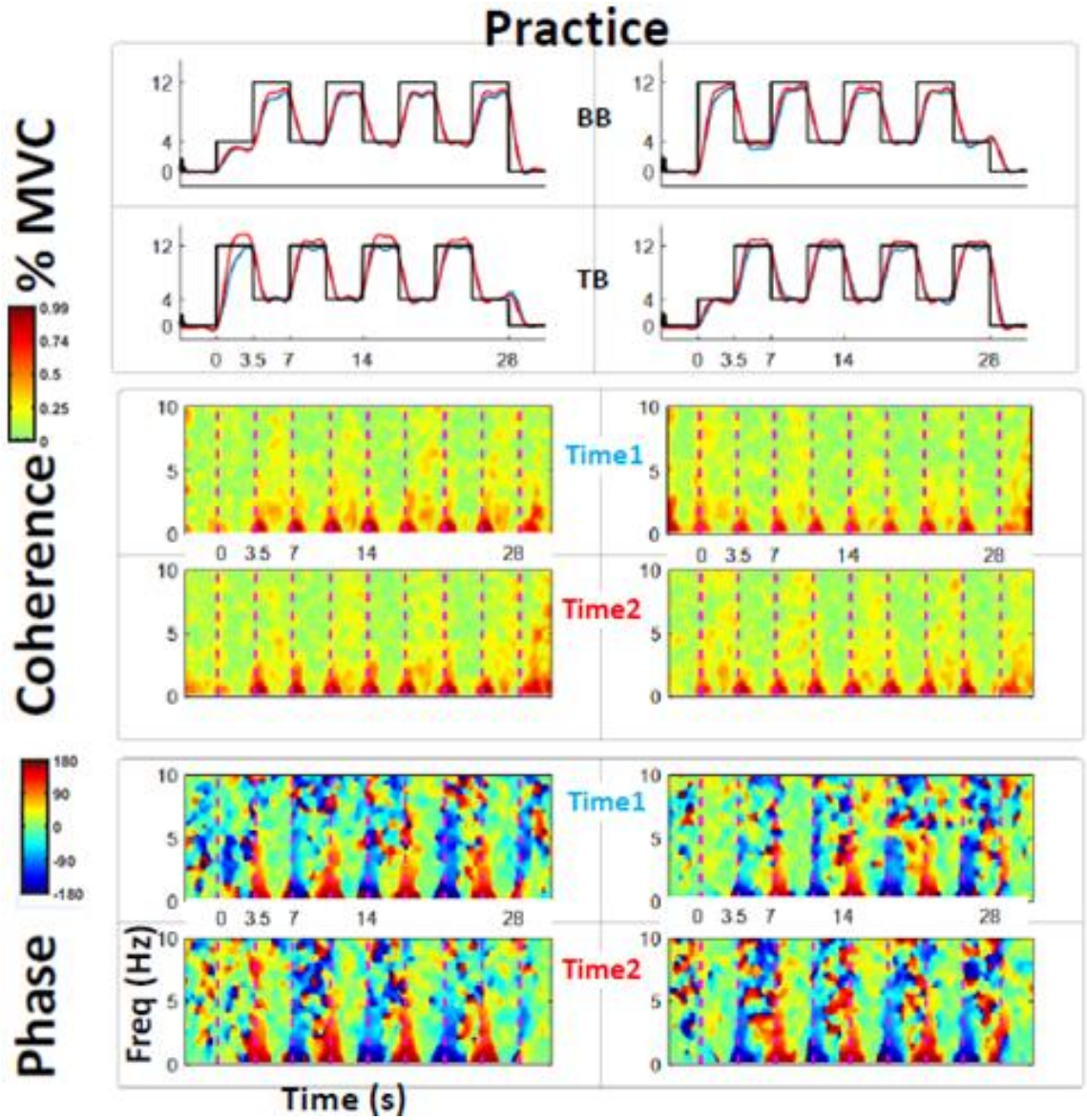

Figure 9 Signals grand average during cocontraction practice. Target level VL-even (left column), and target level VL-odd (right column) across trials in 20 subjects: Top 2 rows, time series data (top: BB, bottom: TB; time1: 1st half of trials, time2: 2nd half of trials); Rows 3&4, amplitude coherence between BB and TB first (1st-8th trials) and second half (9th-16th trials) for each target level of practice sessions; Similarly, rows 5&6 show phase coherence corresponding to rows 3&4. The x-axis is a measure of time between -4 and 32 s.

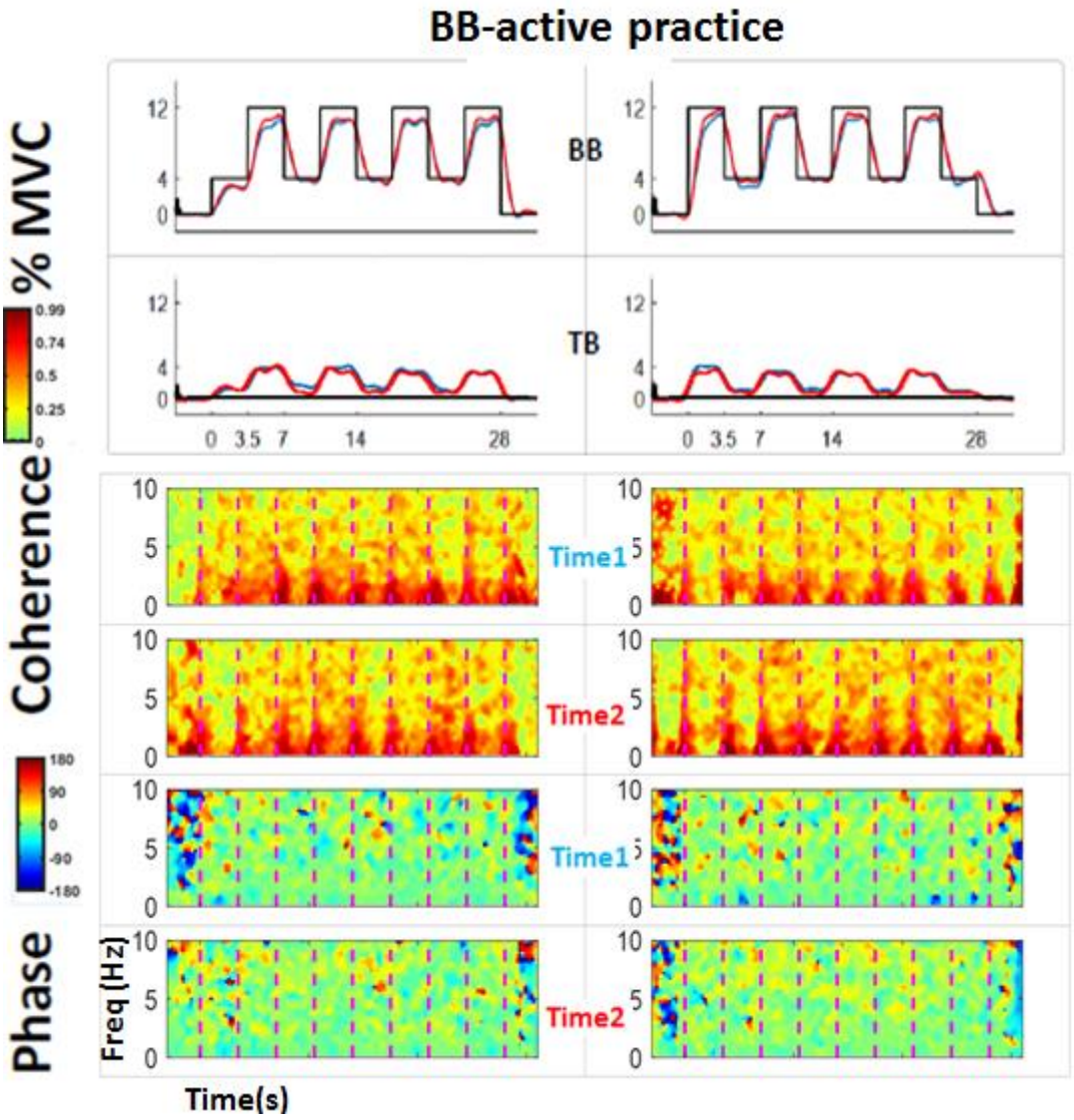

Figure 10 Signals grand average during contraction practice when BB is active (TB is idle). Target level VL-even (left column), and target level VL-odd (right column) across trials in 20 subjects: Top 2 rows, time series data (top: BB, bottom: TB; time1: 1st half of trials, time2: 2nd half of trials); Rows 3&4, amplitude coherence between BB and TB first (1st-4th trials) and second half (5th-8th trials) for each target level of practice sessions; Similarly, rows 5&6 show phase coherence corresponding to rows 3&4. The x-axis is a measure of time between -4 and 32 s.

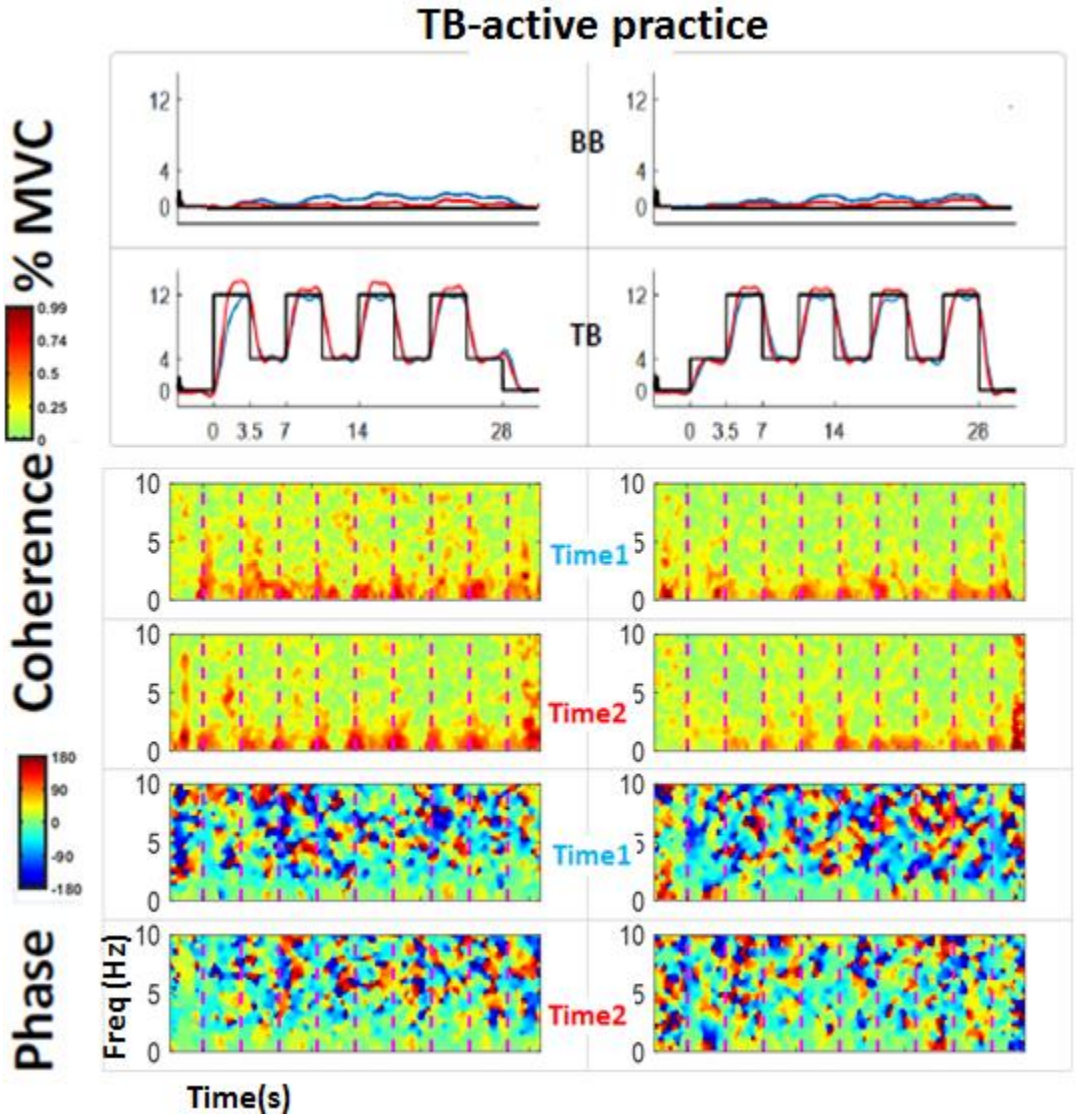

Figure 11 Signals grand average during contraction practice when TB is active (BB is idle). Target level VL-even (left column), and target level VL-odd (right column) across trials in 20 subjects: Top 2 rows, time series data (top: BB, bottom: TB; time1: 1st half of trials, time2: 2nd half of trials); Rows 3&4, amplitude coherence between BB and TB first (1st-4th trials) and second half (5th-8th trials) for each target level of practice sessions; Similarly, rows 5&6 show phase coherence corresponding to rows 3&4. The x-axis is a measure of time between -4 and 32 s.

To quantify the in-phase metric between muscles, probability density function (pdf) ranging between 0 ± 180 degrees was first extracted. The pdf for each phase coherence

target level (BB-LOW / BB-HIGH) was calculated in the 0-3 Hz range and across the 21 s (test) for EMG phase coherence (Figure 12). In-phase metric was then computed as the area within 0 ± 5 degrees of pdf distribution. In other words, it is the percentage of in-phase per each target level.

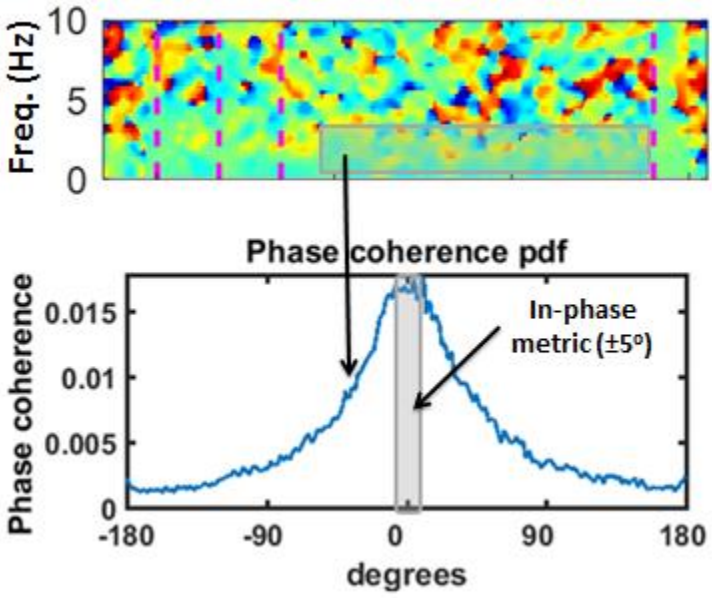

Figure 12 Probability density function (pdf) of phase coherence and its in-phase metric. The pdf is extracted from the time-frequency phase coherence window of interest. In-phase metric calculation defined as the percentage of probability density function between 0 ± 5°. The x-axis in the top panel is a measure of time between -4 and 32 s.

As for practice protocol, the Cocontraction group was designed so subjects voluntarily produce out-of-phase low-frequency correlated EMG oscillations between muscles. To examine the characteristics of EMG oscillations during the intervention in this group, EMG coherence and EMG phase between muscle pairs were calculated

similarly as above except for the extraction of the samples depending on temporal windows of interest.

To quantify a measure for potential neuromuscular fatigue, median power frequency was computed using power spectral density estimate using the last 21 s of each trial during steady contraction.

Steady-state vs. transient-state

Due to possible underlying neural differences, each task trajectory was divided into a steady and transient cocontraction traces. The steady cocontraction test was covered in section 3.1.2. The alternating practice contraction and cocontraction during intervention traces are transient (section 3.1.3). In other words, they change the activation level in a short duration. Likewise, the initial reaching and first alternating activation level for both test and practice are transient traces.

Each trial starts with transient activation of muscles from rest (reaching) that last for about 3.5s (Figure 13). Such activation is denoted as varying level 1 (VL1). This is followed by an alternation of activation level between the two targets (LOW becomes HIGH and vice versa). The 3.5s is denoted as varying level 2 (VL2). Both VL1 and VL2 are transient states common to test and practice. For the cocontraction test (Figure 13-I), a steady constant level (CL) follows and lasts for 21s; this will be the main focus of aim-I. On the other hand, during practice, a repetitive alternating target (VL-rep) that lasts for 3 cycles of 21s (Figure 13-II) is explored in aim-II.

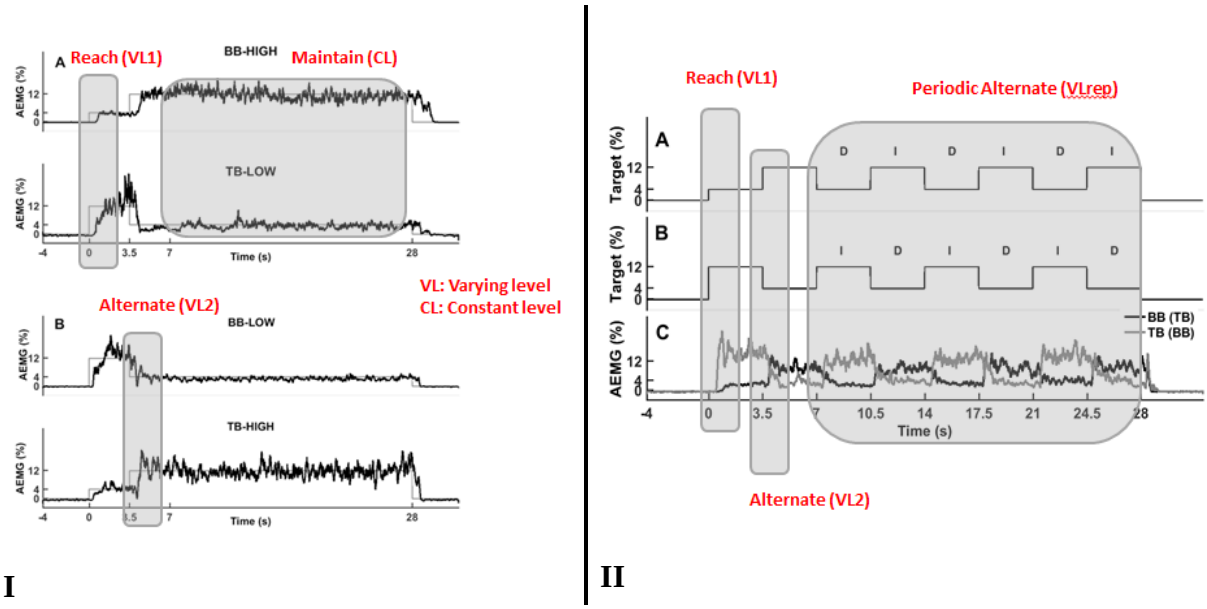

Figure 13 Differentiation between transient varying level and steady constant level. I) Cocontraction test with labels for each stage for both target level conditions: Reach, varying level 1 (VL1); Alternate, varying level 2 (VL2); Maintain, constant level (CL). II) co/contraction practice with reach (VL1), alternate (VL2), and repetitive periodic alternate for 3 cycles (VL-rep).

Stimulus-locked vs. Response-locked

Data were initially analyzed based on stimulus-locked responses (i.e., the subject's temporal reaction relative to when stimulus appeared on screen). However, different subjects have different alertness and reaction time. For better accuracy, and to extract finer responses during transient initiation stage, trials were segmented based on their response rather than stimuli (Figure 14). To identify response time stamps, peaks of maximum deviation (derivative of AEMG signal) were located while limiting peaks between 0-3.5secs of each half cycle. Then a window of 3 s around peaks was extracted for each trial and target level.

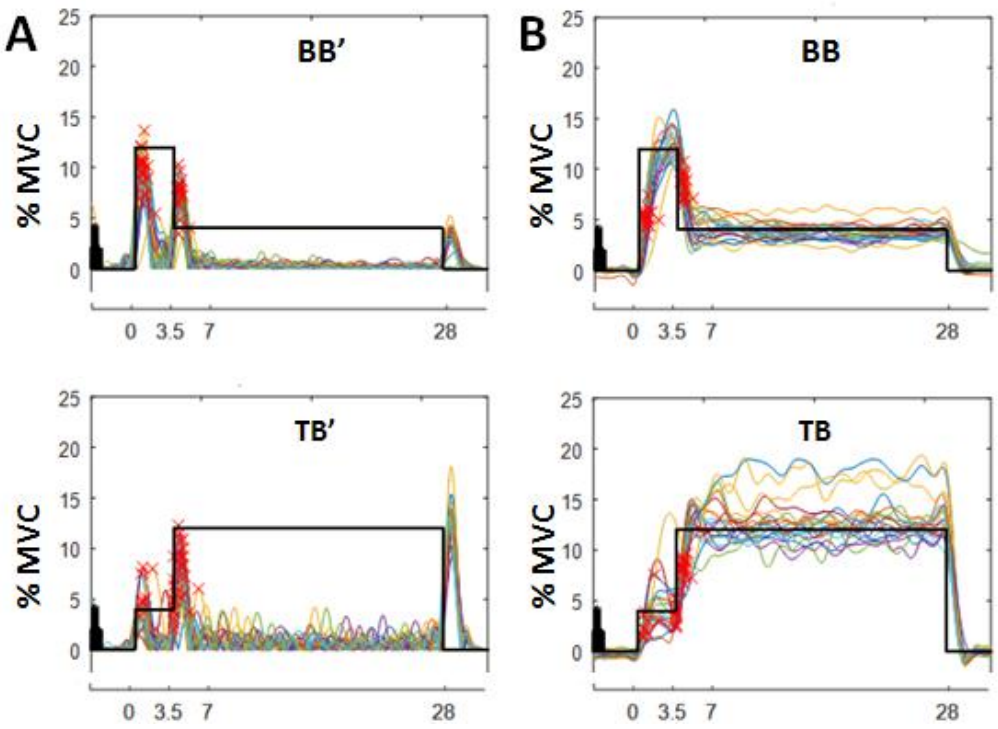

Figure 14 Response-locked maximum AEMG drop or increase. A, derivative of AEMG (BB' and TB') with maximum peaks denoted with X for each of the 20 subjects during BB-LOW cocontraction test. B, Corresponding AEMG (BB and TB) with the location of the maximum drop or increase in %MVC. The x-axis is a measure of time between -4 and 32 s.

3.1.6 Statistical analysis

For testing accuracy and variability of AEMG in the steady cocontraction test, a four-way analysis of variance (ANOVA) was performed on MSE and variance of AEMG with factors being time (before and after intervention period), muscle (BB and TB), target level (BB-LOW / TB-HIGH and TB-LOW / BB-HIGH), and group (Control, Contraction, and Cocontraction) with repeated measures. Dependent variables for oscillatory characteristics of EMG in the steady cocontraction test included EMG power for each muscle and EMG coherence and EMG phase for each pair of muscles, all < 3

Hz. EMG power was tested with a four-way ANOVA with factors being time, muscle (BB, TB, and BR), target level, and group with repeated measures. EMG coherence and EMG phase were tested with a four-way ANOVA with factors being time, muscle pair (BB-TB, BR-TB, and BB-BR), target level, and group with repeated measures. EMG in-phase coherence was tested with a three-way ANOVA after taking the difference between times (in-phase coherence measures after practice were subtracted from in-phase measures before practice) resulting in three factors being muscle pair (BB-TB, BR-TB, and BB-BR), target level, and group. For assessing neuromuscular fatigue, median power frequency of raw EMG during steady contractions was tested with a three-way ANOVA with factors being time (before the steady cocontraction test, immediately before the intervention, and after the steady cocontraction re-test post intervention), muscle (BB and TB), and group with repeated measures. When appropriate, post hoc comparisons were performed using Tukey's test. Linear regression analysis was performed between each of the Oscillation-related variables (i.e., EMG power, EMG coherence, and EMG phase) and the performance-related variables (i.e., MSE and variance) across subjects for each muscle and muscle pair before and after the intervention period. Pearson product-moment correlation coefficient (r) was obtained for these correlations. An alpha level of 0.05 was chosen for determining statistical significance. $P < 0.05$ and $P < 0.01$ are noted when significant.

As for practice protocol (cocontraction and contraction), statistical analysis was calculated similarly as above except for the extraction of the samples depending on temporal windows of interest and number of target level conditions.

In what follows, aim-I will deal with steady cocontraction while aim-II will explore intervention in more details especially the transient aspect of the signal. For the more detailed description of experiment I methodology, refer to (2).

3.2 Aim-I Slow oscillations are associated with steady cocontraction performance.

Aim-I builds the foundation with two objectives: 1) determine whether there is an underlying association between the low-frequency correlated neural oscillations between muscles and the performance of steady unbalanced cocontraction across individuals and 2) determine whether a bout of out-of-phase cocontraction practice reduces the in-phase low-frequency correlated neural oscillations and improves the performance of steady unbalanced cocontraction of antagonistic muscles in healthy young adults.

3.2.1 Correlation between oscillations and performance

In the first goal, performance variables were not influenced by group. Therefore, subjects of all groups were put together to increase statistical power in this examination. Correlation coefficients were determined between the correlated oscillation and the performance related variables across subjects in the steady cocontraction tests.

Correlation coefficients between EMG coherence and the performance variables across subjects are summarized in Figure 15 for various muscle pairs at each target. Collectively, significant positive correlations between EMG coherence and performance variables were found only in 6 out of 24 cases (25% frequency) before the intervention period when all muscle pairs and targets were collapsed. After the intervention period, significant positive correlations were found in 17 out of 24 cases (71% frequency): 7 out of 12 cases (58% frequency) for the TB-LOW / BB-HIGH target and 10 out of 12 cases (83% frequency) for the BB-LOW / TB-HIGH target. Note however that the correlation coefficients were no larger than 0.7 because of the multiple components present, the large number of data points (60 subjects), and possible interference of action potentials.

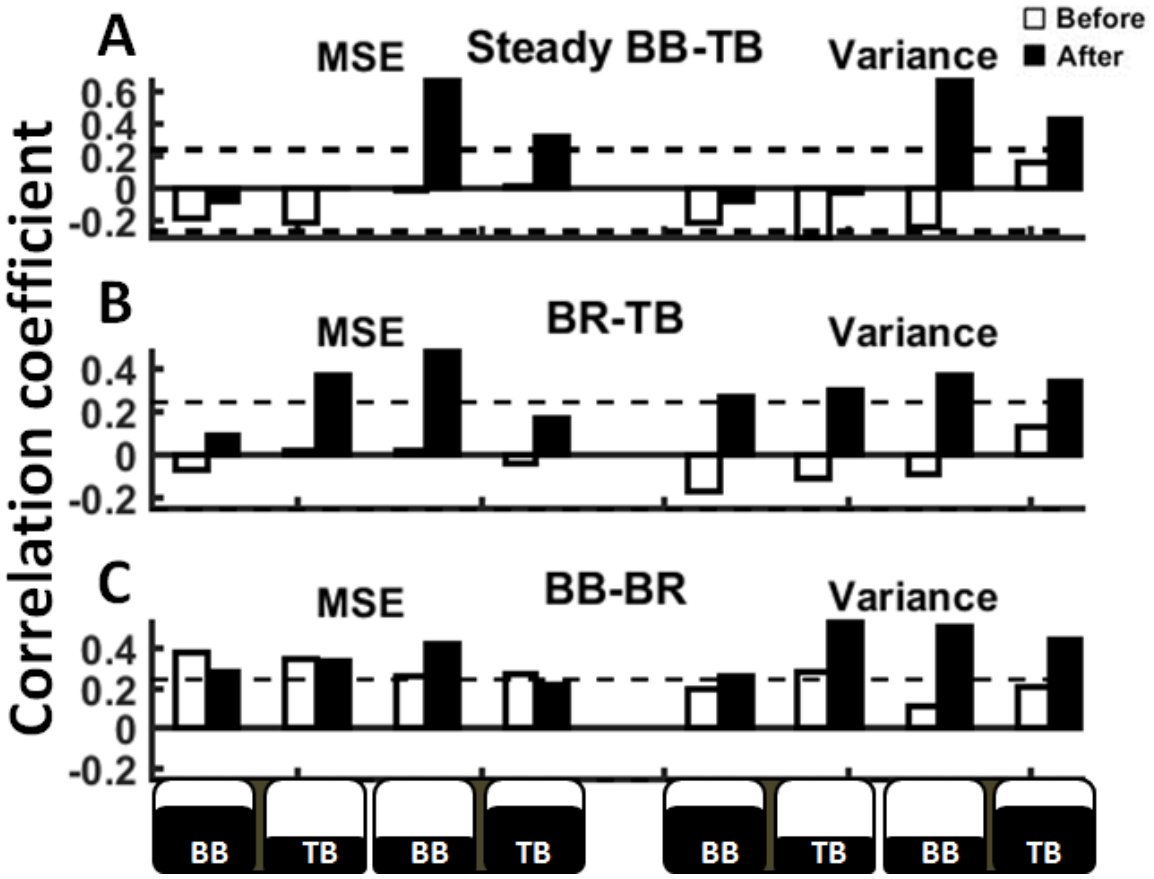

Figure 15 Correlation coefficient between performance variables (MSE and variance) and EMG coherence (A: BB-TB pair, B: BR-TB pair, C: BB-BR pair) before (open bars) and after (filled bars) the intervention period. On the x-axis, BB HIGH and TB LOW is one target pair, and BB LOW and TB HIGH is another target pair. Broken horizontal lines represent correlation coefficient at *P* = 0.05. LOW: 4%MVC target; HIGH: 12%MVC target; MSE, mean squared error.

3.2.2 Oscillations

The second goal was to examine if out-of-phase cocontraction practice acutely reduces the correlated neural oscillations and improves steady cocontraction performance. To determine whether correlated oscillations were changed differently depending on the type of intervention, the statistical significance of the interaction of time × group was looked for in EMG coherence, EMG phase, and EMG power < 3 Hz.

For coherence of EMGs, there was a main effect of time ($P < 0.01$); EMG coherence was reduced by 6% after the intervention period (Table 2). Other main effects included group, muscle pair, and target level. For phase of EMGs, there was a main effect of muscle pair but was not a significant effect of time or group with the mean value being < 2 degrees. For low-frequency EMG power, the measure was smaller by 14% after the intervention period with the main effect of time (Table 2). Other main effects included muscle and target level. None of the three comparisons (coherence, phase, and power) had any significant interaction that contained time × group interaction.

3.2.3 Performance

In the assessment of accuracy, there was a main effect of time ($P < 0.01$), revealing reduced MSE of AEMG by 33% after the intervention period (Table 2). Additionally, MSE of AEMG was 40% greater in TB compared with BB, and 110% greater in HIGH target compared with LOW ones. There was no significant interaction on MSE of AEMG that contained time × group interaction. In the assessment of variability, there was a main effect of time ($P < 0.01$), showing a decreased variance of AEMG by 30% after the intervention period. For other main effects of group, the variance of AEMG was lower in Cocontraction compared with Contraction by 30% and Control by 29%, 32% greater in TB compared with BB, and 125% greater in HIGH target compared with LOW ones. There was no significant interaction on the variability of AEMG that contained time × group interaction. Additionally, there was no significant interaction across target level conditions.

Table 2 Performance variables and EMG oscillations during steady cocontraction test in each group before and after the intervention period.

Group	Cocontraction		Contraction		Control		Average	
	Before	**After**	**Before**	**After**	**Before**	**After**	**Before**	**After**
MSE %MVC	6.94 (8.29)	4.67 (8.17)	7.81 (10.66)	5.24 (5.85)	8.69 (9.06)	5.72 (8.91)	7.81 (9.38)	5.21** (7.73)
Variance %MVC	2.71 (2.53)	1.95 (1.71)	3.80 (5.27)	2.89 (3.46)	3.99 (4.42)	2.54 (3.33)	3.50 (4.25)	2.46** (2.96)
Power	18.80 (9.09)	15.25 (9.87)	19.34 (7.81)	16.28 (8.96)	17.91 (8.30)	16.93 (8.68)	18.69 (8.41)	16.15* (9.19)
Coherence	0.448 (0.066)	0.414 (0.044)	0.459 (0.068)	0.432 (0.066)	0.435 (0.058)	0.419 (0.043)	0.447 (0.065)	0.421* (0.053)
Phase	1.42 (7.33)	1.33 (9.28)	1.04 (8.56)	1.34 (8.54)	1.90 (9.08)	1.03 (9.21)	1.45 (8.33)	1.23 (9.00)

MSE, mean squared error; Power, mean area of event-related spectral perturbation; Coherence, mean area of event-related amplitude coherence between muscles; Phase, corresponding phase coherence; Average, averaged data across groups; MVC, maximal voluntary contraction; *, $P < 0.05$; **, $P < 0.01$. Values are mean (standard deviation) across subjects.

3.2.4 Potential neuromuscular fatigue

The median power frequency of raw EMG during the steady contraction was compared as an indirect measure of neuromuscular fatigue. There was only a significant main effect of muscle (85.6 ± 14.2 Hz in TB vs. 78.9 ± 12.2 Hz in BB, $P < 0.01$), but not time or group. When collapsed across groups and muscles, median power frequency of raw EMG was 83.1 ± 13.5 Hz before the steady cocontraction test, 82.3 ± 14.3 Hz immediately before the intervention, and 81.3 ± 13.3 Hz after the steady cocontraction retest post intervention ($P > 0.05$). There were no significant interactions.

3.2.5 Discussion

This aim-I study intended 1) to determine whether there is an underlying association between the low-frequency correlated neural oscillations between muscles and the performance of steady unbalanced cocontraction across individuals and 2) to determine whether a bout of out-of-phase cocontraction practice reduces the in-phase low-frequency correlated neural oscillations and improves the performance of steady unbalanced cocontraction of antagonistic muscles in healthy young adults. The major findings are: 1) there were positive correlations between low-frequency EMG coherence and performance variables (i.e., mean squared error of AEMG and variance of AEMG) across subjects, which became more prevalent after the intervention period; and 2) there were marginal reductions in low-frequency EMG amplitude coherence and large improvements in performance variables after the intervention period, but the type of intervention did not necessarily influence the reductions in these variables..

The presence of significant positive correlations between EMG coherence and both mean squared error and variance of AEMG in the majority of cases after the intervention period indicates that accuracy and steadiness of steady cocontraction tend to be degraded in individuals who have greater low-frequency correlated oscillations between muscles. The magnitude of low-frequency neural oscillations is suggested to be one of the major contributors to the steady performance in both simulation (13, 46) and experimental studies (34, 38, 52) on contractions primarily within agonistic muscles. In the current study, the absence of significant positive correlations between EMG power in individual muscles and performance variables in most cases indicates that the amount of independent neural oscillations in each muscle is not associated with the steady

performance when the steady task is antagonistic cocontraction. This is a new set of intriguing findings suggesting that people who tend to perform steady cocontraction less skillfully are not those who have greater low-frequency neural oscillations in each muscle but greater correlated oscillations between muscles. Hence, the results support that capability for steady cocontraction performance is related to the amount of low-frequency correlated neural oscillations.

The used steady test was unique not only because it was a cocontraction task but also because it used unbalanced activation levels between antagonistic muscles. Maintaining two different activation levels in antagonistic muscles requires the motor command to concurrently excite both muscles while partially inhibiting one of the muscles as steady as possible. Concurrent excitation of multiple muscles involves low-frequency common oscillations in motor unit discharges: the ‘‘common drive’’ of central origin (10). As an indirect measure of common oscillations of pools of motor units, low-frequency correlated oscillations in rectified EMG have negligible time lags (<50 ms) between antagonistic elbow muscles (51). Very slight deviations of EMG phase from zero during steady cocontractions confirm that correlated oscillations in the current study were also in phase practically. In the presence of this in-phase common drive, the unbalanced cocontraction requires partial inhibition for adjusting to a lower target level with one of the muscles. Because spinal Ia reciprocal inhibition is strongly depressed during cocontraction (24, 40), this inhibition is likely to involve central mechanisms, including reciprocally organized anti-phase drive between antagonistic muscles (11). It is unknown whether the decreased corticospinal excitability with improved cocontraction performance (42) is related to this implied inhibition.

The correlations between EMG coherence and performance variables emerged after the intervention period likely because of the elimination of other factors that can influence performance. Before the initial steady cocontraction test, subjects were familiarized in two trials with the requirements of the task, including the production of unbalanced cocontraction with the target muscles and visuomotor coordination between their muscle activities and target lines on the monitor. Less prevalent positive correlations between performance variables and EMG coherence before the intervention period indicate the involvement of such other factors. Considerable improvements in performance (~30%) and marginal reductions in EMG coherence (6%) after the intervention period demonstrate that performance and EMG coherence do not change with corresponding magnitudes. This no correspondence also implies that factors not associated with EMG coherence may influence cocontraction performance. Before the intervention period, performance was low probably due to the involvement of continued familiarization and explorations of the novel task for understanding and satisfying the demanding requirements. A substantial improvement in performance ensued after the intervention period when the explorations were assumingly less. Nonsystematic variability of such familiarization and explorations as well as the consequent performance across subjects before the intervention can conceal the underlying correlations between performance variables and EMG coherence.

The degree of significant positive correlations between EMG coherence and performance variables was not uniform or high across muscle pairs ($r < 0.66$). It should be noted that, despite smoothing, AEMG used for providing visual feedback and assessing performance still has a large number of high-frequency components

(originating from the shape of motor unit spikes) that are not directly related to the control of muscle activation level. This study purposefully used such signals, so visual feedback responds to the activation changes intuitively without delay, which is not possible with substantial low-pass filtering. Hence, the limited degree of significant correlations is inevitable in this research design. Although the main focus was on low-frequency correlated oscillations in the current study, they cannot be the sole neural mechanism that determines the performance of steady cocontraction. For example, steady cocontraction performance is suggested to be associated with excitability of corticospinal neurons and Ia presynaptic inhibition (24, 42). It is possible that the contributions of listed and undefined other factors are variable depending on the task. Nonetheless, it is important to note that significant positive correlations between performance variables and EMG coherence were present in the muscle pairs (BR–TB and BB–BR) that were not specifically used in visual feedback or task requirements. This interesting finding ensures that the significant correlations were observed not because of using the same original signal sources (i.e., EMG) between the assessments of performance and the correlated neural oscillations but because of fundamental activation characteristics across muscle pairs.

In testing the second hypothesis of aim I, subjects in the Cocontraction group were expected to achieve greater acute reductions in EMG coherence and accompanying performance variables than other groups since they were the only group to practice out-of-phase cocontraction trials. This was not the case based on the absence of a significant interaction of time and group on EMG coherence and performance variables. The out-of-phase cocontraction practice was designed with the expectation of attenuating in-phase

low-frequency correlated oscillations by voluntarily tracking the target that required the repetition of out-of-phase low-frequency correlated oscillations between antagonistic muscles (Aim II section 3.3.2.1). Voluntary production of out-of-phase low-frequency correlated oscillations during the practice is confirmed by EMG phase around 160^{o} or -145^{o} in the antagonistic pairs in the Cocontraction group. Although EMG mean phase was somewhat deviated from the expected 180^{o} probably because of the difficulty of quickly alternating unbalanced cocontractions, the intervention goal of producing out-of-phase activation of antagonistic muscles was accomplished. The current findings with this practice are thus against the second hypothesis of the specific effect of out-of-phase cocontraction practice on sharp reductions in correlated neural oscillations and accompanying improvements of steady cocontraction performance. It is possible that the currently used conscious production of out-of-phase oscillations may not be able to influence the unconscious production of in-phase oscillations. In the literature, the acute effects of practice on steady cocontraction performance have only been tested in distinct protocols: steady cocontraction practice with leg muscles (24, 42). Hence, the current results are new essential findings that demonstrate the limited acute adaptability of (unconsciously produced) low-frequency correlated neural oscillations due to a bout of consciously produced out-of-phase oscillations via cocontraction practice at least in arm muscles.

One might think the invariant EMG coherence may imply the inability of the correlated oscillations for acute alterations. Indeed, low-frequency correlated oscillations during steady cocontraction are not altered acutely between leg agonist muscles, for example, because of neuromuscular fatigue (4). However, the low-frequency correlated

oscillations are acutely adaptable at least between the BB and the TB based on an acute increase in low-frequency correlated oscillations between the muscles due to neuromuscular fatigue (51). The invariant median frequency of raw EMG in the present study also eliminates the possible confounding effect of neuromuscular fatigue. Thus, the current results against the second hypothesis would rather imply the independence of in-phase common drive from the out-of-phase drive. It is possible that the balance of using descending pathways of in-phase common drive and out-of-phase drive depends on the task and is not easy to be altered with an acute bout of intervention. Nonetheless, it would be interesting to examine whether long-term training (e.g., practice several days per week for several weeks) with the out-of-phase cocontraction practice can modulate the low-frequency correlated oscillations during steady cocontraction.

3.2.6 Conclusions

The amount of in-phase low-frequency correlated neural oscillations between muscles was associated with the capability of healthy young adults for maintaining steady activation level during cocontraction of antagonistic muscles. The practice of enforcing out-of-phase low-frequency drive to antagonistic muscles did not specifically reduce the in-phase low-frequency correlated oscillations (as inferred from mean amplitude or mean phase coherence measures) or improve steady cocontraction performance acutely. These preliminary findings suggest that individuals with less correlated neural oscillations tend to perform steady cocontraction more skillfully, and the low-frequency correlated oscillations may not be acutely modulated by one bout of out-of-phase cocontraction

practice, as assessed by mean of phase coherence. The findings suggest that cocontraction should be evaluated not only for the amplitude of neural activity but also the coherence and phase of correlated oscillatory neural activity between cocontraction muscles. Aim-II, on the other hand, will address similar questions using the pdf distribution of phase coherence instead of mean phase coherence and clarify or even reverse the current conclusions.

3.3 Aim-II Modulation of neuromuscular oscillations through interventions.

This study was not able so far to uncover the role that intervention practice played, if any exist, in reducing correlated oscillations while possibly improving performance. On the other hand, for steady cocontraction, a relationship between correlated oscillations and performance was uncovered; however, it is not clear if such findings will extend to transient cocontractions. Therefore the main objectives of this aim are 1) to determine whether a bout of out-of-phase cocontraction practice reduces the in-phase low-frequency correlated neural oscillations in steady and transient unbalanced cocontraction of antagonistic muscles across individuals and 2) to determine whether there is an underlying association between the low-frequency correlated neural oscillations between muscles and the performance of transient static unbalanced cocontraction during practice across individuals. All analyses in this section used the EMG recordings obtained in experiment I.

3.3.1 In-phase synchrony during steady cocontraction

Phase coherence was investigated in aim-I using mean of event-related coherence. Alternatively, phase coherence was analysed using a different approach. For each time-frequency window, a probability distribution function was extracted then an in-phase metric that represents the probability density within phase 0 ± 5° was calculated (Figure 12). The in-phase coherence was used for the corresponding range (phase 0 ± 5°) to assess synchrony between muscles, together with amplitude coherence, in addition to evaluating the relationship between neural oscillations and output performances.

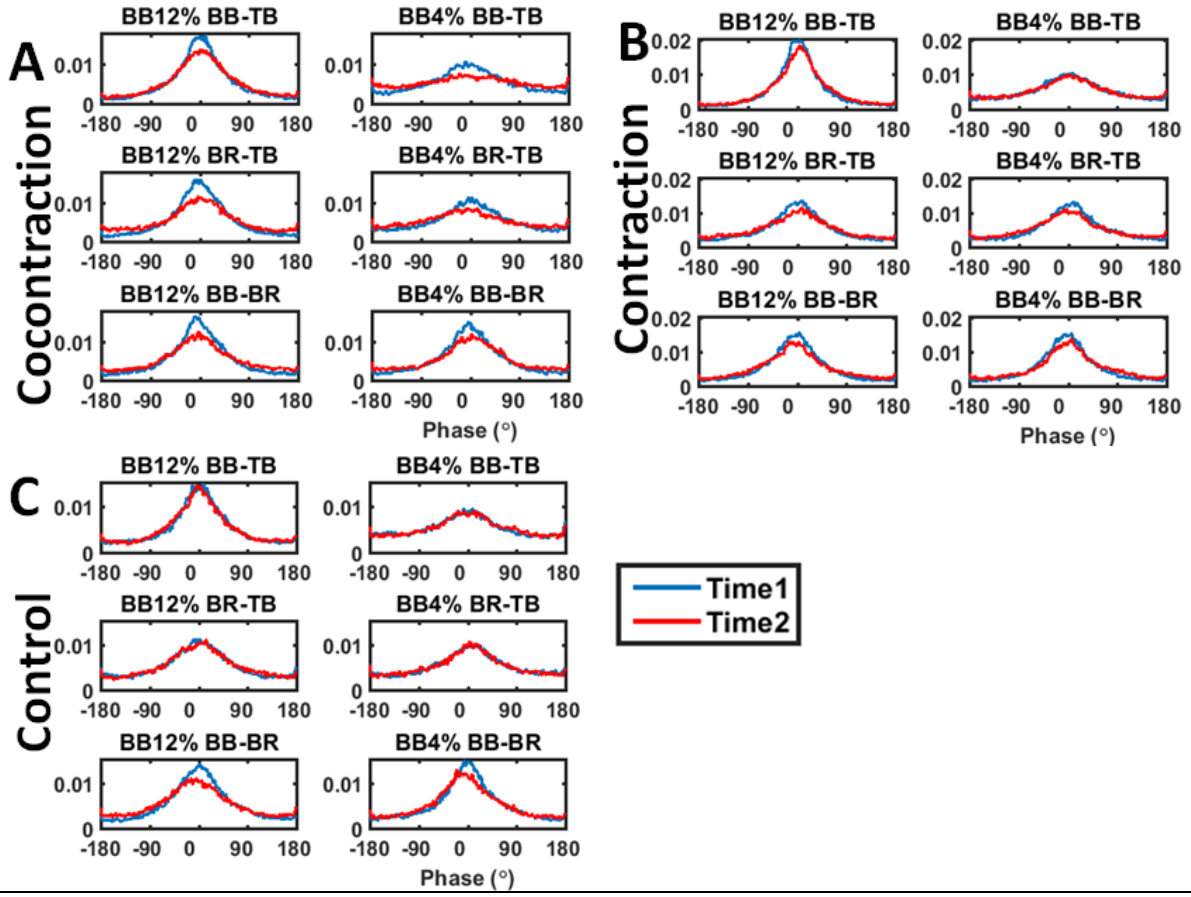

Figure 16 Phase pdf distribution for 3 test groups: A, Cocontraction, B, Contraction, C, Control, before vs. after intervention for both target level conditions. Column 1 and 2 correspond to target level 1 (BB HIGH, 12%) and target level 2 (BB LOW, 4%). Three rows for each muscle pairs (BB-TB, BR-TB, and BB-BR). Time1 (before intervention) vs. Time2 (after intervention).

The first application of in-phase measure was to investigate differences across three intervention groups in the in-phase coherence during steady cocontraction. Figure 16 illustrates phase coherence pdf for each group (cocontraction, contraction, control), target level (BB-HIGH, BB-LOW), muscle pair (BB-TB, BR-TB, and BB-BR), and time (before and after intervention) during the steady cocontraction. Figure 19 (top right) illustrates the in-phase coherence metric before and after the intervention period in each

muscle pair target level and group. Out of the three groups, Cocontraction had the most in-phase drop after the intervention. It is almost non-existent for the control group except for agonist muscles (Figure 16-C).

Difference in in-phase coherence between times (Δ in-phase coherence) was tested with repeated measures of a three-way ANOVA with factors being group, target level, and muscle pair. There was a main effect of group with a decrease of in-phase coherence by 16% on average across target levels, muscle pair, and groups (24% cocontraction, 14% contraction, and 8% control, $P < 0.001$, Table 4). Post hoc analysis confirmed that there is difference between Cocontraction and Control groups ($P < 0.0005$). No interaction was observed between factors. As a non-statistical observation, most of the drop in the Control group is in agonist muscle pair BB-BR (10% drop) while in-phase either increased or did not change for antagonist pairs (BB-TB or BR-TB). There was also a main effect of muscle pair ($P < 0.05$).

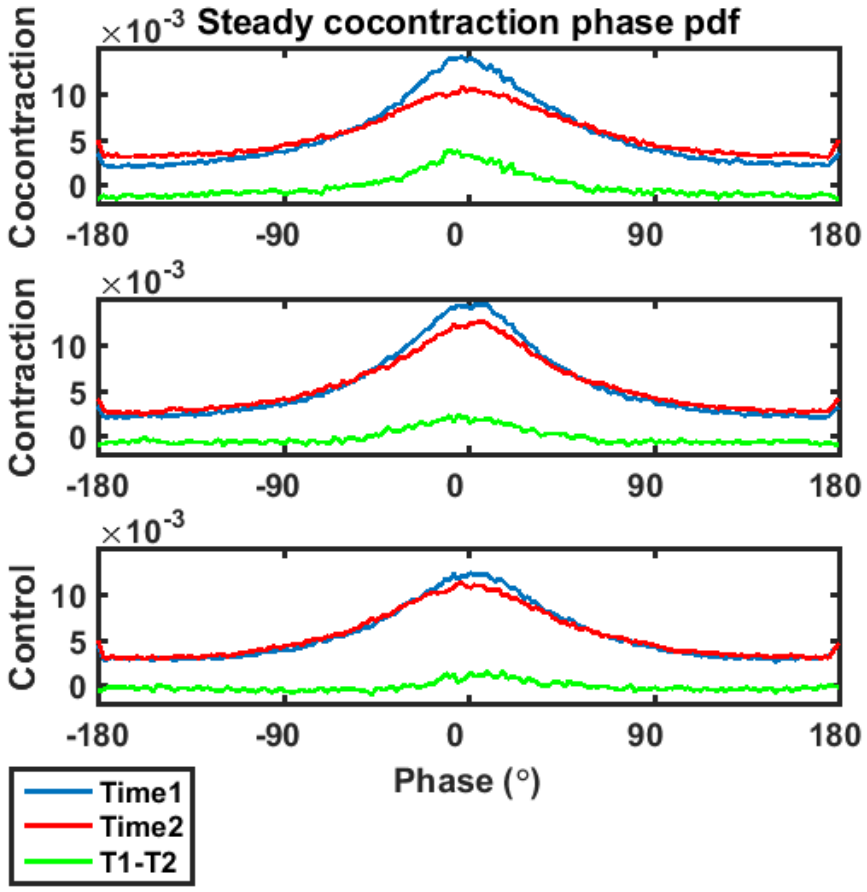

Figure 17 Phase pdf distribution during steady cocontraction for 3 test groups after collapsing target level and muscle pair: Cocontraction, Contraction, and Control, before (Time1) and after (Time2) the intervention and their difference (T1-T2).

Table 3 Amplitude and in-phase EMG coherence during <u>steady cocontraction</u> test in each group before and after the intervention period.

Group	Cocontraction		Contraction		Control		Average	
	Before	After	Before	After	Before	After	Before	After
Coherence	0.448 (0.066)	0.414 (0.044)	0.459 (0.068)	0.432 (0.066)	0.435 (0.058)	0.419 (0.043)	0.447 (0.065)	0.421* (0.053)
In-phase%	8.34 (3.46)	6.31 (2.35)	8.64 (3.49)	7.39 (3.44)	7.29 (2.93)	6.66 (2.78)	8.09 (3.29)	6.79** (2.86)
Correlation coefficient	0.780	0.637	0.794	0.834	0.718	0.648	0.764	0.706

Coherence, mean area of event-related amplitude coherence between muscles (same data as presented in Table 2); In-phase, corresponding percentage phase coherence between 0 ± 5°; Correlation coefficient between amplitude and in-phase coherences; Data across groups were pooled. Average, averaged data across groups; MVC, maximal voluntary contraction; *, *P* < 0.05; **, *P* < 0.01. Values are mean (standard deviation) across subjects.

Table 4 In-phase EMG coherence differences between times (before and after intervention during steady cocontraction test in each group.

Group	Cocontraction	Contraction	Control
Δ **In-phase%**	2.03	1.25	0.63**
	(1.70)	(1.54)	(1.51)

Δ In-phase, percentage of phase coherence differences between 0 ± 5°; Data across groups were pooled. **, *P* < 0.01 difference between Cocontraction and Control Groups (post hoc 3-way ANOVA analysis). Values are mean (standard deviation) across subjects.

The relationship between metrics of correlated oscillations and output performance (MSE and variance) were examined before and after the intervention period, using in-phase coherence (Figure 18-B) displayed side by side with amplitude coherence bar plots (Figure 18-A) when data were pooled across groups for comparison purposes between the two types of coherences. Note the overall similarity between the two figures although amplitude coherence case is a bit more significant than the in-phase coherence case (especially for BB-TB pair). Additionally, the correlation coefficients between the two metrics of correlated oscillations were illustrated for each muscle pair, target level, and group (Figure 19, bottom). Furthermore, the correlation coefficient between these metrics were computed before and after the intervention period, in which data were pooled across muscle pairs and target levels (Table 3, last row): After the intervention,

amplitude and in-phase coherence in cocontraction and Control groups became less correlated while in Contraction group, they became more correlated.

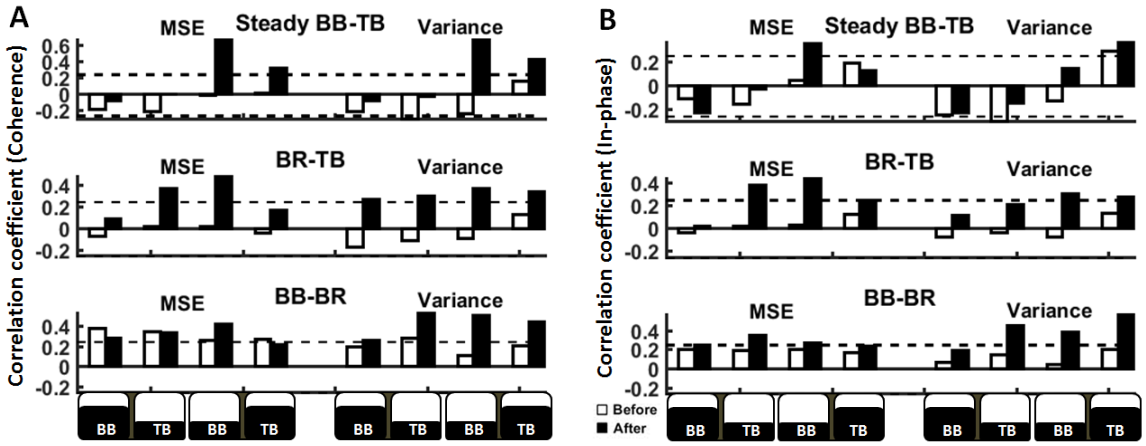

Figure 18 Correlation coefficient between performance variables (MSE and variance in the specified muscle on the x-axis) and A, EMG amplitude coherence (replicated from Figure 15) vs. B, EMG in-phase coherence. (Top: BB-TB pair, middle: BR-TB pair, bottom: BB-BR pair) before (open bars) and after (filled bars) the intervention period. On the x-axis, BB HIGH and TB LOW is one target pair, and BB LOW and TB HIGH is another target pair. Broken horizontal lines represent correlation coefficient at *P* = 0.05. LOW: 4%MVC target; HIGH: 12%MVC target; MSE, mean squared error.

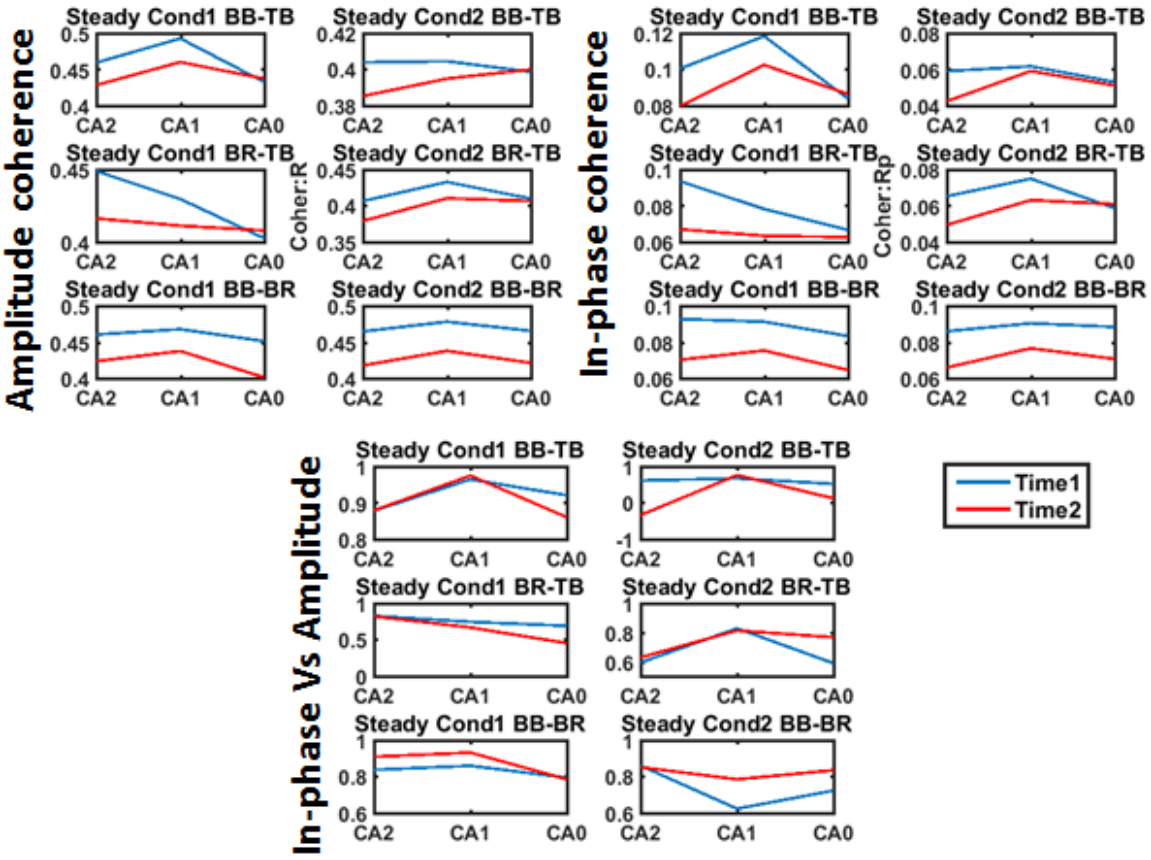

Figure 19 Amplitude vs. in-phase coherence comparison during steady cocontraction: Top left, amplitude coherence for cond1 (BB-HIGH) in column 1, and cond2 (TB-HIGH) in column 2. Three rows for muscle pairs (BB-TB, BR-TB, and BB-BR). On the x-axis, three groups, cocontraction (CA2), contraction (CA1), and control (CA0). Y-axis are measures of intermuscular coherence (between 0 and 1) comparison before vs. after intervention; Top right, in-phase coherence percentages (between 0 ± 5^{o}) for same 3 intervention groups, muscle pair, target level and times; Bottom, in-phase vs. amplitude correlation coefficient for same 3 intervention groups, muscle pairs, target levels, and times.

3.3.2 Intervention during static transient stage

A detailed analysis of the effect of transient and intervention in influencing the properties of correlated oscillations follows. During the intervention period for Co/Contraction groups, subjects practiced matching alternating targets. Trials consisted

of a reaching event (VL1), and a first varying level (VL2), followed by six varying level events (VL-rep) broken down into two classes, odd (VL-odd) and even (VL-even) segments depending on the target sequence (Figure 20). In the Cocontraction group, subjects produced concurrent our-of-phase activation of antagonistic muscles alternately across trials (3.3.2.1). In the Contraction group, subjects used the same alternating target template but were instructed to activate only the flexor (BB) or extensor (TB) at a time in each trial (3.3.2.2).

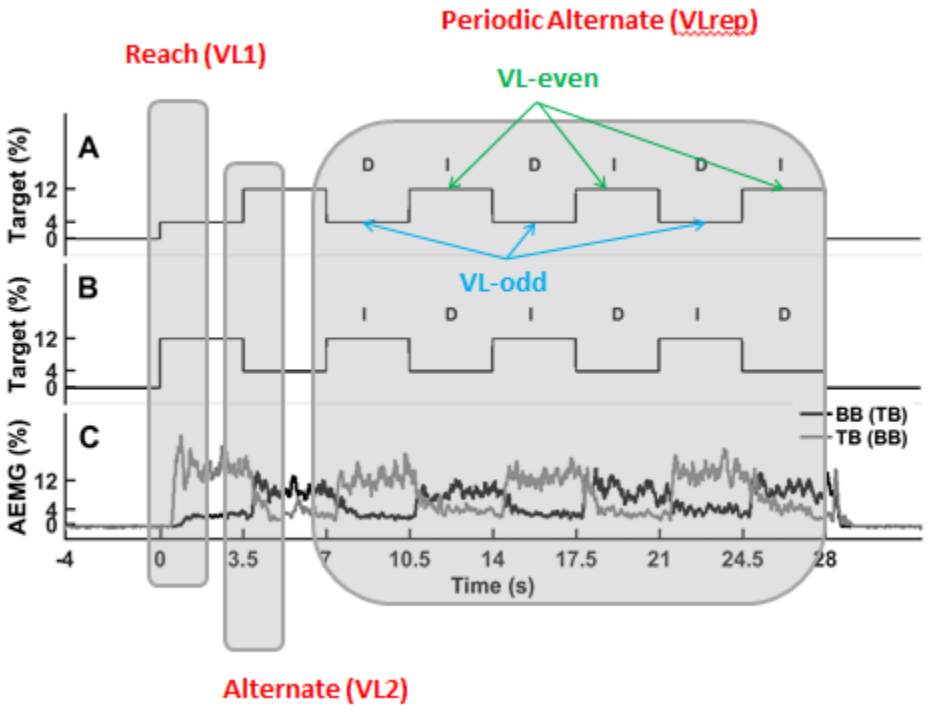

Figure 20 Trial events for both Co/Contraction groups: Reach (VL1), Alternate (VL2), Periodic alternate (VL-odd and VL-even). Varying level (VL).

3.3.2.1 Correlated oscillations during cocontraction practice (Cocontraction group).

In the Cocontraction group, subjects performed out-of-phase activation of antagonist muscles during the intervention period (Figure 20). Performance measures as well as EMG coherence and EMG phase < 3 Hz during the intervention were determined in each target sequence assignment, depending on BB targeting the D (Decreasing) or I (Increasing) segments in VL-rep in Figure 20. Within the practice trials, the first half (1^{st}-8^{th}) and second half (9^{th}-16^{th}) of the 16 trials for each target level were separately analyzed to examine the effect of practice time. The independent variables for ANOVA included segment (D and I), muscle (BB and TB), coherence muscle pair (BB-TB, BR-TB, and BB-BR), and time (first and second halves).

There was significant accuracy (MSE) main effect in the segment (7.13±7.98 for D segments vs. 15.23±12.22 for I segments, P<0.01), and time (reduced MSE with time, P<0.05, Table 5). There was also an interaction between muscle x segment (P<0.01). For variability (variance), the significant main effects were muscles (5.88±3.96 for BB vs. 8.27±6.20 for TB, P<0.01) and segment (5.32±4.28 for D segments vs. 8.84±5.88 for I segments, P<0.05). Effect of time was not significant (Table 5). Only interaction was between muscle x segment (P<0.01).

There was an interaction of muscle pair and segment on EMG coherence (P < 0.01). EMG coherence between the BB–TB pair was 0.426 ± 0.048 for D segments and 0.458 ± 0.057 for I segments. For the BR–TB pair, EMG coherence was 0.440 ± 0.055 for D segments and 0.467 ± 0.057 for I segments. For the agonistic BB–BR pair, EMG coherence was 0.561 ± 0.067 for D segments and 0.545 ± 0.063 for I segments. There was no significant effect of time (Table 5).

Table 5 Performance variables and EMG oscillations during <u>transient cocontraction</u> practice in ant/agonist groups for first and second half periods VL-even and VL-odd combined.

Muscles	BB-TB		BR-TB		BB-BR		Average	
	Time1	Time2	Time1	Time2	Time1	Time2	Time1	Time2
MSE %MVC	-	-	-	-	-	-	12.26 (11.06)	10.10* (9.15)
Variance %MVC	-	-	-	-	-	-	7.13 (5.23)	7.02 (4.94)
Coherence	0.425 (0.054)	0.435 (0.057)	0.433 (0.058)	0.443 (0.060)	0.551 (0.070)	0.541 (0.065)	0.470 (0.061)	0.473 (0.060)
In-phase %	5.81 (4.37)	5.33 (3.56)	5.64 (3.85)	4.94 (3.62)	16.3 (6.22)	15.1 (6.31)	8.45 (4.50)	8.85 (4.66)

MSE, mean squared error; Coherence, mean area of event-related amplitude coherence between muscles; In-phase, corresponding percentage phase coherence between 0 ± 5^o; Muscle pairs, BB-TB, BR-TB, and BB-BR; Average, averaged data across all muscles pairs; MVC, maximal voluntary contraction; Time 1, first half trials; Time 2, second half trials; *, $P < 0.05$; Values are mean (standard deviation) across subjects.

For in-phase coherence, the only significant main effect was coherence muscle pair (5.57±3.97 BB-TB, 5.29±3.74 BR-TB, 15.68±6.27 BB-BR; $P<0.01$). The others being time (Table 5) and segment were not significant. The only interaction was between segment x coherence muscle pair ($P<0.01$).

To examine if out-of-phase EMG oscillations were produced between antagonistic muscles, the deviation of the EMG phase from 180^o (i.e., complete anti-phase) was determined for the antagonistic pairs. In reference to TB, the deviation of EMG phase in BB–TB pair was 20.8^o ± 42.0 ^{o} for D segments for BB (i.e., I segments for TB) ($P < 0.01$ compared with 90^o) and -38.0^o ± 42.4^o for I segments for BB ($P < 0.01$ compared with -

90^o). Similarly, the deviation of EMG phase in the BR–TB pair was $22.7^o \pm 45.1^o$ for D segments for BR ($P < 0.01$ compared with 90^o) and $-34.5^o \pm 46.7^o$ for I segments for BR ($P < 0.01$ compared with -90^o). The positive and negative values indicate that BB and BR followed and preceded TB, respectively. These deviations from 180^o demonstrate that the average EMG phase between the antagonistic muscles was 159.2^o, -142.0^o, 157.3^o, and -147.5^o. In addition, the EMG phase between agonistic muscles was determined to examine if EMG oscillated in phase. In reference to BB, EMG phases in the agonistic BB–BR pair were different from 0^o but only slight deviations for both segments ($P < 0.01$): $0.047^o \pm 0.23^o$ for D segments for BB and $0.067^o \pm 0.22^o$ for I segments for BB. Alternatively, per pdf of phase coherence (Figure 21), data for VL-odd and VL-even are presented for each target level, muscle pair, and time during out-of-phase cocontraction practice. It is clear that out-of-phase trials are flattening in-phase coherence for antagonist muscles with no effect on agonist muscle pair (BB-BR). There was no statistical difference between the first and the last half of trials due to repetition as pointed out by one-way ANOVA comparing the effect of time after collapsing target levels and muscle pairs (P values >>0.05).

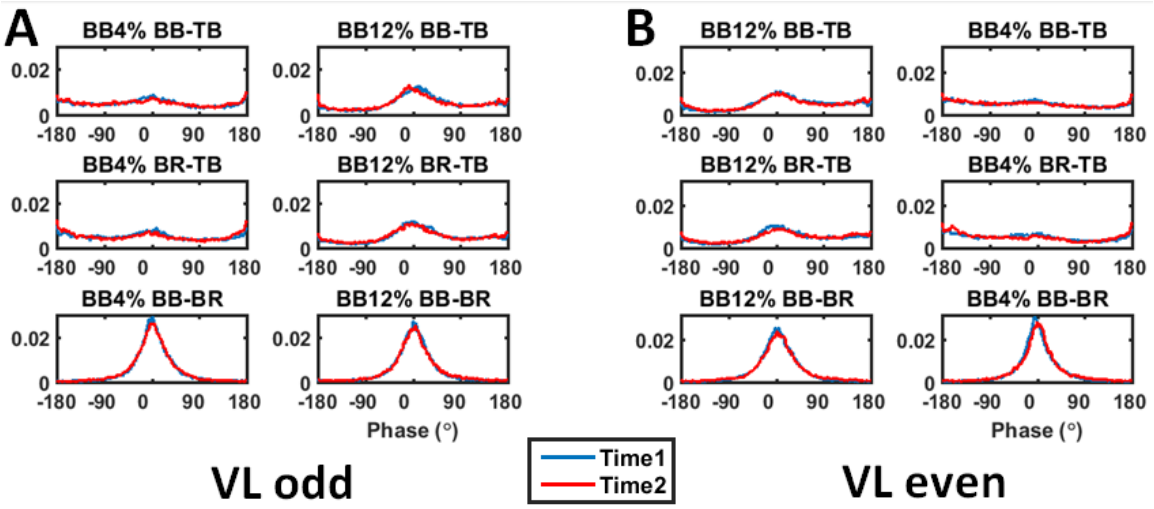

Figure 21 Pdf of phase coherence during cocontraction practice. A, VL-odd segment. Left column BB HIGH; Right column TB HIGH. From top to bottom rows: BB-TB, BR-TB, and BB-BR. B, same for VL-even.

Correlation coefficients between performance measures (MSE and variance) and amplitude coherence during the VL-odd and VL-even periods in the first and second halves of cocontraction practice trials are illustrated in Figure 22. It follows that subjects who had higher coherence at least in the BB-HIGH tend to have a higher error (across both varying levels and all three muscle pairs). It supports a linear relationship between the two. It implies that repetition of practice cocontraction task clarified such relationship. Such trends are present in four cases for MSE (33%) and 1 case for variance in VL-even. Treating cycle's statistics for each subject as different measures, to simulate more participants for VL-rep, 7 out of 12 cases became statistically significant for MSE (58%), and four out of 12 for variability (33%). However, such comparison mixes the intra-subject variability and inter-subject variability, and therefore does not substitute for running more subjects. It is rather an interesting observation that needs to be verified. On the other hand, note again that the correlation coefficients are below 0.7

due to the presence of multiple components and possible interference of action potentials. Such low correlation coefficients are common in physiological data.

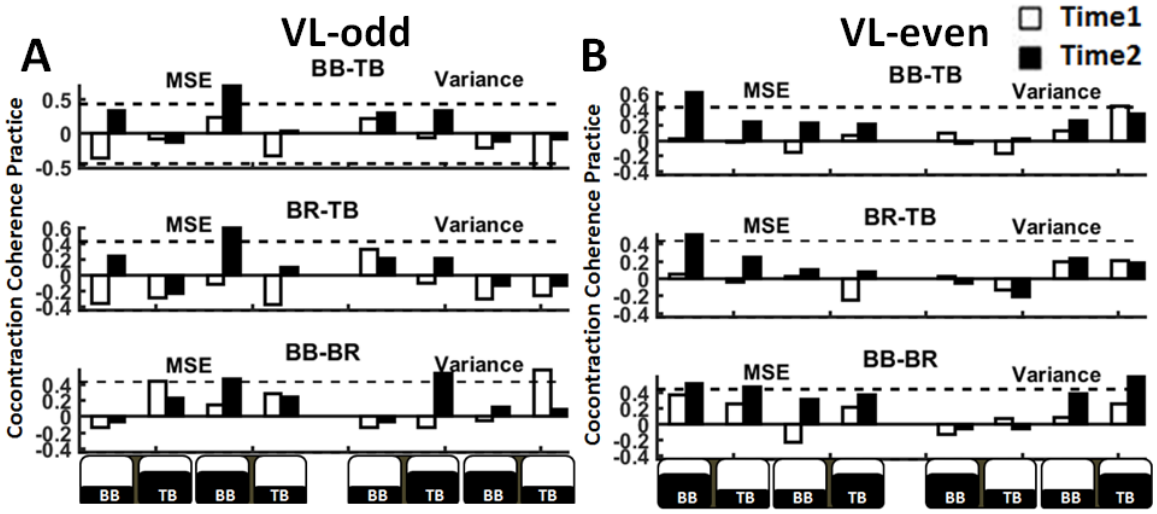

Figure 22 Correlation coefficients during transient alternating cocontraction practice for VL-odd (A) and VL-even (B). Association between performance variables (MSE and variance in the specified muscle on the x-axis) and EMG amplitude coherence (Top to bottom: BB-TB pair, BR-TB pair, and BB-BR pair) time1 (1st half) and time2 (2nd half) corresponds to 1st to 8th trials and 9th to 16th trials for each target level. On the x-axis, BB HIGH and TB LOW is one target pair, and BB LOW and TB HIGH is another target pair. Broken horizontal lines represent correlation coefficient at *P* = 0.05. LOW: 4%MVC target; HIGH: 12%MVC target; MSE, mean squared error.

3.3.2.2 Correlated oscillations during contraction practice (Contraction group).

Subjects in the Contraction group were instructed to activate only one agonist (BB or TB) at a time to match the alternating target (Figure 20) during the contraction practice in the intervention period. Measures of performance and correlated oscillations for the periodic alternate sequence (VL-rep) were obtained in the same manner as in the previous

section for Cocontraction group. The independent variables for ANOVA included active muscle (BB and TB), segment (D and I), coherence muscle pair (BB-TB, BR-TB, and BB-BR), time (first and second halves).

There was significant accuracy (MSE) main effect in segment (3.74±2.85 for D segments vs. 8.13±7.00 for I segments, $P<0.01$). No time or muscle effect was found for accuracy performance measure. As for variability (variance), there was no main effect of time, active muscle, or segment. Table 6 displays results for performance measures averaged across time.

Table 6 Performance variables and EMG oscillations across times during transient contraction practice in ant/agonist muscles for VL-even and VL-odd combined.

Muscles	BB-TB	BR-TB	BB-BR	Average
MSE	-	-	-	5.93
%MVC				(4.92)
Variance	-	-	-	4.40
%MVC				(2.76)
Coherence	0.633	0.577	0.611	0.607
BB active	(0.085)	(0.082)	(0.059)	(0.076)
Coherence	0.540	0.546	0.559	0.548
TB active	(0.070)	(0.065)	(0.093)	(0.076)
In-phase %	15.85	12.59	13.08	13.84
BB active	(7.19)	(5.79)	(5.23)	(6.07)
In-phase %	9.22	9.39	9.56	9.40
TB active	(5.20)	(4.45)	(5.85)	(5.17)

MSE, mean squared error; Coherence, mean area of event-related amplitude coherence between muscles (either BB or TB active); In-phase, corresponding percentage phase coherence between 0 ± 5^{o} (either BB or TB active); Muscle pairs, BB-TB, BR-TB, and BB-BR; Average, averaged data across muscle pairs; MVC, maximal voluntary contraction; Values are mean (standard deviation) across subjects.

For amplitude coherence, there was a main effect of active muscle (0.608±0.0715 BB active, 0.551±0.080 TB active; $P<0.01$). Also, there was an interaction between active muscle and coherence muscle pair ($P<0.01$).

For in-phase coherence, the only significant main effect was active muscle (13.65±5.86 BB active, 9.43±5.34 TB active; $P<0.01$). The effects of time, segment, and coherence muscle pair were all non-significant. The only interaction was between muscle active and coherence muscle pair ($P<0.01$).

As for the correlation between coherence and measures of performance across time, no statistically significant results were found.

When amplitude coherence values were numerically compared for average values without statistical comparisons, it was higher during contraction (Table 6) than cocontraction (Table 5) by around 18%. BB active amplitude coherence was 10% higher compared to TB active. It is 45% higher as well for in-phase coherence. Another observation was that the coherence values were comparable between the agonist and antagonist muscles as opposed to the cocontraction cases where the agonist muscle coherence is usually higher than that of the antagonist muscles.

Regarding phase coherence, Figure 23 illustrates pdf for the VL-odd / VL-even segments collapsed across target level and muscle pair. The main difference between TB-active and BB-active phase coherence was that the former in-phase was lower ($P < 0.05$). On the other hand, distributions were similar for the first half of trials compared to the last half. There was no in-phase coherence effect of time.

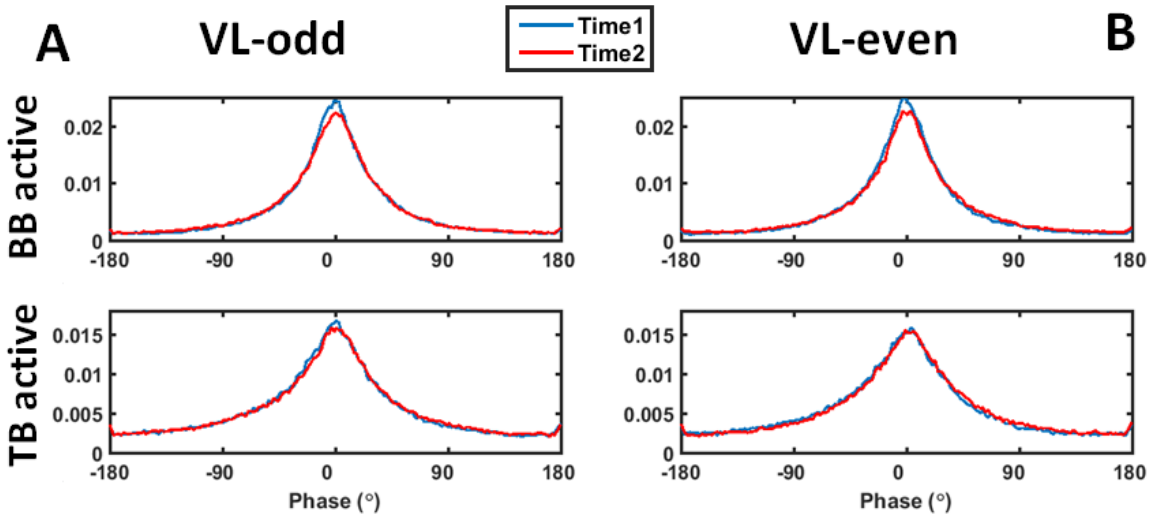

Figure 23 Pdf of phase coherence during contraction practice averaged across target level and muscle pair. A, VL-odd, BB active (TB idle) on top; TB active (BB idle) bottom plot. Panel B, the same for VL-even.

3.3.2.3 Correlated oscillations during steady contractions

In addition to the steady cocontraction test and the intervention, each subject performed three trials of steady contraction per each muscle (BB or TB) throughout the experiment (before and after test 1, then after test 2) in all groups. These trials were analyzed to extract amplitude and in-phase coherences during steady single muscle activations. Independent variables for ANOVA included time (before and after intervention), active muscle (BB and TB), and group (Cocontraction, Contraction, Control).

For in-phase coherence, there was a 7% drop with time (6.05±2.22 before vs. 5.63±2.04 after, $P<0.05$). Also, the in-phase coherence of TB active (Figure 24) was lower by 21% compared to BB active (6.54±2.39 BB active vs. 5.14±1.87 TB active,

P<0.05, Table 7). There was no group effect. For amplitude coherence, there was no significant main effect of time, group, or active muscle.

Table 7 Amplitude and in-phase EMG oscillations during <u>steady contraction</u> in each group averaged across time.

Group	Cocontraction	Contraction	Control	Average
Coherence BB active	0.71 (0.032)	0.70 (0.039)	0.69 (0.042)	0.70 (0.038)
Coherence TB active	0.69 (0.044)	0.69 (0.028)	0.69 (0.028)	0.69 (0.034)
In-phase% BB active	7.08 (2.36)	6.98 (3.06)	5.57 (1.75)	6.54 (2.39)
In-phase% TB active	4.83 (1.55)	5.31 (1.88)	5.27 (2.19)	5.14 (1.87)

Coherence, mean area of event-related amplitude coherence between muscles; In-phase, corresponding percentage phase coherence between 0 ± 5^{o}; Two target level conditions for the type of coherence, either BB or TB active; Average, averaged data across groups; MVC, maximal voluntary contraction; Values are mean (standard deviation) across subjects.

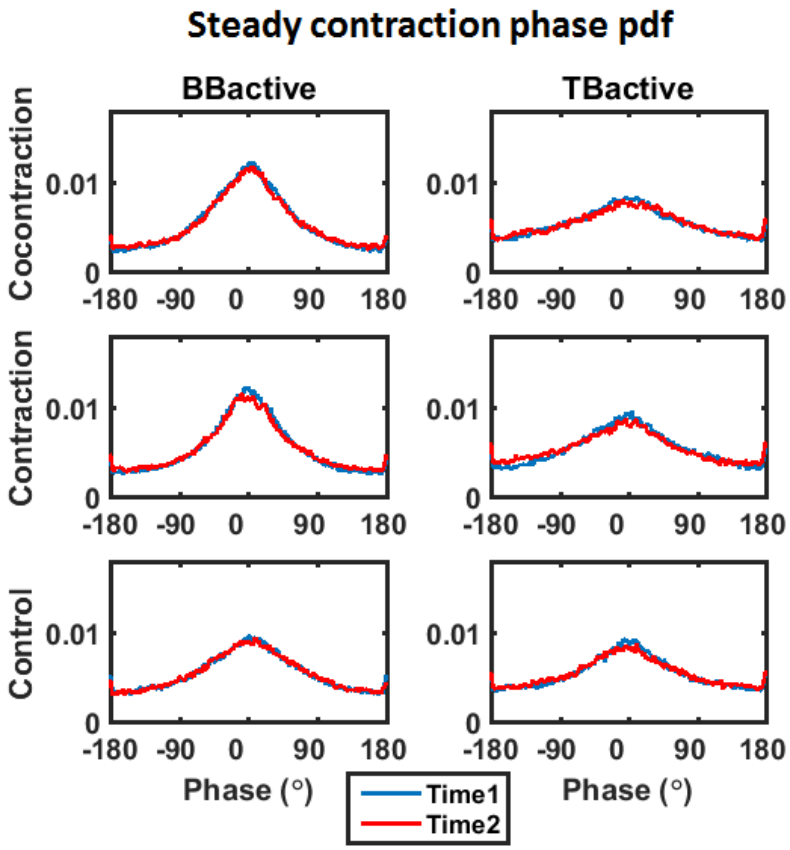

Figure 24 Pdf of phase coherence during steady contraction for all 3 groups: Left, BB is active (TB is idle): From top to bottom rows: Cocontraction, Contraction, and Control groups. The right column is the same when TB is active (BB is idle).

3.3.2.4 Correlated oscillations and performance during transient cocontraction test (VL1, VL2)

All subjects completed Cocontraction tests before and after intervention. The first part of each trial (transient) consisted of reaching target (VL1), followed by an alternation of target activation level (VL2). Various characteristics of this transient period were analyzed.

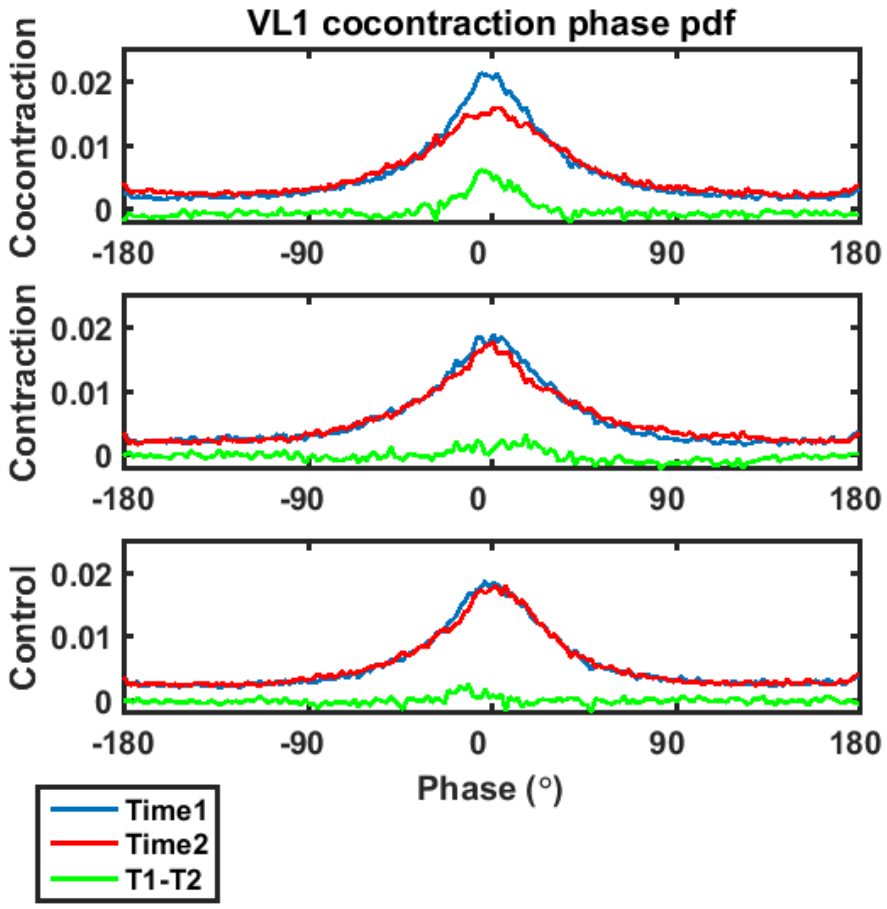

Figure 25 Phase pdf distribution during VL1 cocontraction for 3 test groups after collapsing target level and muscle pair: Cocontraction, Contraction, and Control, before (Time1) and after (Time2) the intervention and their difference (T1-T2).

For VL1, in-phase coherence decreased by 26%, 7%, and 5% for Cocontraction, Contraction and Control groups respectively (Table 8, Figure 25) with group main effect ($P < 0.005$). In-phase coherence for VL2 decreased after intervention (Table 9, Figure 26) for Cocontraction (by 29%), Contraction (by 19%), and Control (by 12% mainly in agonist muscles). There was a main effect of group ($P < 0.05$).

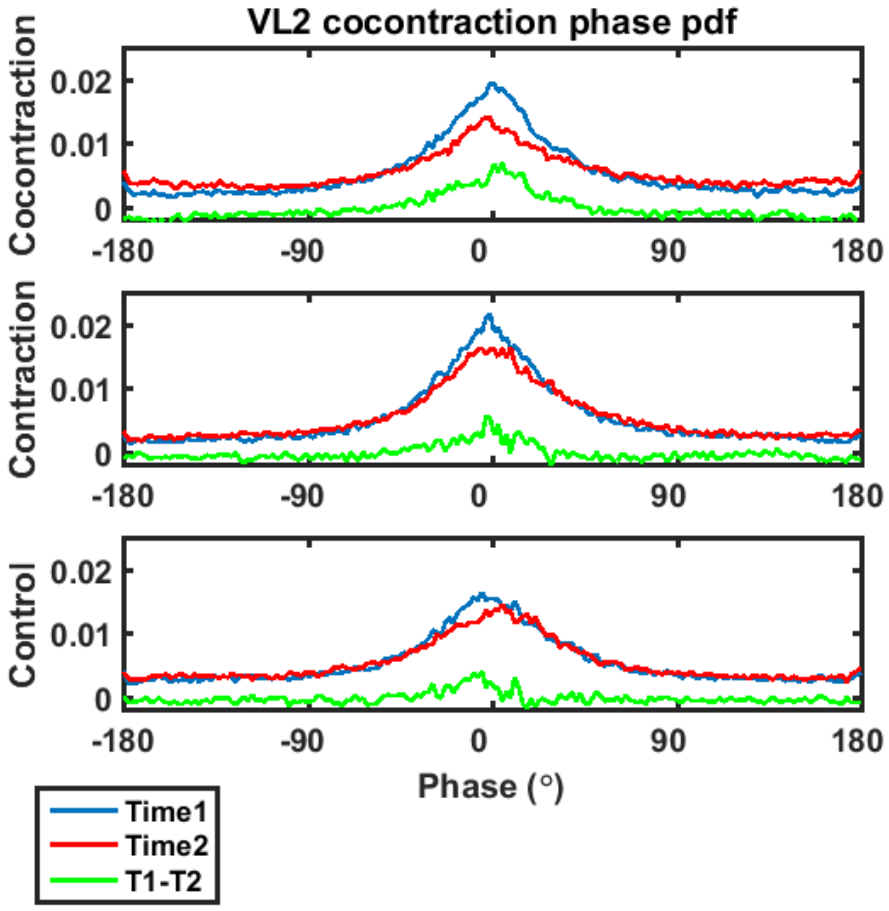

Figure 26 Phase pdf distribution during VL2 cocontraction for 3 test groups after collapsing target level and muscle pair: Cocontraction, Contraction, and Control, before (Time1) and after (Time2) the intervention and their difference (T1-T2).

Overall, there was little to no significant correlated oscillations effect in amplitude coherence during the initial stage of reaching the target (VL1) and adjusting after the first alternation (VL2). In the beginning of each trial, subjects were not accustomed to the fast changing target level yet; they were still trying to adjust. Both a positive and negative correlation coefficients were observed during these stages that were non-significant for the majority of cases (Figure 27) with a trend toward negative association between amplitude coherence and performance metrics. On the other hand, Figure 29 illustrates

the correlation coefficient between performance measures and correlated oscillations for BB-TB pair during VL2 using FFT stimulus-locked, FFT response-locked, and wavelet stimulus-locked processing. All these variations revealed similar relationships.

EMG amplitude coherences were tested with a four-way ANOVA with factors being time, muscle pair (BB-TB, BR-TB, and BB-BR), target level, and group with repeated measures. For VL1 (Table 10), there was a main effect in amplitude coherence for target level and muscle pair ($P < 0.001$), and group (Cocontraction: 0.519 ± 0.119, Contraction: 0.493 ± 0.121, Control: 0.514 ± 0.13, $P < 0.01$). There was also interaction in target level x muscle pair ($P < 0.001$), and time x muscle pair ($P < 0.05$). For VL2 (Table 11), there was an amplitude coherence main effect in muscle pair ($P < 0.001$), and time (coherence decreased by 2%, $P < 0.05$). Interaction was found in time x muscle pair ($P < 0.001$), and target level x muscle pair ($P < 0.01$).

Δ in-phase coherences were tested with a three-way ANOVA with factors being muscle pair (BB-TB, BR-TB, and BB-BR), target level, and group with repeated measures. Δ in-phase coherence for VL1 (Table 8) had a group main effect ($P < 0.005$). Post hoc analysis results showed that Cocontraction group was different from both Contraction group ($P < 0.05$) and Control group ($P < 0.01$). The only interaction was between target level and group ($P < 0.05$). As for VL2 (Table 9), a group main effect was found ($P < 0.05$). Post hoc analysis revealed that Cocontraction group was different from Control group ($P < 0.05$). There was no interaction found.

Table 8 In-phase EMG coherence differences between times (before and after intervention during VL1 test in each group.

Group	Cocontraction	Contraction	Control
Δ **In-phase%**	3.23	0.81*	0.50**
	(4.78)	(2.47)	(2.81)

Δ In-phase, percentage of phase coherence differences between 0 ± 5°; Data across groups were pooled. *, *P* < 0.05 difference between Cocontraction and Contraction Groups; **, *P* < 0.01 difference between Cocontraction and Control Groups (post hoc 3-way ANOVA analysis). Values are mean (standard deviation) across subjects.

Table 9 In-phase EMG coherence differences between times (before and after intervention during VL2 test in each group.

Group	Cocontraction	Contraction	Control
Δ **In-phase%**	3.24	2.24	1.13*
	(3.33)	(2.71)	(2.24)

Δ In-phase, percentage of phase coherence differences between 0 ± 5°; Data across groups were pooled. *, *P* < 0.05 difference between Cocontraction and Control Groups (post hoc 3-way ANOVA analysis). Values are mean (standard deviation) across subjects.

Performance measures

The independent variables for ANOVA included muscle (BB and TB), target level (BB-HIGH and BB-LOW), time (before and after intervention), and group (Cocontraction, Contraction, Control). For VL1 (Table 10), in the assessment of accuracy, there was a main effect of time (MSE of AEMG decreased by 29%, $P < 0.001$), target level, and muscles ($P < 0.001$). The only interaction was between target level and muscle ($P < 0.001$). In the assessment of variability, there was a main effect of time (variance of AEMG increased by 20% $P < 0.01$), muscle ($P < 0.01$), and target level ($P < 0.05$). Interaction target level x muscle ($P < 0.001$); time x muscle ($P < 0.05$); group x muscle ($P < 0.05$).

For VL2 (Table 11), in the assessment of accuracy, there was a main effect of time (MSE of AEMG decreased by 40%, $P < 0.001$) and group (Cocontraction: 20 ± 18, Contraction: 27 ± 20, Control: 26 ± 18, $P < 0.001$). Only interaction was between target level and muscle ($P < 0.001$). In the assessment of variability, main effect was found in group (Cocontraction: 10 ± 7, Contraction: 12 ± 9, Control: 12 ± 8, $P < 0.001$), and target level ($P < 0.05$). Only interaction for variance was between target level and muscle ($P < 0.05$).

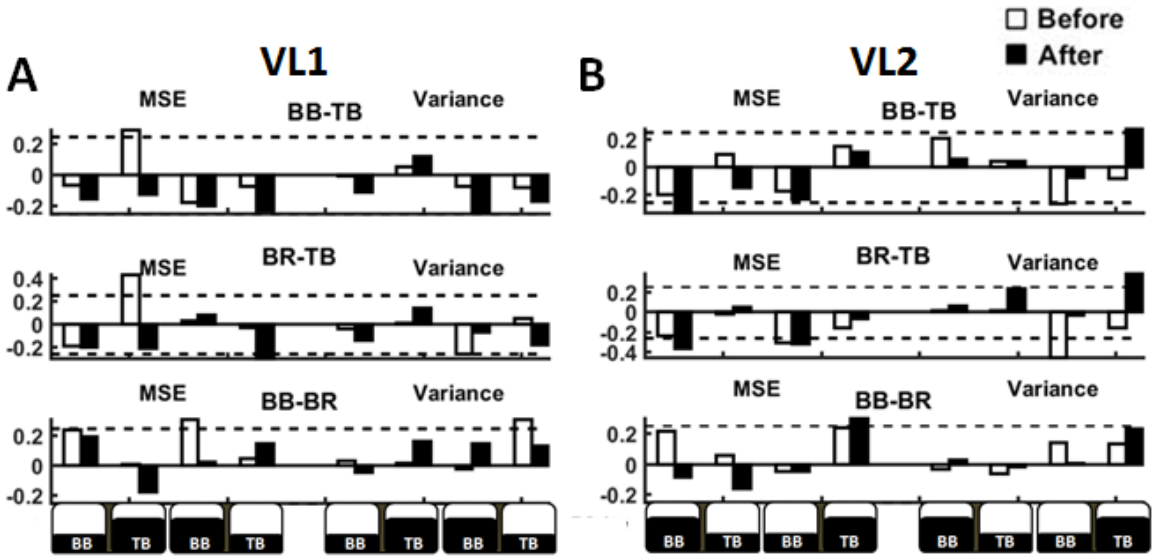

Figure 27 Correlation coefficient between performance variables (MSE and variance) and EMG coherence (BB-TB, BR-TB, and BB-BR pairs) before (open bars) and after (filled bars) the intervention period for VL1 (A) and VL2 (B). On the x-axis, BB HIGH and TB LOW is one target pair, and BB LOW and TB HIGH is another target pair. Broken horizontal lines represent correlation coefficient at $P = 0.05$. LOW: 4%MVC target; HIGH: 12%MVC target; MSE, mean squared error.

Table 10 and Table 11 summarize mean square error, variance, power, amplitude coherence, and in-phase coherence for the three groups (Cocontraction, Contraction, and Control) before and after practice during the cocontraction test for both VL1 and VL2.

Reach, alternate, and maintain are three classes of activities during cocontraction test and practice that have different requirements of muscle activations with potentially different strategies associated with them across groups. So far, performance measures were compared to correlated oscillations only during the same type of activation (example performance during VL1 to correlated oscillations during VL1). Alternatively, activation of different types could be compared to each other. Performance measures during transient varying levels (VL1: reach and VL2: alternate) were compared to correlated oscillations during the steady test. However, no significant correlations were found.

Table 10 Performance variables and EMG oscillations during <u>VL1 cocontraction</u> test in each group before and after the intervention period.

Group	**Cocontraction**		**Contraction**		**Control**		**Average**	
	Before	**After**	**Before**	**After**	**Before**	**After**	**Before**	**After**
MSE %MVC	30.62 (28.06)	19.30 (19.70)	33.30 (28.58)	23.60 (21.69)	31.34 (26.62)	24.66 (20.57)	31.75 (27.67)	22.52** (20.71)
Variance %MVC	10.16 (9.45)	13.45 (13.24)	10.92 (9.01)	12.75 (10.68)	11.04 (11.63)	12.36 (11.72)	10.71 (10.06)	12.85** (11.89)
Power	16.47 (7.55)	15.43 (6.86)	18.40 (7.23)	17.02 (5.54)	17.58 (7.66)	17.61 (7.60)	17.48 (7.50)	16.68 (6.77)
Coherence	0.534 (0.132)	0.503 (0.105)	0.508 (0.130)	0.479 (0.111)	0.521 (0.134)	0.508 (0.125)	0.521 (0.132)	0.497** (0.114)
In-phase %	12.55 (5.13)	9.32 (2.90)	10.92 (2.82)	10.10 (2.37)	10.90 (2.88)	10.41 (2.69)	11.45 (3.61)	9.94** (2.65)

MSE, mean squared error; Power, mean area of event-related spectral perturbation; Coherence, mean area of event-related amplitude coherence between muscles; Phase, corresponding phase coherence; Average, averaged data across groups; MVC, maximal voluntary contraction; *, $P < 0.05$; **, $P < 0.01$. Values are mean (standard deviation) across subjects.

Table 11 Performance variables and EMG oscillations during VL2 cocontraction test in each group before and after the intervention period.

Group	Cocontraction		Contraction		Control		Average	
	Before	**After**	**Before**	**After**	**Before**	**After**	**Before**	**After**
MSE %MVC	26.76 (25.60)	12.38 (10.69)	32.64 (22.75)	20.96 (16.28)	30.77 (21.19)	20.40 (13.83)	30.06 (23.28)	17.92** (14.28)
Variance %MVC	10.69 (7.52)	9.64 (5.58)	12.14 (9.76)	11.42 (7.67)	11.64 (8.17)	11.46 (8.82)	11.49 (8.52)	10.84 (7.49)
Power	23.42 (7.38)	20.30 (6.95)	24.14 (6.79)	21.71 (6.51)	22.62 (6.73)	22.40 (6.61)	23.39 (6.98)	21.47** (6.73)
Coherence	0.518 (0.101)	0.502 (0.074)	0.514 (0.110)	0.503 (0.088)	0.506 (0.101)	0.503 (0.096)	0.512 (0.104)	0.502* (0.086)
In-phase %	11.18 (4.46)	7.94 (2.00)	11.88 (2.50)	9.64 (2.05)	9.31 (2.69)	8.17 (2.49)	10.79 (3.22)	8.58** (2.18)

MSE, mean squared error; Power, mean area of event-related spectral perturbation; Coherence, mean area of event-related amplitude coherence between muscles; Phase, corresponding phase coherence; Average, averaged data across groups; MVC, maximal voluntary contraction; *, $P < 0.05$; **, $P < 0.01$. Values are mean (standard deviation) across subjects.

Error vs. variability trade-off during transient varying level

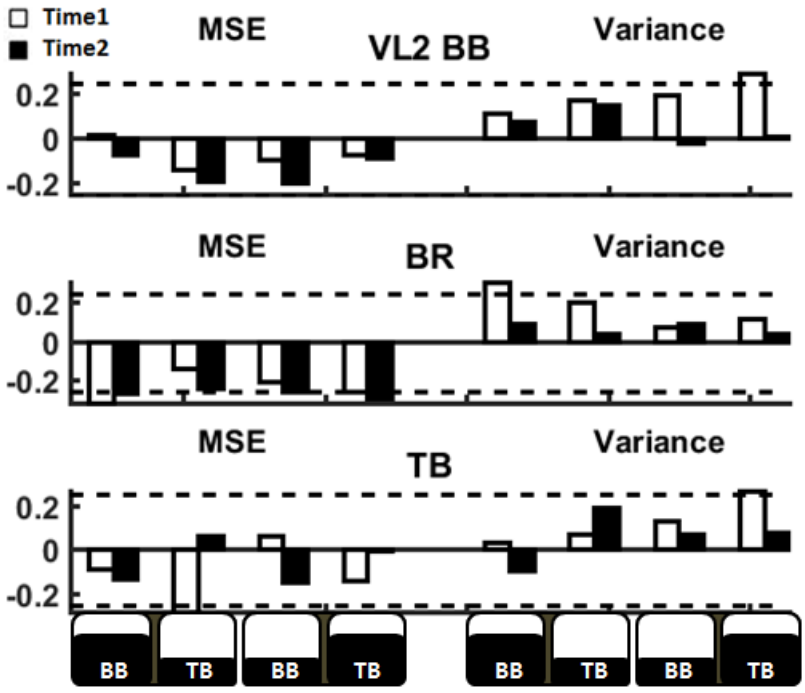

Figure 28. Correlation coefficient between performance and Inter-trial coherence (phase locking) across trials for VL2. Top to bottom (BB, BR, and TB)
On the x-axis, BB HIGH and TB LOW is one target pair, and BB LOW and TB HIGH is another target pair. Broken horizontal lines represent correlation coefficient at *P* = 0.05. LOW: 4%MVC target; HIGH: 12%MVC target; MSE, mean squared error.

Inter-trial coherence vs. error (MSE) during VL2 was mostly negative (Figure 28), i.e., the more consistent the trials were (phase locked), the smaller the error. On the other hand, inter-trial coherence vs. variability (VAR) during VL2 is mostly positive. I.e., the more trials were consistent (phase locked) among each other, the higher the variability was. In other words, subjects were concentrating on one objective above the other during VL2. Additionally, variance stats became inferior in time 2 compared to time 1 during VL2 (mainly, except Control group, whose error decreased the least possibly due to the lack of practice session, confirming the above). During VL1, variance increased in time 2

throughout. Overall, variance performance is of less significance in VL1 & VL2 second session.

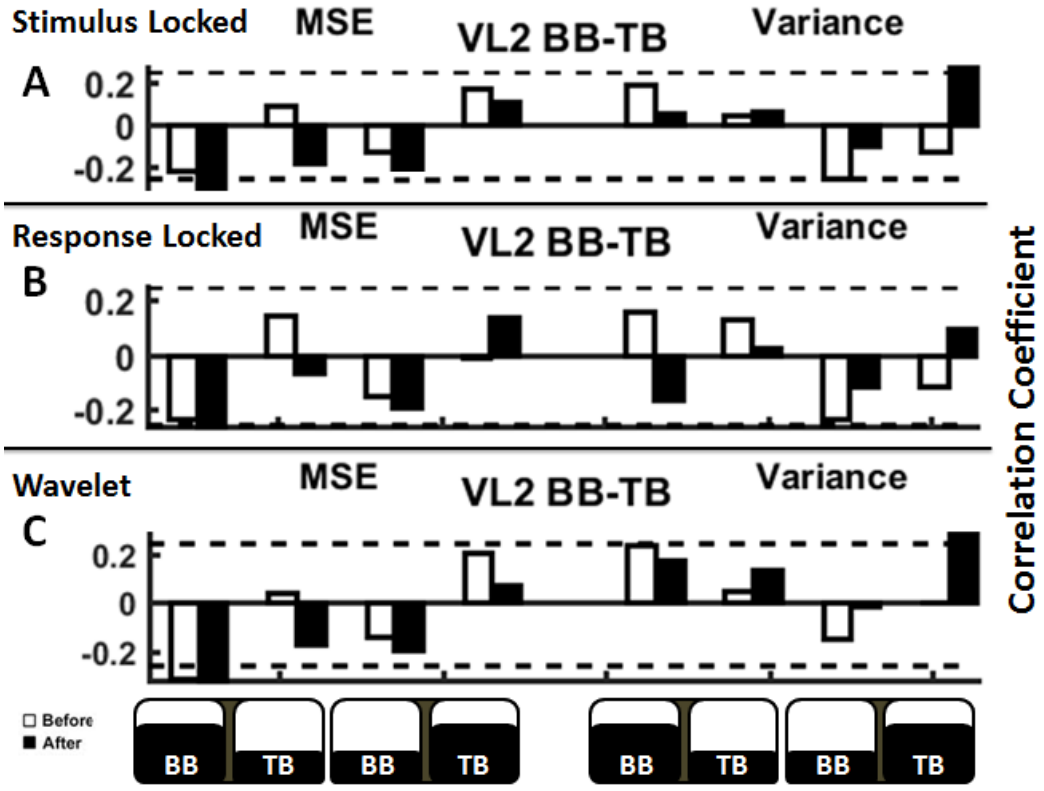

Figure 29 Correlation coefficient comparison between stimulus-locked, response-locked, and wavelet for VL2 BB-TB amplitude muscle pair during the cocontraction test: A, Stimulus-locked (based on FFT); B, Response-locked (based on FFT); C, Stimulus-locked (based on wavelet). On the x-axis, BB HIGH and TB LOW is one target pair, and BB LOW and TB HIGH is another target pair. Broken horizontal lines represent correlation coefficient at *P* = 0.05. LOW: 4%MVC target; HIGH: 12%MVC target; MSE, mean squared error.

This observation of subjects prioritizing one objective over another when the task is challenging was common to cocontraction practice as well. As Figure 22-B illustrates, it

is more likely that either error or variability is significantly related to correlated oscillations but not both.

3.3.3 Involuntary activation of idle muscles during contraction tasks

During contraction tasks (steady or practice), subjects were asked to match given target using single muscle (BB or TB). Instructions did ask subjects to ignore other muscle but did not ask them to still it. Subjects were, however, activating the supposedly idle muscle involuntarily at different inhibition levels. During steady contraction BB-HIGH task, subjects were involuntarily cocontracting their TB muscle (~4% MVC on average) concurrently as they voluntarily activated the BB target muscle (Figure 30-A). On the other hand, when TB-HIGH was the active target, BB was relatively still (~1 %MVC on average); BR was also still with some residue of involuntary activation (~1 %MVC on average). These results were observed during practice intervention as well (Figure 30, C&D, see TB 0% and BB 0% panels). However, the implications for practice are not as straightforward to interpret as in the steady case. During the fast-changing activation level for both muscles during the cocontraction test, the target would either be at HIGH BB or coming for a HIGH BB (same apply for TB). Dissociating the two actions is not obvious. In other words, applying the same logic to Figure 22 is not as straightforward.

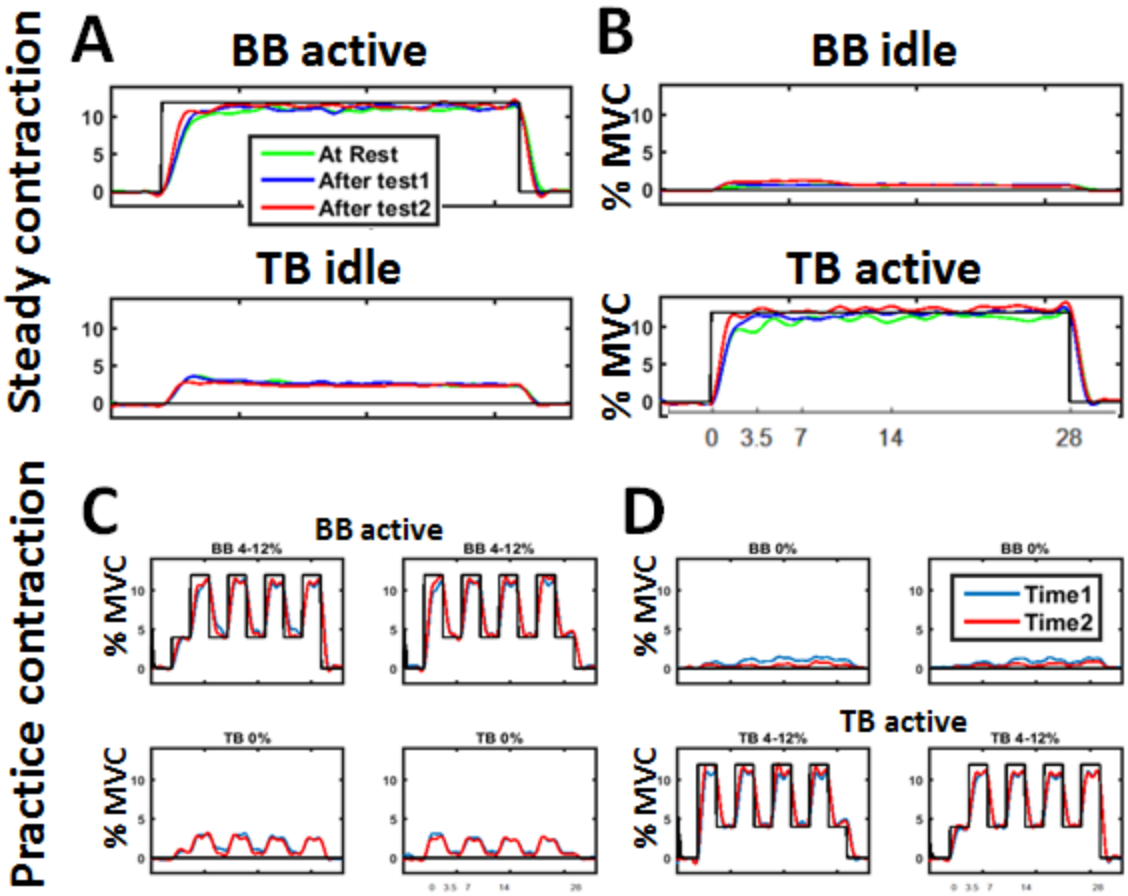

Figure 30 Time series of AEMG during contraction. Steady contraction: A, BB active (12% MVC), TB idle (0% MVC) targets with their corresponding muscle voluntary and involuntary activations; B, BB idle (0% MVC), TB active (12% MVC). Three traces: At rest (before test 1), after test 1, and after test 2. Practice contraction: C, BB active (4-12% MVC) target and idle TB (0% MVC) with their corresponding muscle voluntary and involuntary activations; D, TB active (4-12% MVC) target and idle BB (0% MVC). Visual feedback of target or AEMG was not proved for TB 0% or BB 0% during the task.

3.3.4 Correlation between oscillations and performance revisited

In Aim-1, data during steady cocontraction were analyzed. Since all three groups improved their performance while lowering their coherence in the absence of significant

interaction of group and time in, they were grouped, and linear relationships were assessed for the pooled data. Alternatively, linear relationships were examined for each group individually here.

The coefficient of correlation between amplitude coherence vs. performance variables (MSE, variance) in each group is presented for each muscle pair, target, and time (Figure 31). Cocontraction group (Figure 31-I2) had only two significant cases after intervention (variance when BB-LOW for both antagonist pairs: BB-TB, BR-TB). Contraction group (Figure 31-I1) had 15 out of 24 significant cases in time 2, similar to all groups combined (Figure 31-Ix). The Control group (Figure 31-I0) had four significant cases in BB-TB pair (BB-LOW, TB-HIGH) after the intervention.

A similar analysis for in-phase coherence vs. performance variables is presented in Figure 33. Cocontraction group (Figure 33-I2) had only one case that is significant after intervention (variance in BB-TB when BB-LOW), and it was negatively related (higher in-phase coherence corresponds to lower variance). Contraction group (Figure 33-I1) again had 15 (out of 24) significant cases after the intervention, similar to all three groups combined (Figure 33-Ix). The Control group (Figure 33-I0) had four significant cases in BB-TB pair (BB-HIGH, TB-LOW) after the intervention, and they were all negatively related (higher in-phase coherence corresponds to lower variance).

In both cases (i.e., correlation with amplitude coherence in Figure 31 and with phase coherence in Figure 33), the presence of linear correlation in Contraction group uniquely resembled the net addition of all three groups. In other words, the significant linear relationship may be driven by Contraction group.

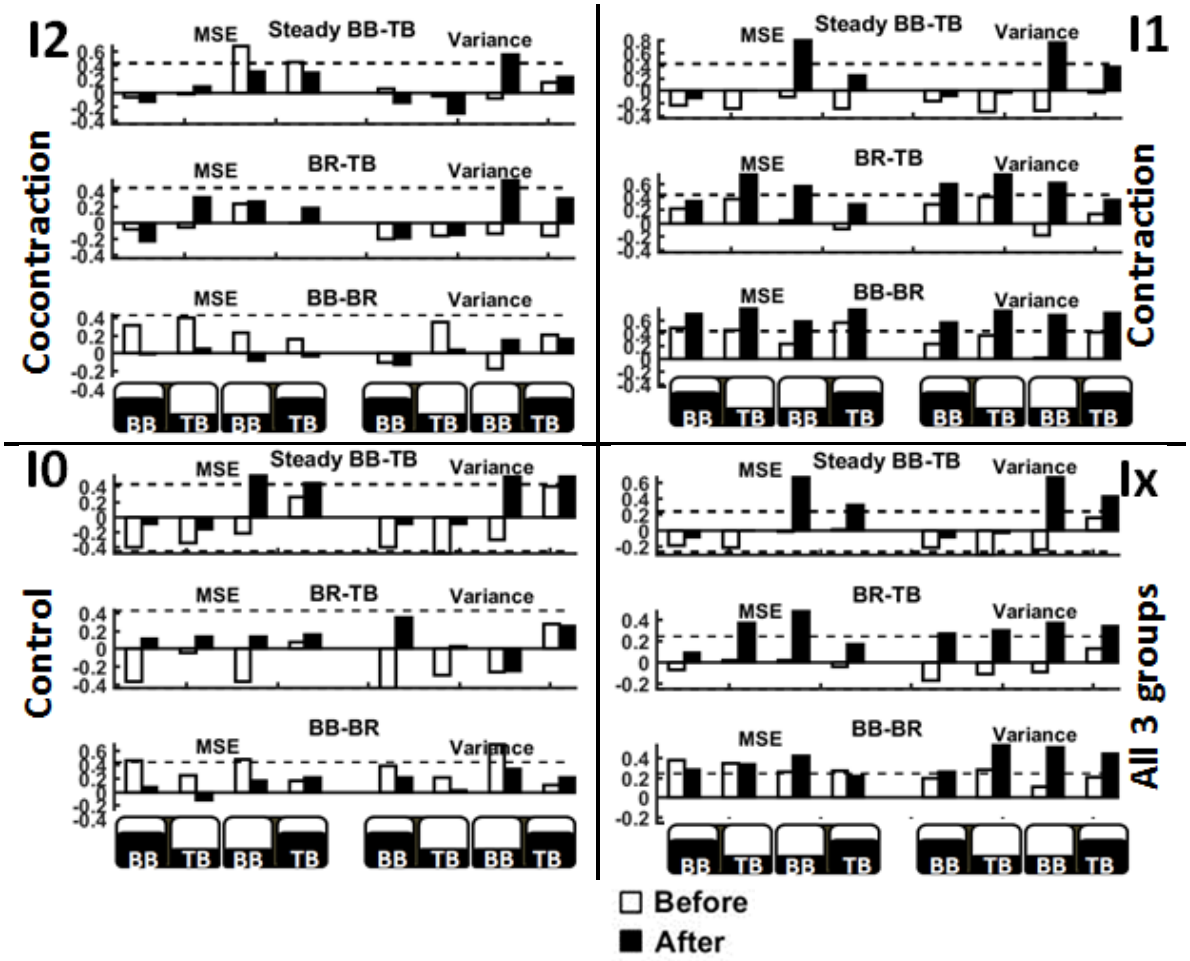

Figure 31 Coefficient of correlation between amplitude coherence and performance variables during steady cocontraction for individual groups: I2) Cocontraction, I1) Contraction, I0) Control, and all 3 combined in Ix) equivalent to Figure 15. Notice the high similarity between I1 and Ix. Per each plot, 3 rows for 3 muscle pairs (BB-TB, BR-TB, BB-BR), first 4 columns (two target level conditions) are for MSE, and the latter 4 are for Variance. On the x-axis, BB HIGH and TB LOW is one target pair, and BB LOW and TB HIGH is another target pair. Broken horizontal lines represent correlation coefficient at $P = 0.05$.

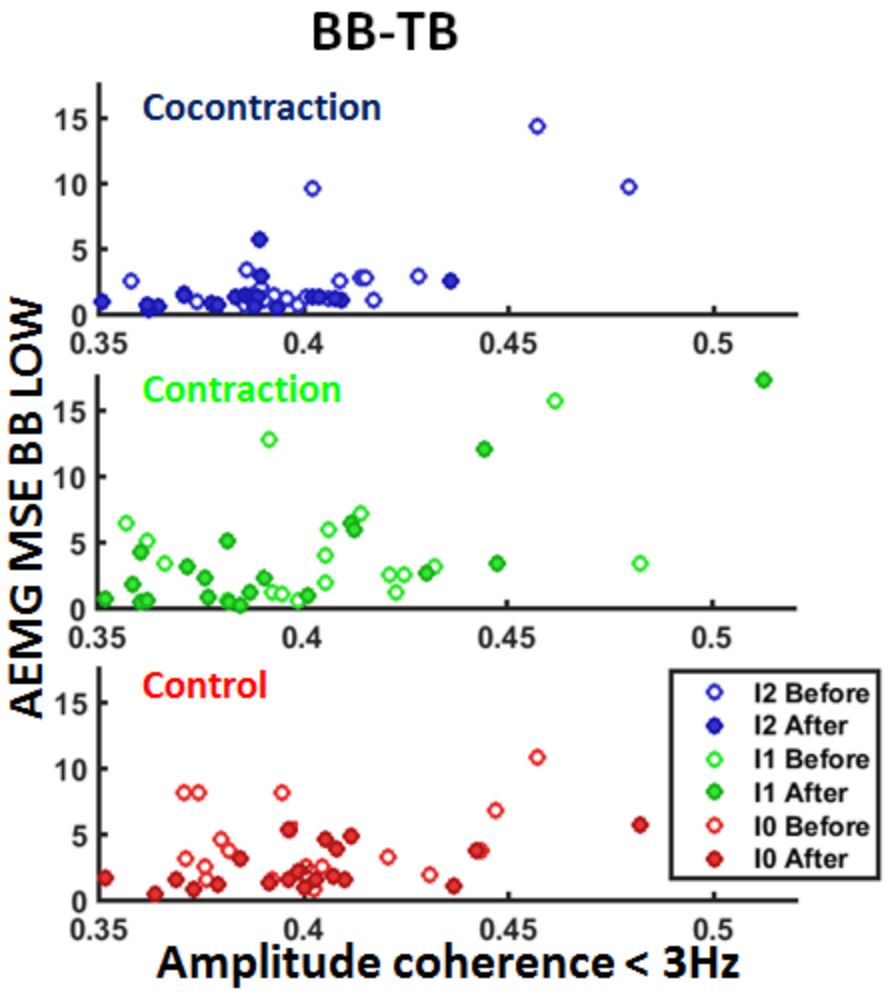

Figure 32 Scatter plot for AEMG MSE BB-LOW vs. amplitude coherence of BB-TB muscles during steady cocontraction in each group: Cocontraction (I2), contraction (I1), and control (I0), before and after the intervention.

In Aim-1, Cocontraction group tended to reduce correlated oscillations on average the most out of all three groups while improving performance reasonably although there was no statistical significance between groups (Table 2). After practice, the distribution of data points appeared to become narrower compared with before practice, and that may have contributed to the absence of significant correlation between AEMG MSE BB-LOW and amplitude coherence case (BB-TB), for example (Figure 32). On the other

hand, contraction and control underwent a smaller improvement in correlated oscillations. As a result, they maintained some spread that preserved or enhanced correlation.

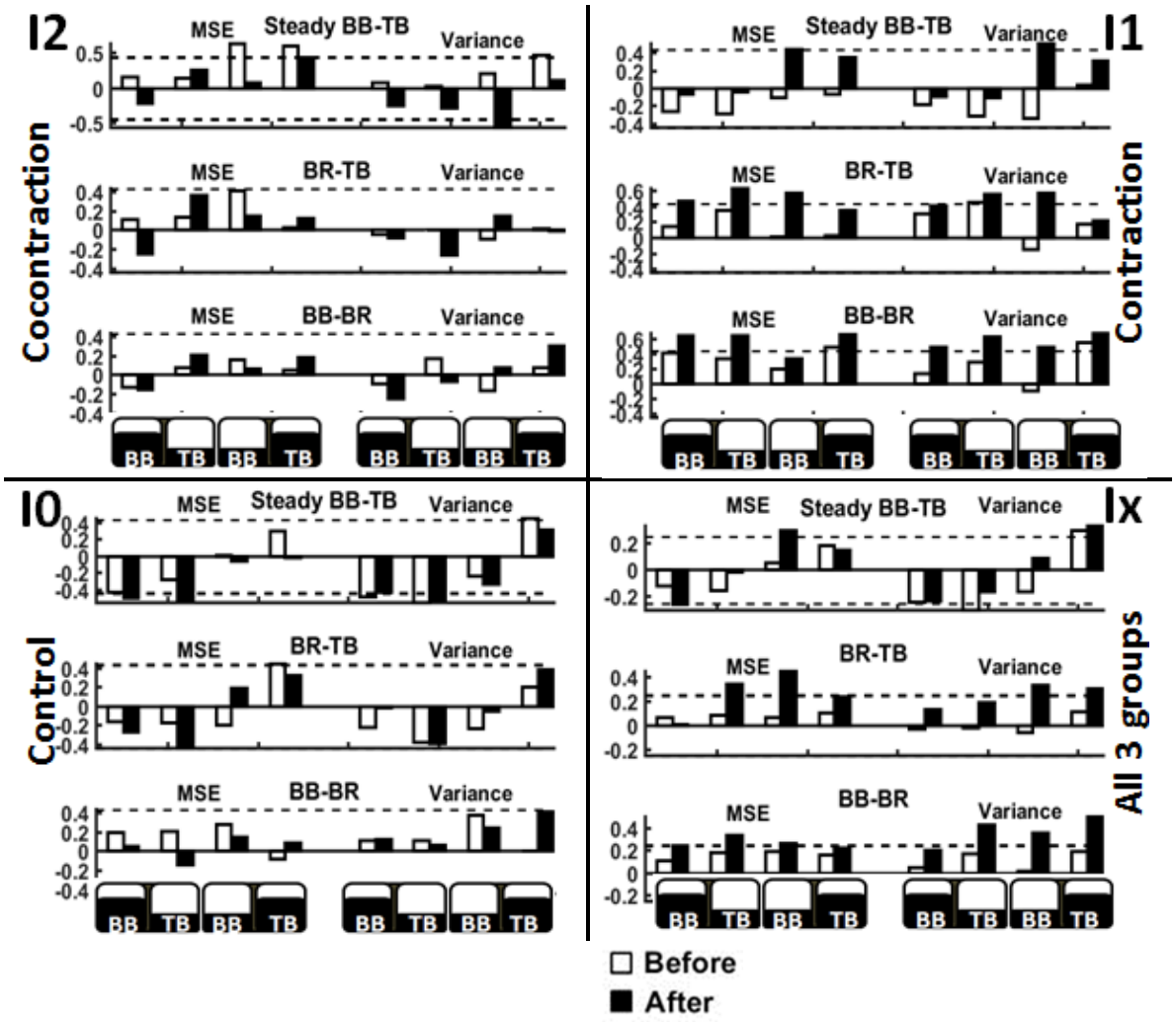

Figure 33 Coefficient of correlation between in-phase coherence and performance variables during steady cocontraction for individual groups: I2) Cocontraction, I1) Contraction, I0) Control, and all three combined in Ix). Notice the high similarity between I1 and Ix. Per each plot, 3 rows for 3 muscle pairs (BB-TB, BR-TB, BB-BR), first 4 columns (two target level conditions) are for MSE, and the latter 4 are for Variance. On the x-axis, BB HIGH and TB LOW is one target pair, and BB LOW and TB HIGH is another target pair. Broken horizontal lines represent correlation coefficient at *P* = 0.05.

3.3.5 Effect of initiation

Table 12 Response times as a measure of initiation for the 1st and 2nd varying levels (VL)

		Cocontraction	Contraction	Control	Average
	Before	1059.8 (338.0)	1231.6 (256.0)	1213.0 (270.0)	1168.1 (299.2)
VL1	**After**	836.8 (285.8)	966.1 (293.6)	1074.5 (283.4)	959.2 (302.5)
	Difference	223.0	265.5	138.4	209.0
	Before	937.7 (292.4)	1017.7 (296.9)	963.9 (279.4)	973.1 (290.4)
VL2	**After**	655.0 (202.8)	834.7 (206.4)	828.6 (285.9)	772.8 (248.3)
	Difference	282.7	183.0	135.3	200.3

Response times (in ms), mean (standard deviation) for different intervention groups (Cocontraction, Contraction, Control, and their averages) before vs. after intervention during the 1st and 2nd varying level of the cocontraction test.

To quantify the effect of the intervention on the initiation of activation to match target level, the response time from the time of a change in the target level to the time at which the maximum AEMG spike increased or decreased (derivative of AEMG) was measured during reaching and alternating stage of test trials. For reaching task from resting to a target (VL1, Figure 20), there was no effect of time or group on the response time. On the other hand, during varying level alternating between muscles (VL2, Figure 20), there was a main effect of time ($P<0.001$), and group ($P<0.001$), but no interaction on the response time (Table 12). Although there was no interaction between time and group, Cocontraction group achieved the largest drop after practice in responding to alternating muscles MVC (Table 12). Cocontraction group became 283 ms faster compared to 183

ms for contraction and 135 ms for Control groups. Note that VL1 target shows up on the screen at a random interval that subjects cannot predict. However, VL2 is always presented on the screen 3.5 s after VL1. Therefore, VL1 is related to alertness while VL2 is associated more with muscle initiation time.

3.3.6 Time-frequency representations

Different time-frequency algorithms (FFT / Wavelet; Amplitude / Phase) were utilized locally for extracting neural oscillations features to infer correlated oscillations (Figure 34). FFT based event-related potential coherence was introduced in section 3.1.5. Wavelet equivalent is to be presented in next section 3.3.6.1. Inter-trial coherence or phase locking, on the other hand, measures coherence between trials of same muscle under different conditions. It quantifies consistencies across trials, potentially revealing strategies in accomplishing tasks.

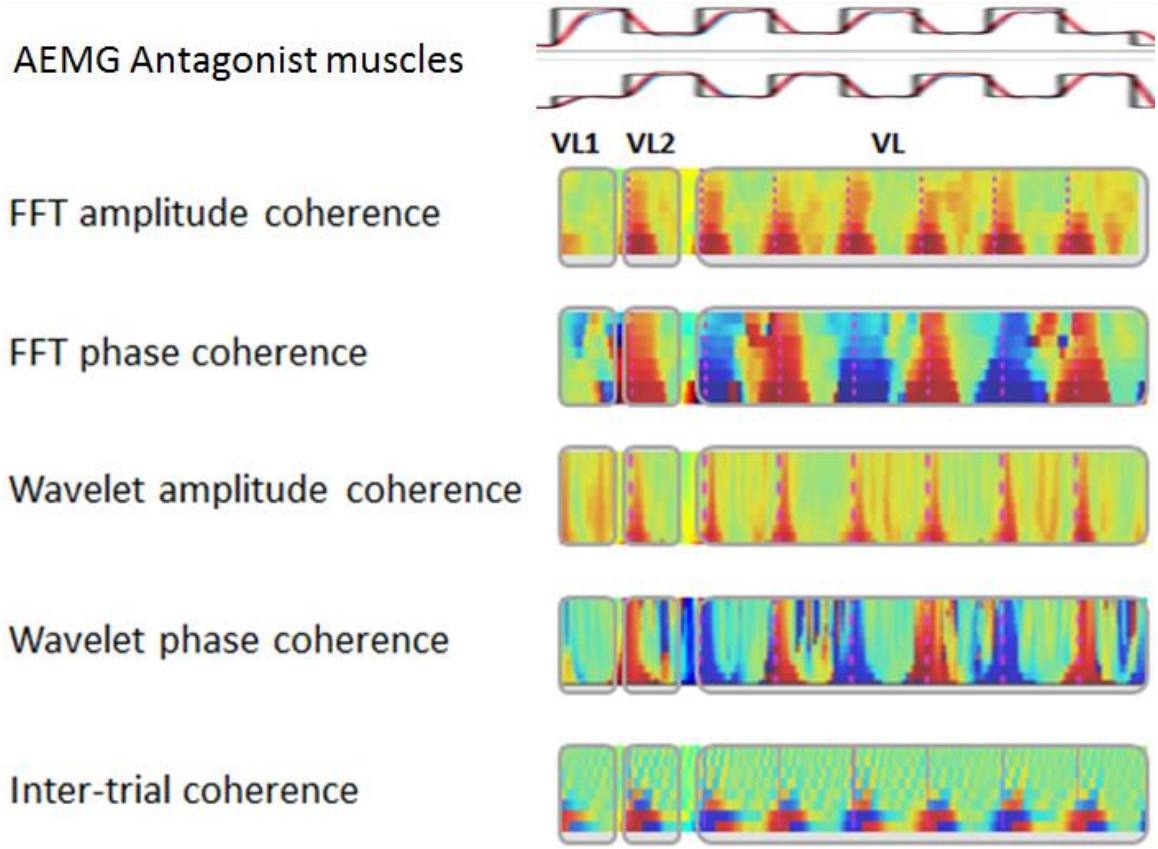

Figure 34 Time-frequency representation used: Event-related FFT / Wavelet, amplitude / phase coherence in addition to inter-trial coherence. Real data from the cocontraction practice of antagonist pair BB-TB with averaged AEMG depicted on top.

3.3.6.1 Wavelet Transform

As discussed earlier, classical methods of time-frequency representation may not be ideal for transient and dynamic coactivation. Wavelet Transform, on the other hand, is more flexible to tune in to temporal or spectral energy as needed. In addition to FFT based event-related coherence, sinusoidal Wavelet Transform was explored as well for the test (Figure 35) and cocontraction intervention practice (Figure 36).

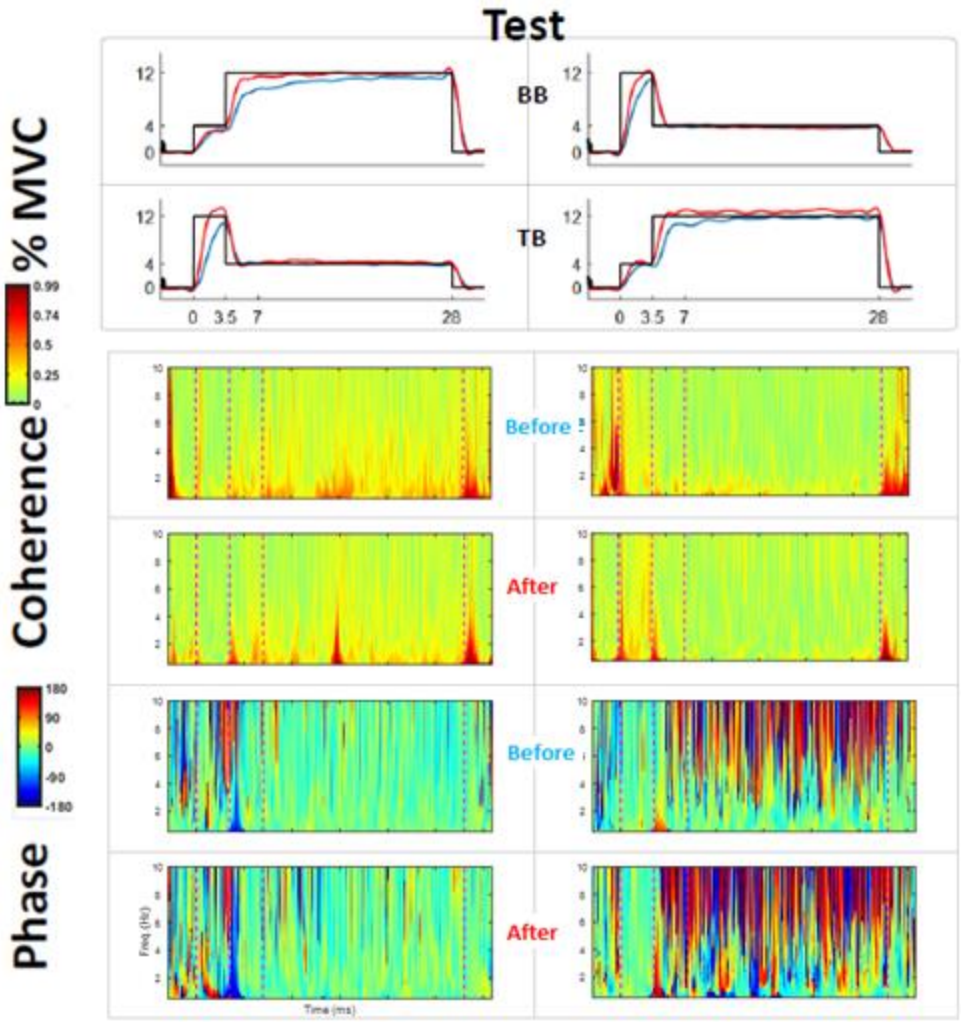

Figure 35 Signals grand average during cocontraction tests using Sinusoidal Wavelet. BB HIGH target level (left column), and TB HIGH target level (right column) across subjects: Top 2 rows, time series data (top: BB, bottom: TB); Rows 3&4, amplitude coherence between BB and TB before and after practice (denoted before and after); similarly, rows 5&6 show phase coherence.

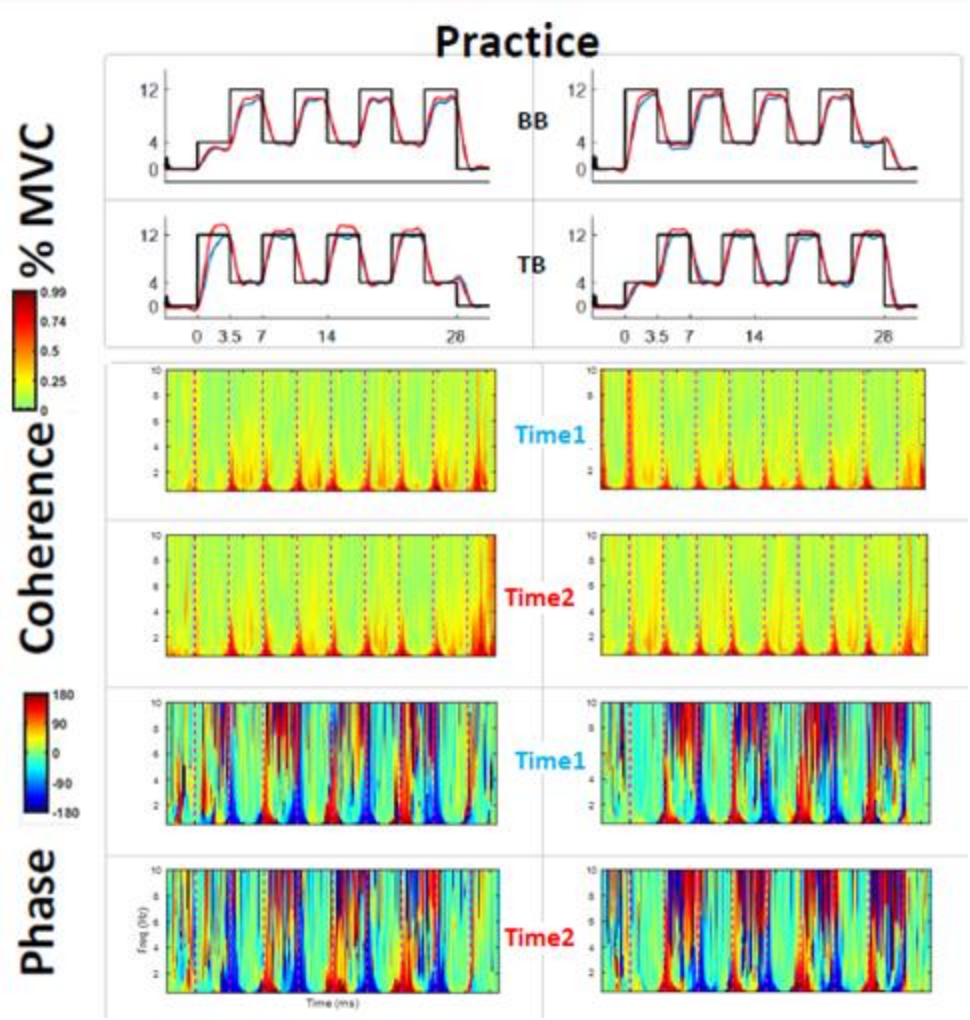

Figure 36 Signals grand average during cocontraction practice using Sinusoidal Wavelet. BB HIGH VL even (left column), and BB HIGH VL odd (right column) across subjects: Top 2 rows, time series data (top: BB, bottom: TB); Rows 3&4, amplitude coherence between BB and TB first and second half of practice sessions for each target level (denoted time1 and time2). Similarly, rows 5&6 show phase coherence during practice.

The Wavelet based coherence delivered comparable results to FFT based coherence (Figure 29) in the low-frequency band (< 3 Hz). One possible reason to why Wavelet did not outperform FFT based event-related coherence is that the low-frequency band is

limited by the number of cycles used. Since the primary analysis was around the low common drive frequencies between 0.5 and 3 Hz, the real power of Wavelet Transform was not exploited. The main benefit would be reached at higher frequencies instead.

3.3.7 Other oscillations

The low-frequency common drive synchrony was investigated so far. How about other higher frequencies? During steady contraction, 20 Hz oscillations were observed in amplitude coherence (BB-TB) for all three groups only when TB was supposed to be active (Figure 37). It was absent during Test (Cocontraction) or Practice (Alternating Co/contraction). Phase coherence is close to zero. This could be tied to tremor oscillations usually observed at 10, 20 and 40 Hz as described in (28, 29 and 49). However, since it is a contraction task, and such oscillations were not observed in BR-TB, one explanation could be that there was crosstalk between BB and TB at the tremor frequency of oscillations. Another plausible explanation is that subjects did not inhibit their BB activation during the TB-HIGH / BB-IDLE task.

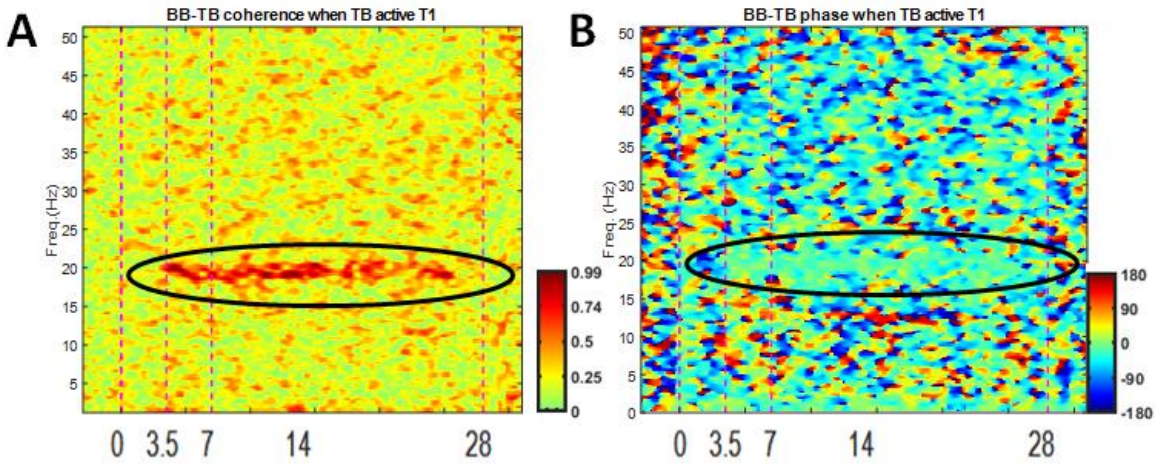

Figure 37 Correlated oscillations between BB and TB at 20 Hz during 12% MVC steady contraction for TB muscle: A, Amplitude coherence; B, Phase coherence.

To this point, this study has looked at low-frequency rectified EMG but how about much higher frequencies? As a quick observation of one of the target level conditions (Figure 38), some clear patterns in coherence and phase can be seen that corresponds to the alternation of activation level between BB and TB muscles. Such oscillations will not be explored but will be left for future investigations.

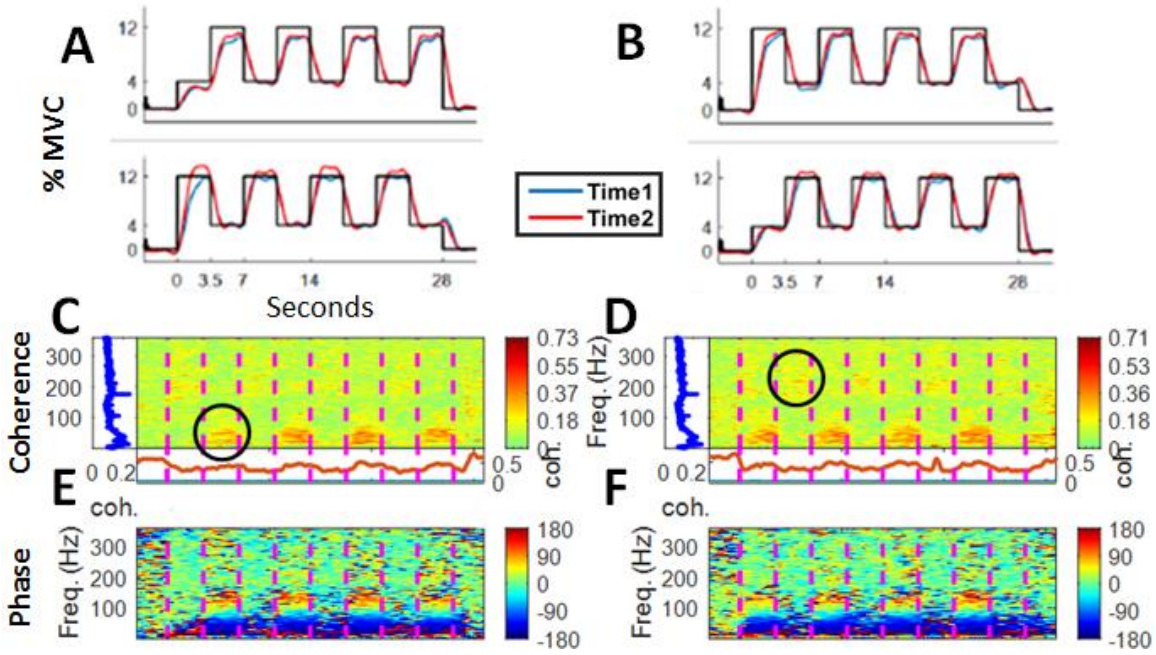

Figure 38 Higher frequencies oscillations for non-rectified cocontraction practice: A, AEMG for cocontraction of BB-TB, C, corresponding coherence and E, corresponding phase. B, D, and F subplots are on opposite-level target sequence compared with A, C, E. Circles highlight the shift in amplitude coherence frequency bands between different activation levels for BB-TB pair.

3.3.8 Discussion

This Aim-II study aimed to: 1) determine whether a bout of out-of-phase cocontraction practice reduces the in-phase low-frequency correlated neural oscillations in steady and transient unbalanced cocontraction of antagonistic muscles across individuals, and to 2) determine whether there is an underlying association between the low-frequency correlated neural oscillations between muscles and the performance of transient static unbalanced cocontraction during practice across individuals. The key findings are as follows: 1) There was significant reductions in low-frequency EMG in-phase coherence in Cocontraction group but not in Control group during steady (Figure 17) and transient (VL1, Figure 25; and VL2, Figure 26) cocontraction after the

intervention period; 2) There were positive correlations between low-frequency EMG coherence (across all three pairs of muscles) and one of the performance variables (i.e., mean squared error of AEMG) during transient alternating target level cocontraction across subjects, which emerged during second half of practice trials only when BB was HIGH (Figure 22).

In-phase synchrony effect during steady cocontraction test. Observed amounts of in-phase low-frequency correlated oscillations are the net results of excitatory and inhibitory input to the motor neurons. Collectively, it is possible that individuals who have lower net in-phase common drive perform better in steady cocontraction by producing less in-phase common drive or by using central inhibition (or both). Lower in-phase correlated oscillations indicates less coupled activity (i.e., more decoupled activity) between muscles, which would help independent control of unbalanced activity between antagonistic muscles (2). This is why it was crucial to quantify a differentiating in-phase measure.

Preserving phase coherence probability distribution revealed more insights as opposed to other metrics such as taking the mean coherence that suffers from cancelation. The following derived in-phase statistics was successful in uncovering the unique role that cocontraction practice played. In-phase coherence revealed a significant reduction in synchrony between muscles through the out-of-phase bout of intervention trials for the Cocontraction group that is almost absent for Control group (Figure 17).

Control group in-phase coherence decreased by 8% after intervention (Figure 16-C) although they did not have any intervention. Such decrease was not significant; actually, it was mostly due to agonist muscles. As Figure 21 demonstrates, the out-of-phase practice trials would put pressure on antagonist muscles (BB-TB) to desynchronize, but not necessarily the agonist ones (BB-BR). The out-of-phase practice had little effect on the mostly in-phase distribution of agonist muscles (BB-BR) compared to the almost flat phase distribution for antagonist muscles (BB-TB). This might explain why there was an in-phase drop in agonist muscles for Control group. In other words, there are other factors in play acting on agonist muscles than the bout of out-of-phase practice trials, possibly repetition. On the other hand, Contraction group decreased their in-phase coherence more significantly (14%) after the intervention. The plausible explanation is that subjects practiced the same out-of-phase intervention using a single muscle, except they could not inhibit the idle muscle as has been shown in Figure 30-A/B.

In addition to the significant difference ($P < 0.0005$) between Cocontraction and Control groups in-phase measures during steady cocontraction, 1) subjects practiced for only 15 min in addition to 37 min of rest in between trials, 2) subjects practiced during intervention, then their in-phase coherence was measured during test, i.e., it is a case of transfer of skill, 3) the Cocontraction group was able to decrease their in-phase coherence by 24% (Table 3) while the Control group decreased their in-phase coherence insignificantly (Figure 16-C) only for agonist muscles (BB-BR) that were not subjected to the out-of-phase practice (Figure 21). This is a supporting argument that a bout of cocontraction practices did influence the in-phase neural oscillations during the test. It would be interesting to have subjects train with out-of-phase cocontraction practice for a

longer duration (e.g., several weeks) and see the influence on modulating the low-frequency correlated oscillations during steady cocontraction.

The amplitude and in-phase coherence metrics measure different effects with some overlap. The fact that in-phase, but not amplitude coherence, uncovered the effect of the intervention is proof of their differences. Not to mention the correlation coefficient between the two is low or even negative under a few cases (Figure 19, bottom plot). On the other hand, both coherences revealed similar relationships as they were correlated with performance measures (Figure 31 vs. Figure 33). In general, the driving force behind isolating muscles could be due to the neural strategies that are associated with: 1) amplitude coherence; 2) in-phase coherence; or 3) both amplitude and in-phase metrics as they were associated with the modulation of neural oscillations.

The fact that both amplitude and in-phase coherences became more correlated with performance variables after the intervention than before for Contraction group, but not cocontraction or control (Figure 31, Figure 33) might support the idea that the latter two groups utilized multiple strategies to achieve their objective in matching the target while Contraction group had more consistency after the intervention. This potentially results in a higher correlation between amplitude and in-phase coherence in the Contraction group due to the unified neural strategy.

Correlated oscillations during cocontraction practice. Significant correlation coefficients between performance measures of accuracy (MSE) in BB and amplitude coherence emerged during BB-HIGH in the second half of the cocontraction practice (Figure 22-B). Four out of 12 cases became significant after practice when there were none before practice. This appearance supports the evidence that repetition of out-of-

phase cocontraction practice trials facilitates the emergence of an association between correlated oscillations and lower error at least for specific muscle and a specific cocontraction task. The importance of such observation is that what was perceived during the steady cocontraction test has some truth during alternating cocontraction practice: Whether it is steady or alternating cocontraction, subjects who achieved lower error are those who tended to have lower correlated oscillations as well. Such a relationship was clarified through repetition as subjects became more familiar with the task in hand. Again, because of the difficulty of the alternating cocontraction practice task, subjects focused on one of the two objectives, either lower error or variability but not necessarily both as revealed by inter-trial coherence (Figure 28). This explains why the relationship was skewed toward one target level for error and toward the other target level for variability in term of significance (Figure 22).

Correlated oscillations during contraction practice. Contraction practice was unique in the sense that one muscle was active at a time throughout the intervention. The task was easier than cocontraction practice, showing greater amplitude coherences by around 18% (not statistically tested, Table 5, Table 6), on average, with no instructed voluntary effort for inhibiting antagonist muscles but to neglect them. Such intervention gave subjects ample time to attend to each target independently habituating to the demands of the task. On the other hand, BB active coherences were higher compared to TB active (10% amplitude, 45% in-phase, Table 6) in line with involuntary activation of idle muscle findings (Figure 30 C&D).

Similarly, steady contraction draws some resemblance to contraction practice. In-phase coherence in TB active is lower than BB active (Table 7). On average, overall coherences during steady contraction are higher than steady cocontraction (Table 3) although no statistical test was performed.

Correlated oscillations during transient cocontraction (VL1, VL2). At least for VL2 and BB-HIGH during cocontraction test (Figure 29), there is a negative association between MSE and correlated oscillations for BB-TB muscle pair. In other words, during the initial stage of the trial (VL2), it is possible that subjects are more susceptible to the common drive due to unfamiliarity with the task even though they practice similar patterns during intervention. Repetition of same pattern within a trial (example VL-rep) might be different than repetition across trials (example VL2).

Possibly for the same reason there was no time x group performance interaction for reaching (VL1) and alternating target level (VL2) during the cocontraction test although both tasks resemble more the alternating cocontraction practice trajectories than the steady target part of test trajectories (Aim-I). Other reasons could be because there was not enough practice, higher frequencies played a part and were outside range of common drive, or cognitive strategies did play a more prominent role.

On the other hand, there was a significant group effect for both VL1 ($P < 0.005$) and VL2 ($P < 0.05$) in low-frequency in-phase correlated oscillations (Figure 25 and Figure 26). During VL1, in-phase coherence decreased in Cocontraction group only (26%). During VL2, in-phase coherence decreased in both Cocontraction (29%) and Contraction (19%) groups after intervention but not in Control group. It was expected for

Cocontraction group to have such in-phase coherence decrease during the test, however, for Contraction group, they did a single muscle contraction. One explanation, similar to steady cocontraction test above, is that due to various inhibition capabilities, subjects activated the antagonist muscles during contraction tasks involuntarily as has been illustrated in section 3.3.3 (Figure 30-C/D). Finally, similar to the steady cocontraction test, there was no clear evidence to tie any relationship between in-phase coherence decrease after practice and performance metrics during VL1 or VL2 because all three groups improved their performance with no significant time x group interaction.

Involuntary activation of idle muscles during contraction tasks. Crosstalk is the effect of capturing surface EMG signal from neighboring muscles that is different from the muscle of interest that is being recorded. The closer the muscles are, the higher the chance for crosstalk. On the other hand, related involuntary activation is the act of failure of inhibiting an antagonist muscle while contracting the muscle of interest that is being investigated. When subjects were asked to activate single muscle during contraction tasks (while ignoring the antagonist muscle), they could not help it but activate the antagonist muscle. Different subjects had different inhibition capabilities. However, the majority had more difficulties inhibiting TB when BB was active than suppressing BB when TB was active (Figure 30). When TB was active, both BB and BR had an involuntary contraction. Hence, this phenomenon cannot be due to crosstalk between BB and TB, but rather an involuntary contraction of idle muscles because TB and BR are farther away from each other, yet BR had similar behavior as BB. This could be due to

activating the deltoid extended shoulder muscle in one case but not the other due to the type of setup.

This differentiation is noteworthy because it may translate to implying that reciprocal inhibition worked better in TB HIGH, but not in BB HIGH in the cocontraction test as well. BB-HIGH was an easier task than TB-HIGH that could have led to less drive to decouple muscles for achieving required objective. This possibly could explain why the relationship between performance and correlated oscillations (Figure 15, Figure 18, and Figure 31) were not as prevalent for antagonist TB muscle when BB was HIGH. This explanation may be straightforward in the steady cocontraction test, but not as evident during cocontraction practice. In the latter, the change of activation level is fast for both muscles. The relationship between practice cocontraction and contraction is not linear. In other words, observing a single muscle changing activation level while the other muscle is idle does not necessarily relate to both muscles changing activation level concurrently. BB and TB trajectories are frequently crisscrossing during cocontraction practice. Therefore, a HIGH or LOW BB (or TB) may not explain results when they are changing activation level throughout trajectory.

Correlation between oscillations and performance revisited. Previously in aim-I, a robust relationship between oscillations and performance was found. Lower coherence between upper arm muscles was associated with better performance after the intervention period when all groups were pooled, with no significant interaction of time and group present on the corresponding measures. However, it is not clear how this relationship is weighted across different groups. Each intervention was designed with a different

expectation in mind: 1) Alternating target levels, during cocontraction practice, were expected to weaken phase synchrony between muscles in the Cocontraction group. 2) Single muscle contraction during intervention could have had the effect of habituating muscles to work independently in the Contraction group. 3) Control group had no task-related intervention, so it should bear effect only due to repetition.

Cocontraction group still have some evidence of linear relationship mainly in antagonist muscles (Figure 31-I2), but such a relationship does not look as prevalent as it was when groups were combined (Figure 31-Ix). Nevertheless, Cocontraction group had the most decrease in coherence (amplitude and in-phase, Table 3), comparable improvement in performance (accuracy and steadiness, Table 2) during steady-state, and the largest drop in initiation time to match the target after intervention (Table 12). Performance and coherence data could have become more closely situated after practice; hence secondary effects were not evidently available especially with participants testing and applying multiple strategies. Compared with steady cocontraction, the linear trend between performance metrics and correlated oscillations for the Cocontraction group is clearer during cocontraction practice of BB-HIGH, on an accuracy measure in BB (Figure 22). For the 12 cases of the MSE measures, there were three significant cases during the test before practice and none after practice; On the other hand, there were no significant cases in the 1st half of cocontraction practice trials, but there were four significant cases in the 2nd half of cocontraction practice trials. It is possible because the task is more difficult in cocontraction practice than steady cocontraction, subjects managed to focus on one single objective only (minimizing error or variability, but not both). Correlation coefficients between inter-trial coherence for MSE had opposite

polarity of the correlation coefficient between inter-trial coherence for variance. I.e., low error correlated with high variability, and high error correlated with low variability during cocontraction practice.

On the other hand, it is possible that the habituation effect for Contraction group played a role in unifying a single strategy for Contraction group that resulted in the highest prevalence in the linear relationship between performance and correlated oscillations among the groups (Figure 31 and Figure 33). For example, correlation coefficients between amplitude coherence and in-phase coherence decreased for both Cocontraction and Control groups, but it increased for Contraction group after intervention (Table 3).

One interesting observation for Control group in BB-TB pair is the positive relationship of performance variables with amplitude coherence (BB-LOW / TB-HIGH, Figure 31-I0), yet the negative relationship with in-phase coherence (BB-HIGH, TB-LOW, Figure 33-I0). In other words, amplitude coherence decoupling was correlated with a lower error for BB-LOW / TB-HIGH; yet, higher in-phase coherence was correlated with a lower error for BB-HIGH / TB-LOW. BB-HIGH and BB-LOW are different in the sense that the former has more difficulty suppressing automatic activation of the antagonist muscle (TB). This could explain the difference between the two, but it is interesting that amplitude and in-phase statistics were complementary in their findings.

Adaptability, transfer of skills from task to another. For Contraction group, subjects may have adjusted their strategies after practice to achieve lower error and

variability during steady cocontraction. But so did Cocontraction and Control groups (Table 2). Contraction group were not asked to decrease correlated oscillations (amplitude and in-phase) during steady cocontraction. However, at least Cocontraction group decreased both their amplitude and in-phase coherence as well (Table 3). Nevertheless, Contraction group practiced repetitive single muscle alternating contractions during the intervention and achieved the largest significant associations between performance and correlated oscillations (15/24 cases were clarified after practice, Figure 31-I1 and Figure 33-I1). On the other hand, there were only 2/24 significant associations present for Cocontraction group after practice (Figure 31-I2 and Figure 33-I2) although there might be other factors in play for this group. There were only 4/24 significant associations for the Control group after the intervention (Figure 31-I0 and Figure 33-I0). Hence, there should be some transfer of skills from contraction practice to cocontraction test observed for Contraction group across muscle pairs (except for BB-TB where it was observed for either BB-LOW or TB-HIGH only, Figure 31-I1 and Figure 33-I1).

On the other hand, Cocontraction group achieved the largest in-phase coherence drop across all groups ($P < 0.001$) during the cocontraction test (Table 3, Figure 17). The Cocontraction group practiced alternating cocontraction trials during the intervention, and the observed effect was perceived during the test. Again, there should be possibly some transfer of skills from practice to test mainly for the in-phase coherence measure in the Cocontraction group that is less evident in the Contraction group (who also did alternating activation level but for a single muscle at a time) and non-existent in the Control group.

Finally, possible tremor frequency oscillations around 20 Hz were identified that could be useful as a vehicle to study various physiological properties. For example, one can compare how the atypical population responds under such stimulus based intervention compared to healthy subjects. However, more work needs to be done to understand the extent of such oscillations fully.

3.3.9 Conclusions

The objectives for this aim-II were to 1) Explore the role of intervention in influencing intermuscular correlated oscillations (amplitude and phase coherences), and 2) See if the relationship between correlated oscillations and output performance still holds for transient activations.

The intervention was designed in order to influence the in-phase correlated oscillations. The practice of enforcing out-of-phase low-frequency drive to antagonistic muscles did reduce significantly the in-phase coherence during steady and transient (VL1 and VL2) cocontraction test for Cocontraction group but not for Control group. On the other hand, the capability of individuals in transient alternating target level cocontraction performance (i.e., mean squared error of AEMG) is associated with the amount of low-frequency correlated neural oscillations during practice only when BB was HIGH.

The various findings that depended on the measure of correlated oscillations confirmed that cocontraction should be evaluated using the amplitude of neural activity, coherence, and phase of correlated oscillatory neural activity between cocontraction muscles. Although amplitude and in-phase coherence are sometimes correlated, each one

capture different type of information as has been shown. However, it is still not clear whether the in-phase coherence is influencing the cocontraction performance and if so, in what way.

Other major observations included: 1) Contraction group had the most prevalent linear relationship between performance and correlated neural oscillations during cocontraction after the intervention period, possibly due to habituation during single target-muscle practice intervention. 2) During VL2, there was no time x group interaction for amplitude coherence or performance measures. However, effect sizes were notable for Cocontraction group compared to others after the intervention. Cocontraction group achieved fastest initiation time, the largest drop in coherence (amplitude, and in-phase), and the largest improvement in performance accuracy. 3) There is some plausible transfer of skills from practice to test for both Cocontraction and Contraction groups. Both groups showed some observed behaviours that cannot be explained only by the effect of repetition.

CHAPTER 4. DYNAMIC COACTIVATION

The associations between the correlated oscillations and the performance measures for static cocontraction were examined, but it is not clear if these findings still hold under dynamic movement. As such, experiment II was designed to investigate the relationship between correlated oscillations and system performance during dynamic coactivation. However, the new experiment is far different from the previous one in so many ways. Accordingly, a static case was introduced and tested in order to connect the two experiments before tackling the dynamic movement in experiment II. A detailed description of methodology and results are presented followed by a discussion of findings.

4.1 Experiment II, Dynamic intermuscular contractions with position feedback

4.1.1 Experimental setup and protocol

4.1.1.1 Subjects

Twenty right-handed healthy young adults (25 ± 3.0 years old, 12 men) without any history of neurological disorder participated in the present study. Handedness was confirmed with the Edinburgh Handedness Inventory (41). All subjects gave their written informed consent per the Institutional Review Board at Georgia Institute of Technology.

4.1.1.2 Experimental setup

Subjects were seated upright on a static high chair with a backrest. Their feet rested on an elevated surface. They held a lever with their right-hand pushing or pulling a robotic device as they fully extended or flexed their arms (Figure 39-B). Surface EMG signal was recorded from two elbow flexor muscles, BB and BR; one elbow extensor muscle TB; two wrist muscles, flexor carpi ulnaris (FCU) and extensor carpi ulnaris (ECU) (Figure 4-B). Similar to experiment I, BR served as a guard against potential crosstalk between BB-TB (or FCU-ECU) muscles. An eight-channel wireless EMG system (Cometa Srl, Milan, Italy) was used to collect five EMG channels acquired at 2000 sample/s, with a 10-500 Hz band-pass filter. At each bipolar electrode site, the skin surface was prepared by gently exfoliating the skin, and cleaning with alcohol.

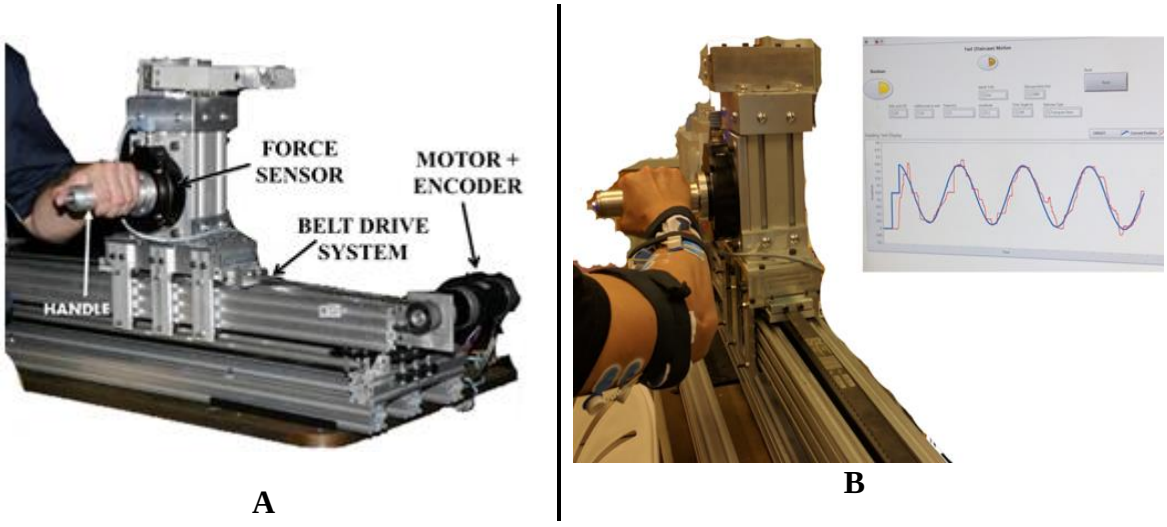

Figure 39 Robotic arm: A, side view; B, Setup during sine wave tracking including position visual feedback.

All the tests conducted in this study were completed using one degree of freedom (DOF) haptic interface (Figure 39), (20), capable of a maximum force of 100N at the

handle. The system set-up included a multi-axis force / torque sensor (ATI Industrial Automation, Apex, NC) with stand-alone controller, a brushless DC motor (Anaheim Automation, Inc., Anaheim, CA) linked to a quadrature optical encoder (US Digital, Vancouver, WA) and controlled by a servo motor drive (Pacific Scientific, CA). The haptic device was digitally operated by a CompactRio real-time controller programmable and deployable through a user interface in LabView (National Instruments, Austin, TX). The haptic device was set up as a conventional controller throughout all experiments generating vibration at the handle that was digitally band-pass filtered between 15 and 30 Hz using LabView. The purpose of the added vibration was to ensure that subjects coactivate their muscles throughout the experiment even when holding robotic arm steadily.

Mechanical output (MECH) signals acquired were force (FRC) in Newton (N) and position (POS) in cm. Derived measures, velocity (VEL) and acceleration (ACC) were computed by taking the first and second derivative of position measured in cm/s and cm/s^2 respectively. Stiffness (STF) was computed as force divided by displacement (N/cm). The position of the robotic arm was also used for providing visual feedback to the subjects as they were tracking targets. All kinetic / kinematic signals were sampled at 1000 samples/s and down-sampled to be logged around 30 Hz.

4.1.1.3 Experimental protocol

MVC was performed at the beginning of the experiment to obtain maximum AEMG for BB, BR, TB, FCU, and ECU muscles in all subjects as described in section 2.2.2. All participants performed two independent target-tracking tests using the position of the

robotic arm, either a set of sine or square waves. Each set consisted of ten trials of a single waveform. Sets were randomized across subjects. The tasks were conducted by dynamically tracking the target wave flexing and extending the elbow joint for BB, BR, and TB, and the wrist flexor and extensor (FCU and ECU) with shoulder joint movement providing joint stability (No surface EMG was acquired for shoulder muscles).

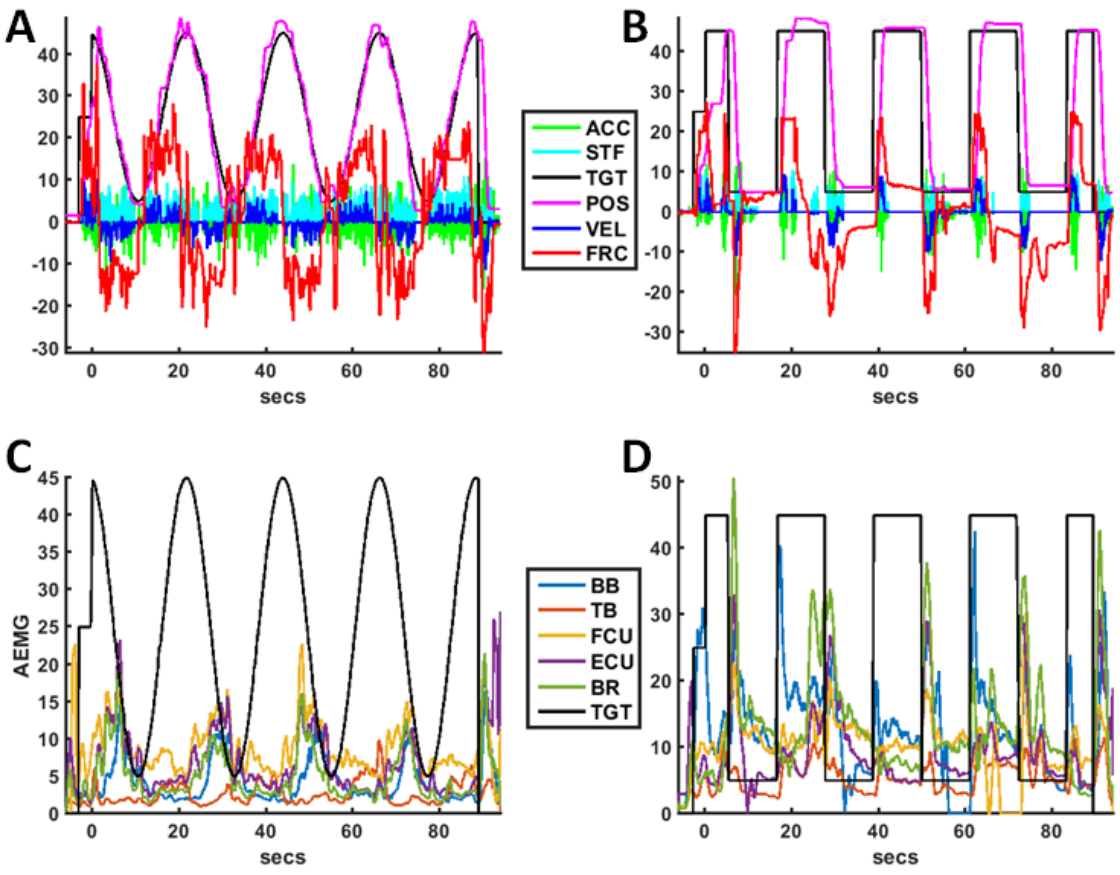

Figure 40 Single trial MECH and AEMG signals: Kinetic / kinematic top (ACC, acceleration; STF, stiffness; TGT, target; POS, position; VEL, velocity; and FRC, force); A, Sine target; B, Square target; AEMG bottom (BB; TB; FCU; ECU; BR; TGT). C, Sine target; D, Square target; Force (N), Position (cm), Velocity (cm/s), Acceleration (cm/s^2), Stiffness (N/cm), AEMG (% MVC).

Current target waveforms, sine, and square-wave trajectories were chosen to capture different features while equating power between target trajectories: square wave trajectory is mostly steady, with abrupt changes at the edges. Sine wave trajectory is gradual, with an inflection at peaks. Both trajectories have a positive concavity. Each trajectory played a different role in testing the current hypotheses. For example, steady coactivation (hold position for square trajectory) is comparable to aim-I target level condition by design, an opportunity to connect and compare both aims for replication purposes.

It is worth mentioning that experiment II was designed after the conclusion of aim-I. The consensus then implied that there is no effect of intervention. Therefore, experiment II explored only the effect of repetition. On the other hand, Experiment II contrasts with experiment I in four main aspects: 1) Experiment II is dynamic where participants are pulling or pushing a robotic arm to match a target in addition to a static task; 2) Subjects did receive visual feedback of position (as opposed to muscle activation); 3) Participants exercised unintentional muscle activations (as opposed to intentional ones) since their main focus is on tracking trajectory rather than the amount of contractions. 4) Vibration was added to tasks to ensure coactivation during experiment II.

4.1.2 Coactivation Test

Subjects were presented with target templates (sine or square waveform) in addition to robotic arm position displayed on the screen as visual feedback. In all templates, the baseline was at an initial zero reference with extended arm of the subject, followed by four cycles of pulling / pushing or holding action (Figure 39-B). A full cycle went from a

fully extended arm to fully flexed and back extended in about 22 s. Subjects were instructed to "match the target as fast, accurate, and stable as possible." The travel distance of the device arm that corresponds to a half cycle is 0.61 meter. A total of ten trials per each waveform were tracked with each trial consisting of four cycles (Figure 40 single trial; Figure 41 average across subjects with task annotation). Each trial was 100 s long with 40 s of rest between trials. There was a short push / pull segments at start and end of the trial for about 12 s as subjects aligned device position. Subjects rested for two minutes after five trials.

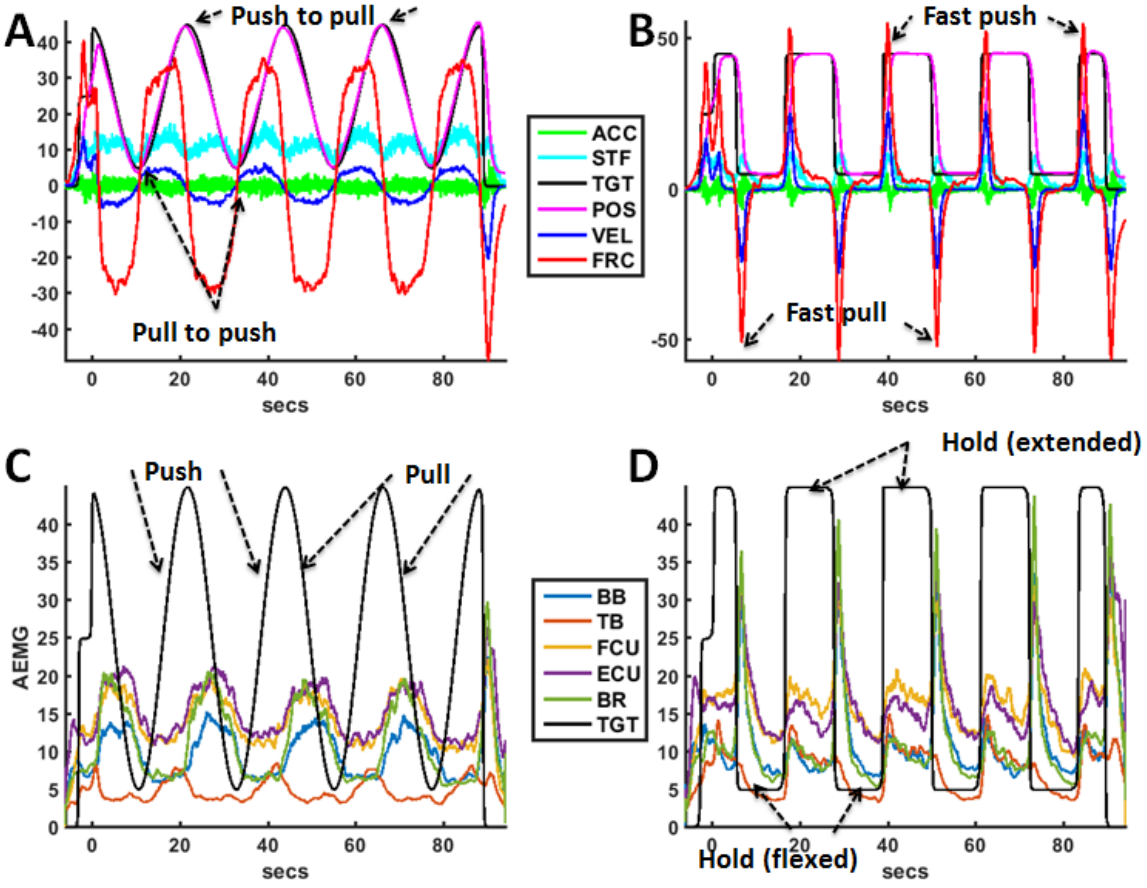

Figure 41 MECH and AEMG signals averaged across ten trials and 20 subjects: Kinetic / kinematic top (ACC, acceleration; STF, stiffness; TGT, target; POS,

position; VEL, velocity; and FRC, force). AEMG bottom (BB; TB; FCU; ECU; BR; TGT). Differentiation between transient and steady-state segments descriptions overlaid: A, Reverse direction coactivation, push to pull vs. pull to push transition; C, Slow coactivation (sine quasi-constant velocity) with a pull or push for steady-state. B, Fast coactivation (square transient): push or pull; D, Steady coactivation hold in place with either flexed or extended arm. Force (N), Position (cm), Velocity (cm/s), Acceleration (cm/s^2), Stiffness (N/cm), AEMG (% MVC).

4.1.3 Slow, steady, fast, and reverse coactivation

For each waveform, sine and square targets, activations were separated into either a transient (reverse / fast-changing) or steady-state (quasi-constant velocity or hold) segments. In sine-wave trajectory (Figure 41, A&C), slow coactivation during the quasi-linear target was referred to a quasi-constant velocity segment. In this segment, subjects were either pushing or pulling the robotic arm lever in one direction for a window lasting about 7 s each. Relatively shorter activations where target segments changed from pull (flex) to push (extend) or push to pull were labeled as reverse direction coactivation (transient segments), each lasting for about 3 s. For square-wave trajectory (Figure 41, B&D), subjects were holding their arms steadily at either end (flexed or extended) at zero velocity for about 7 s. These steady coactivation segments in the square-wave trajectory are comparable to aim-I steady cocontraction trials in the sense that they require static contraction for maintaining a constant target value. During fast pulling or pushing while moving the robotic arm from one end to the other for about 3s, segments were categorized as fast pull / push segments.

4.1.4 Data analysis

The amplitude of EMG signal was computed as follows: After the mean value of the raw EMG signal was subtracted, it was full-wave rectified and smoothed using a moving average window of 250 samples (125 ms) after removing outliers (large non-physiological spikes) and replacing them by neighboring samples. The signal was then normalized by the maximal value during MVC for each muscle (AEMG). To assess the variability in maintaining steady coactivation (zero velocity in square target), slow coactivation (quasi-constant velocity in sine target) or simply tracking transient targets (fast coactivation in square target; reverse direction coactivation in sine target), the standard deviation (variability) and mean of AEMG (mean activation) were calculated across each target segment (7 s for steady-state and 3 s for transient).

Because of the unintentional coactivation nature of the experiment, and the fact that visual feedback was based on position rather than AEMG activation (as in experiment I), there was some higher rate of outliers in the AEMG data. Accordingly, for each waveform (sine / square), target direction (pull / push), target state (steady-state / transient), and muscle, variability measures across segments were normalized as a percentile within each group after removing outliers. Distributions were confirmed to have changed from 1/frequency shape to a more Gaussian-like as expected. Similar normalization was applied to mean values of AEMG.

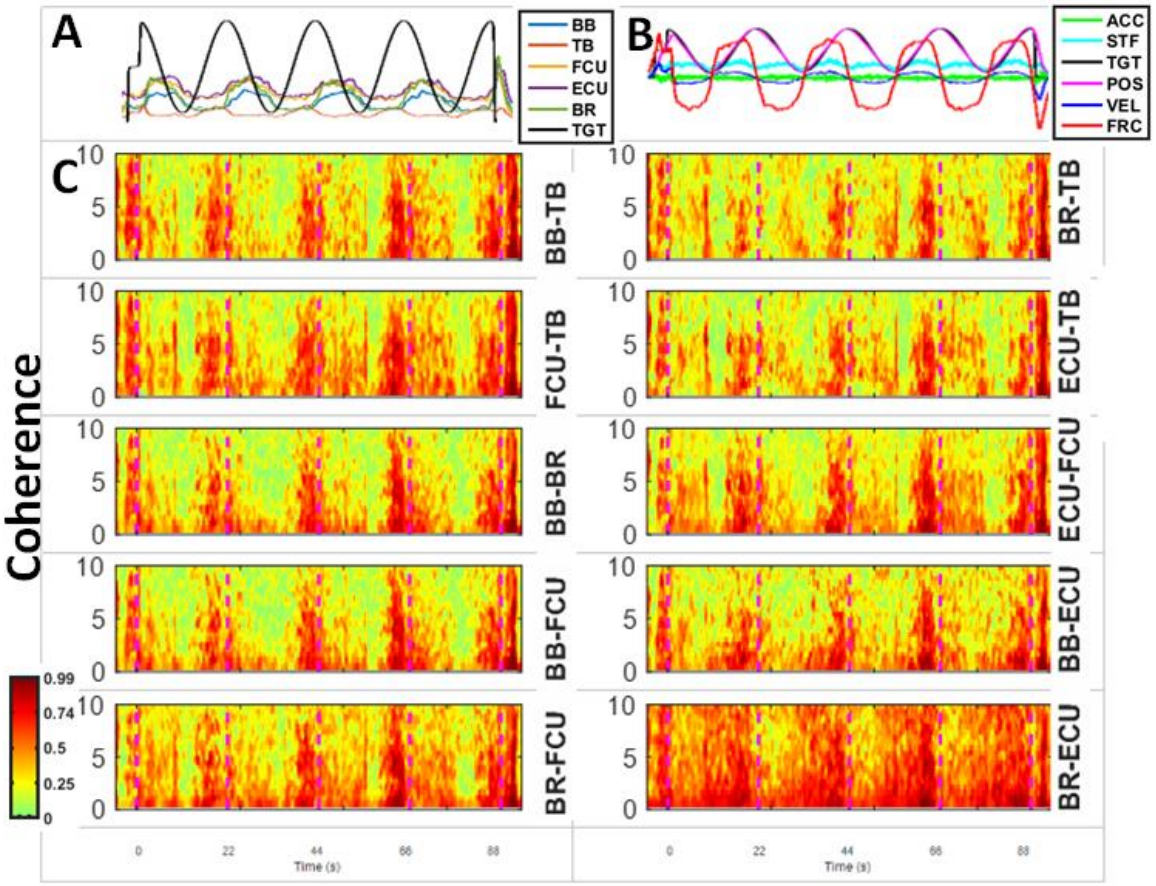

Figure 42 Sine wave AEMG, MECH, and coherence average plots across 20 subjects; A, AEMG (0-88s) for 5 muscles (BB; TB; FCU; ECU; BR; TGT); B, Corresponding kinetic / kinematic data (ACC, acceleration; STF, stiffness; TGT, target; POS, position; VEL, velocity; and FRC, force); C, Event-related amplitude coherence (0-10 Hz) for ten pairs of muscles (BB-TB, BR-TB, FCU-TB, ECU-TB, BB-BR, ECU-FCU, BB-FCU, BB-ECU, BR-FCU, and BR-ECU).

To assess the accuracy in matching the target trajectory (i.e., slow deviations from the target), the root mean squared error (RMSE) between POS and target was calculated for the same time windows (7 s for the steady-state segment, and 3s for the transient segment). Standard deviation and mean were computed for all five mechanical output signals (ACC, FRC, POS, STF, and VEL). Any linear trend in FRC was removed before computing standard deviation.

For assessing the oscillatory characteristics of EMG signals, the following processing was performed. An 8^{th} order Butterworth high-pass filter of 15 Hz cutoff was applied for each 100 s long trial, using a zero-phase forward and reverse digital IIR filter. After removing the mean value, the signal was full-wave rectified. Five trials for each subject per waveform were concatenated together into a 500 s long segment, mean subtracted. To assess the power content of oscillations in addition to phase and amplitude coherence between muscles, the same procedure was followed as described in section 3.1.5. Estimates of the event-related spectral perturbation (ERSP), the event-related phase coherence (ERPCOH), and the event-related linear coherence (ERLCOH) (12) were computed. Equations: **(2), (3)**, and **(4)** respectively. Inter-trial coherence (ITC) (12), a measure of the event-related phase-locking across trials in time and frequency (Figure 34, bottom plot) was computed in the 0-3 Hz range as well. A Hanning window with a size of 2,048 samples (1.024 s) and 1,024 samples (0.512 s) overlap was used for all time-frequency analysis. Phase (Figure 43 & Figure 45) and amplitude (Figure 42 & Figure 44) coherences were applied on all ten pairs of muscles (BB-TB, BR-TB, FCU-TB, ECU-TB, BB-BR, ECU-FCU, BB-FCU, BB-ECU, BR-FCU, and BR-ECU) due to low-frequency correlated oscillations, here referred to as "common drive", do not differentiate between agonist or antagonist muscles. Correlated oscillations were computed using both FFT and sinusoidal Wavelet methods. Mainly FFT based time-frequency analysis is expanded on and is shown throughout this aim since they gave similar results at low frequencies.

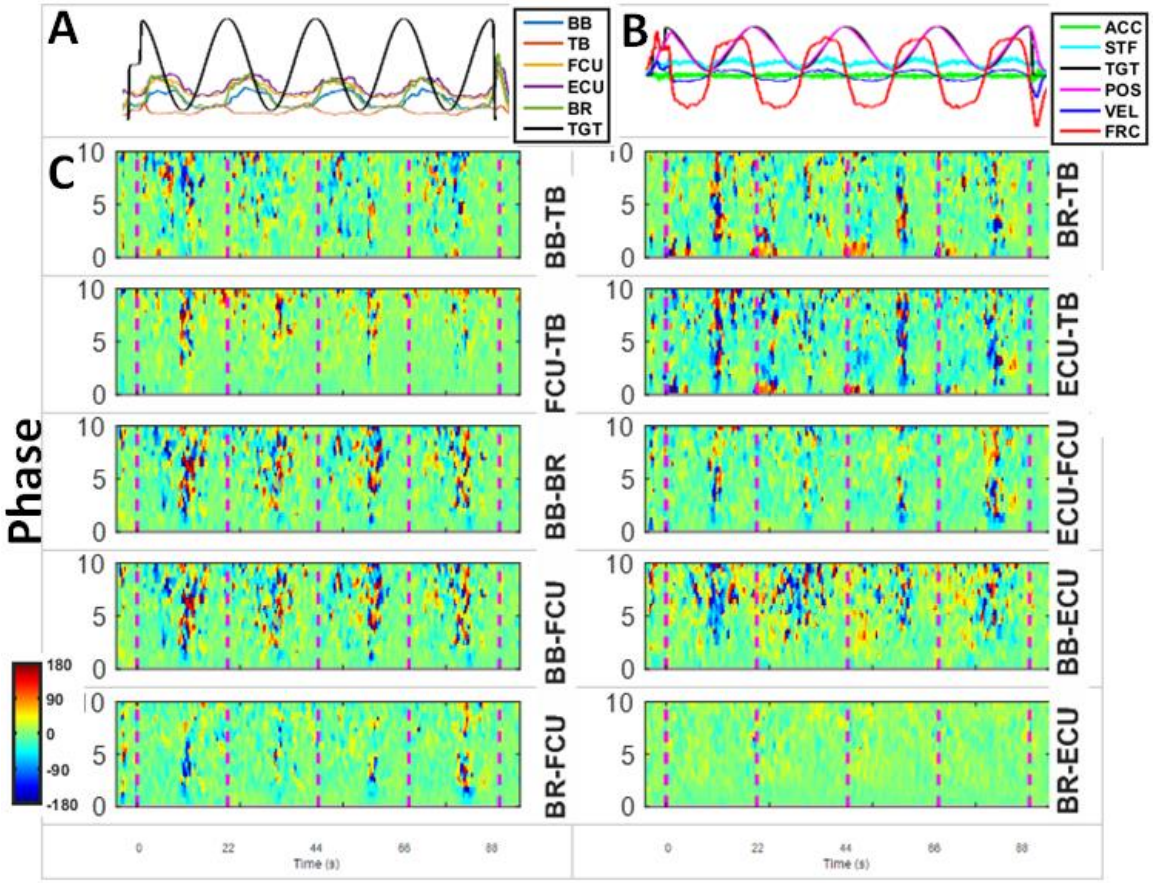

Figure 43 Sine wave AEMG, MECH, and phase coherence average plots across 20 subjects: A, AEMG (0-88s) for 5 muscles (BB; TB; FCU; ECU; BR; TGT); B, Corresponding mechanical output data (ACC, acceleration; STF, stiffness; TGT, target; POS, position; VEL, velocity; and FRC, force); C, Event-related phase coherence (0-10 Hz) for ten pairs of muscles (BB-TB, BR-TB, FCU-TB, ECU-TB, BB-BR, ECU-FCU, BB-FCU, BB-ECU, BR-FCU, and BR-ECU).

In line with experiment I, the focus was on the 0 to 3 Hz range for extracting power and coherence measures. For spectral power (EMG power), amplitude coherence (EMG coherence) and phase coherence (EMG phase), a mean value in the 0-3 Hz range were computed across the 7 s window for the steady-state target segments or 3 s for the transient target segments. These measures were grouped and averaged across corresponding signals for time (first or second set of trials), direction (pull or push), state

(steady-state or transient) and waveforms (sine or square), were grouped and averaged. Each subject had a single measure for each waveform, direction, state, and time.

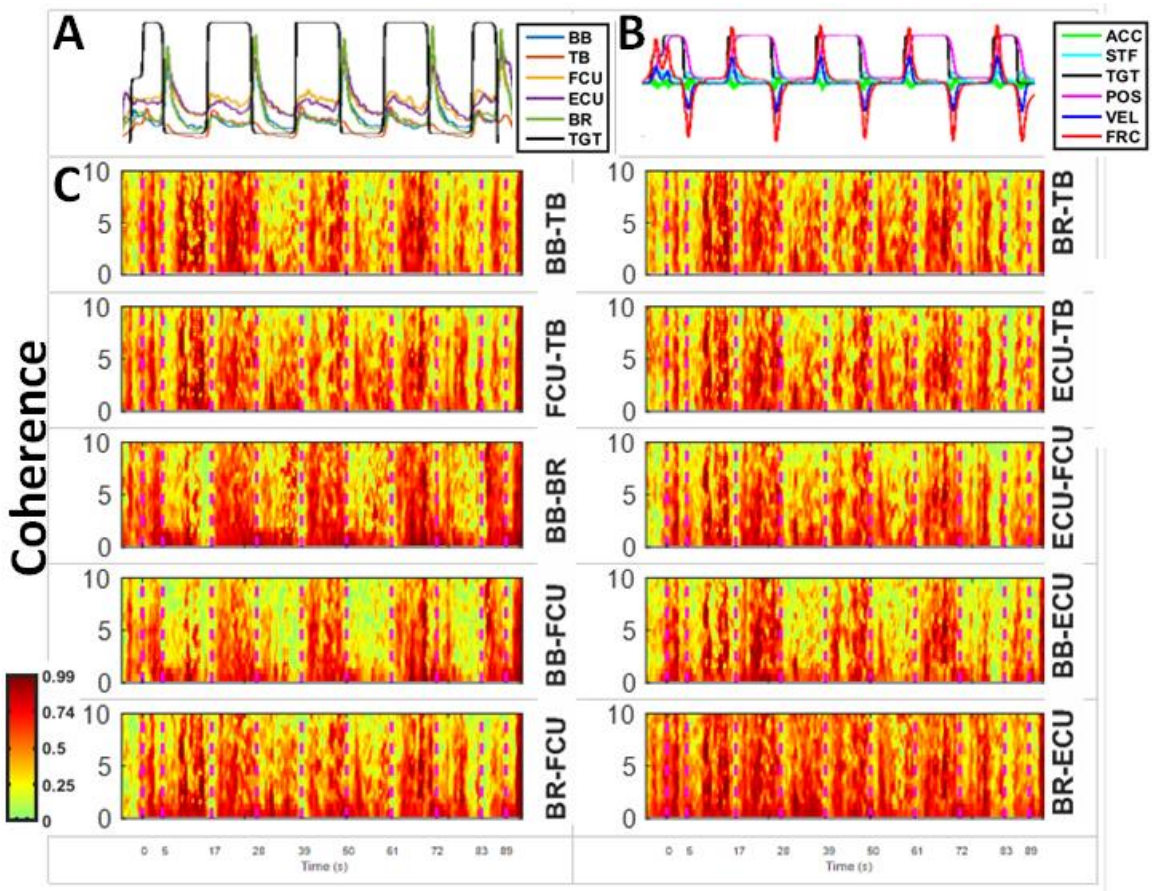

Figure 44 Square wave AEMG, MECH, and coherence average plots across 20 subjects. A, AEMG (0-88s) for 5 muscles (BB; TB; FCU; ECU; BR; TGT); B, Corresponding kinetic / kinematic data (ACC, acceleration; STF, stiffness; TGT, target; POS, position; VEL, velocity; and FRC, force); C, Event-related amplitude coherence (0-10 Hz) for ten pairs of muscles (BB-TB, BR-TB, FCU-TB, ECU-TB, BB-BR, ECU-FCU, BB-FCU, BB-ECU, BR-FCU, and BR-ECU).

The mean of event-related phase coherence suffered from cancelation effects. Alternatively, probability density function ranging between 0 ± 180 degrees was

extracted for each target segment in the 0-3 Hz range and across the temporal window of interest (Figure 12). The in-phase measure was then quantified as the area within 0 ± 5 degrees of pdf distribution.

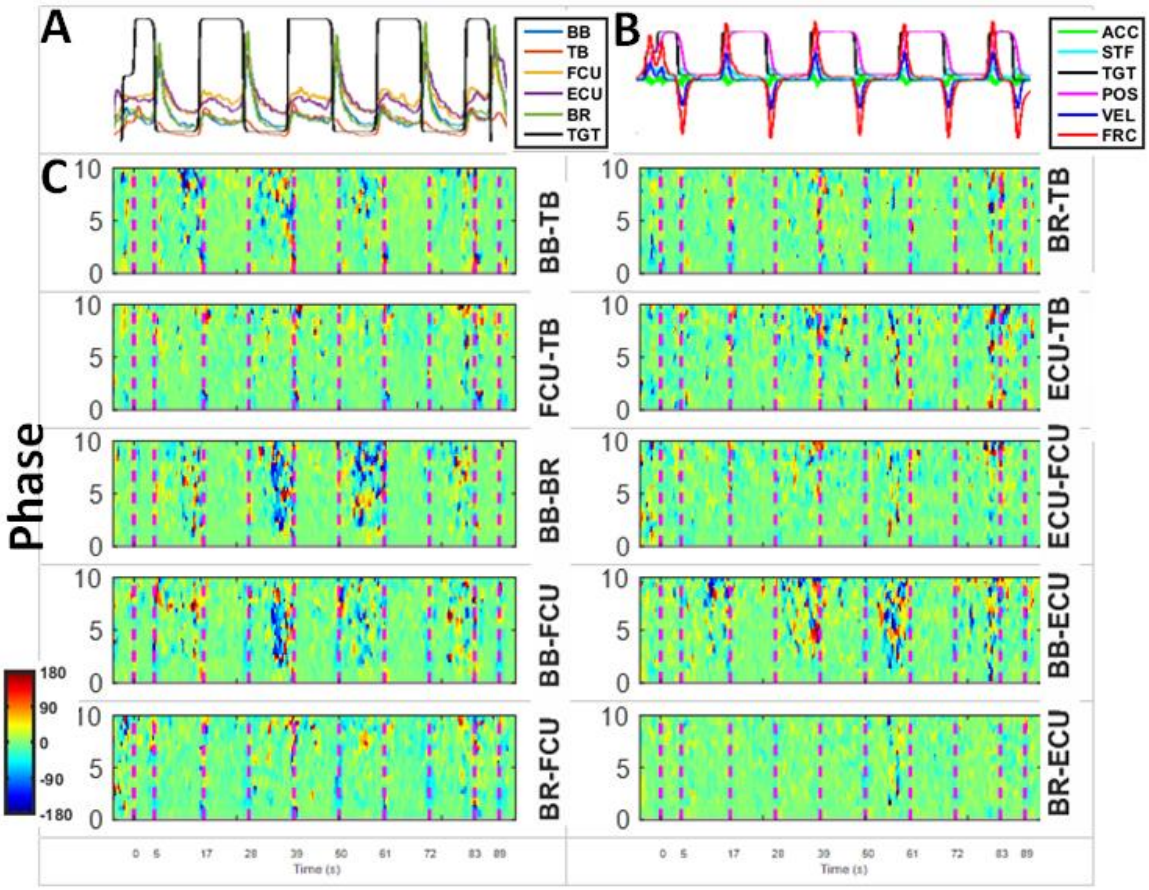

Figure 45 Square wave AEMG, MECH, and phase coherence average plots across 20 subjects: A, AEMG (0-88s) for 5 muscles (BB; TB; FCU; ECU; BR; TGT); B, Corresponding mechanical output data (ACC, acceleration; STF, stiffness; TGT, target; POS, position; VEL, velocity; and FRC, force); C, Event-related phase coherence (0-10 Hz) for ten pairs of muscles (BB-TB, BR-TB, FCU-TB, ECU-TB, BB-BR, ECU-FCU, BB-FCU, BB-ECU, BR-FCU, and BR-ECU).

4.1.5 Statistical analysis

At the beginning, the effect of time on correlated oscillations measures (phase and amplitude coherence), power, neural output (mean or standard deviation of AEMG), and mechanical output were tested with a three-way ANOVA (time x direction x muscle or time x direction x muscle pair coherence). Since there was little effect of time, then the focus shifted to the influence of direction and muscle (or direction and muscle pair) after dropping time. For testing mean activation level or variability of AEMG for each muscle; or mechanical output accuracy of position matching target, variability of MECH signals, a two-way analysis of variance (ANOVA) was performed on μ-AEMG, σ-AEMG, RMSE of POS, or σ-MECH (ACC, FRC, POS, STF, and VEL) with factors being muscle (BB, TB, BR, FCU, and ECU), and target direction (pull and push) with repeated measures. Dependent variables for oscillatory characteristics of EMG test included: EMG power for each muscle, coherence, and phase for each pair of muscles, all at frequencies < 3 Hz. EMG power was tested with a two-way ANOVA with factors being muscle (BB, TB, BR, FCU, and ECU) and target type with repeated measures. EMG coherence and phase were tested with a two-way ANOVA with factors being muscle pair (BB-TB, BB-ECU, TB-FCU, BR-TB, BR-FCU, BB-FCU, BB-BR, ECU-TB, ECU-FCU, BR-ECU) and target direction (pull, push) with repeated measures. Linear regression analysis was performed between each of the oscillation-related variables (i.e., EMG: power; coherence; and phase) and the performance-related variables (i.e., μ-AEMG, σ-AEMG, RMSE-POS, and σ-MECH) across subjects for each muscle and muscle pair. Pearson product-moment correlation coefficient (r) was obtained for these correlations. An alpha level of 0.05 was chosen for determining statistical significance. $P < 0.05$ and $P < 0.01$ are noted when significant.

4.2 Aim-III Slow oscillations are associated with mechanical output during dynamic coactivation while controlling a vibrating object.

In aim-I, this study established that greater decoupling of muscles is associated with better performance during static steady cocontraction. Aim-III explores generalization of such finding by testing similar hypotheses in a dynamic environment after an attempt to tie the two aims: 1) Determine whether there is an underlying association between the low-frequency correlated neural oscillations between muscles and the mean activation level and variability of AEMG during steady coactivation task across individuals, 2) Determine whether there is an underlying association between the low-frequency correlated neural oscillations between muscles and the mechanical output performance and characteristics (a- position accuracy, and b- endpoint stiffness) during slow coactivation task across individuals.

There was little to no effect of time, so all data were combined across trials. Correlations between coherences (amplitude or in-phase) with neural or mechanical output were then investigated.

4.2.1 Steady coactivation

Static steady coactivation at either end of the square target was designed with aim-I in mind. Since the task was stationary where subjects coactivate their muscles, the position is constant hence no kinematics data to analyze. Only force statistics of mechanical output are of value to assess (Table 16): μ-FRC decreased (flexed, 13.6%; extended,

20%) and σ-FRC decreased (flexed, 16%; extended, 11%, $P < 0.05$) with time. As for coherence between muscles, there was no significant change in amplitude or in-phase through repetition (Table 14). There was no significant change in neural output (μ-AEMG and σ-AEMG) with time as well.

On the other hand, the only significant correlation between coherence and neural output is a negative relationship (Figure 46) between muscle pairs and μ-AEMG (i.e., higher coherence corresponds to lower μ-AEMG) in some muscles during the holding tax at each end of the square-wave trajectory. The relationship between coherence and variability of AEMG during steady coactivation was neither significant nor consistent (Figure 47).

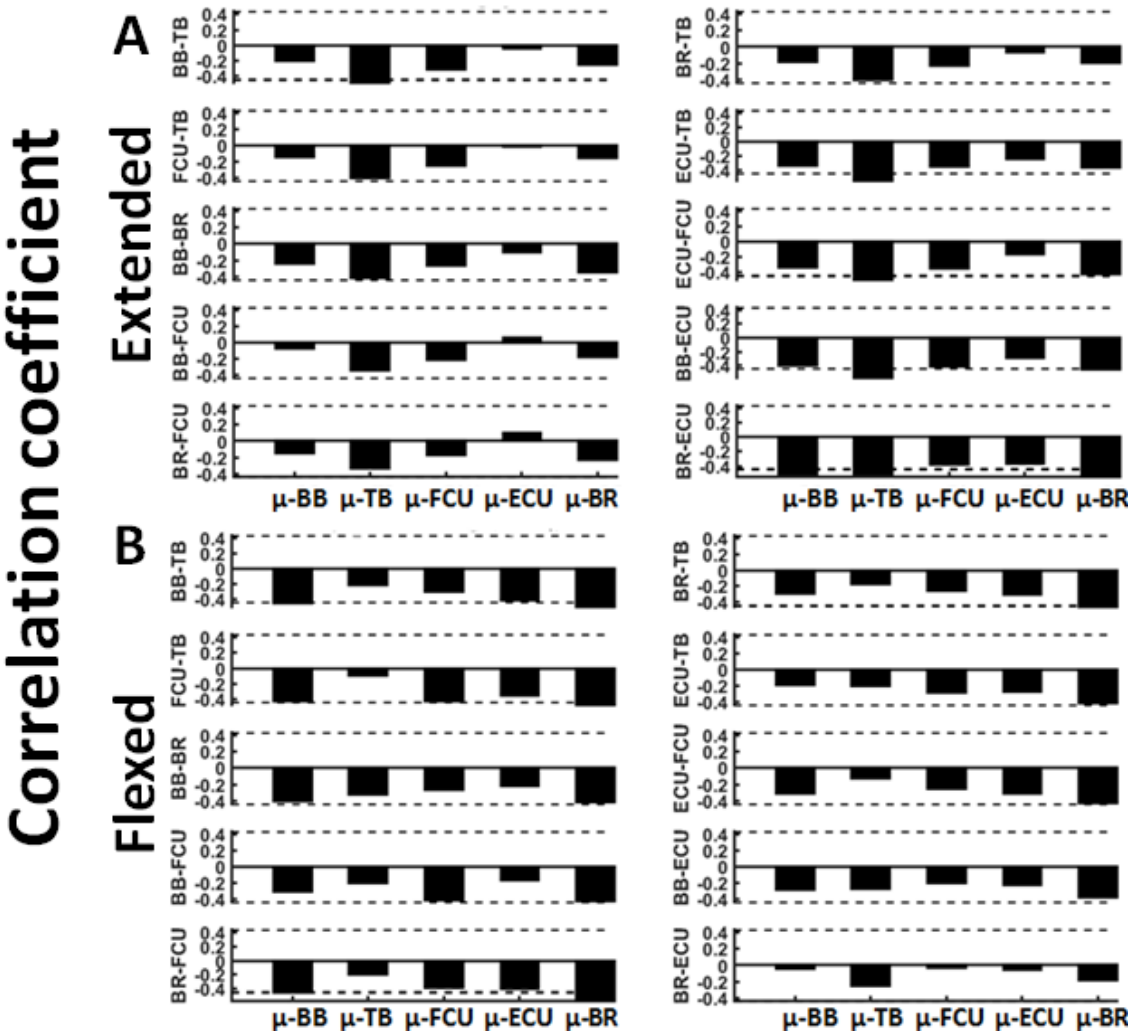

Figure 46 Correlation coefficients between μ-AEMG and coherence for all tested muscle pairs during steady coactivation at each end of the square-wave target: A, Extended arm, muscle pairs (BB-TB, FCU-TB, BB-BR, BB-FCU, BR-FCU, BR-TB, ECU-TB, ECU-FCU, BB-ECU, and BR-ECU); μ, mean AEMG (BB, TB, FCU, ECU, and BR); B, Flexed arm. Broken horizontal lines represent correlation coefficient at *P* = 0.05.

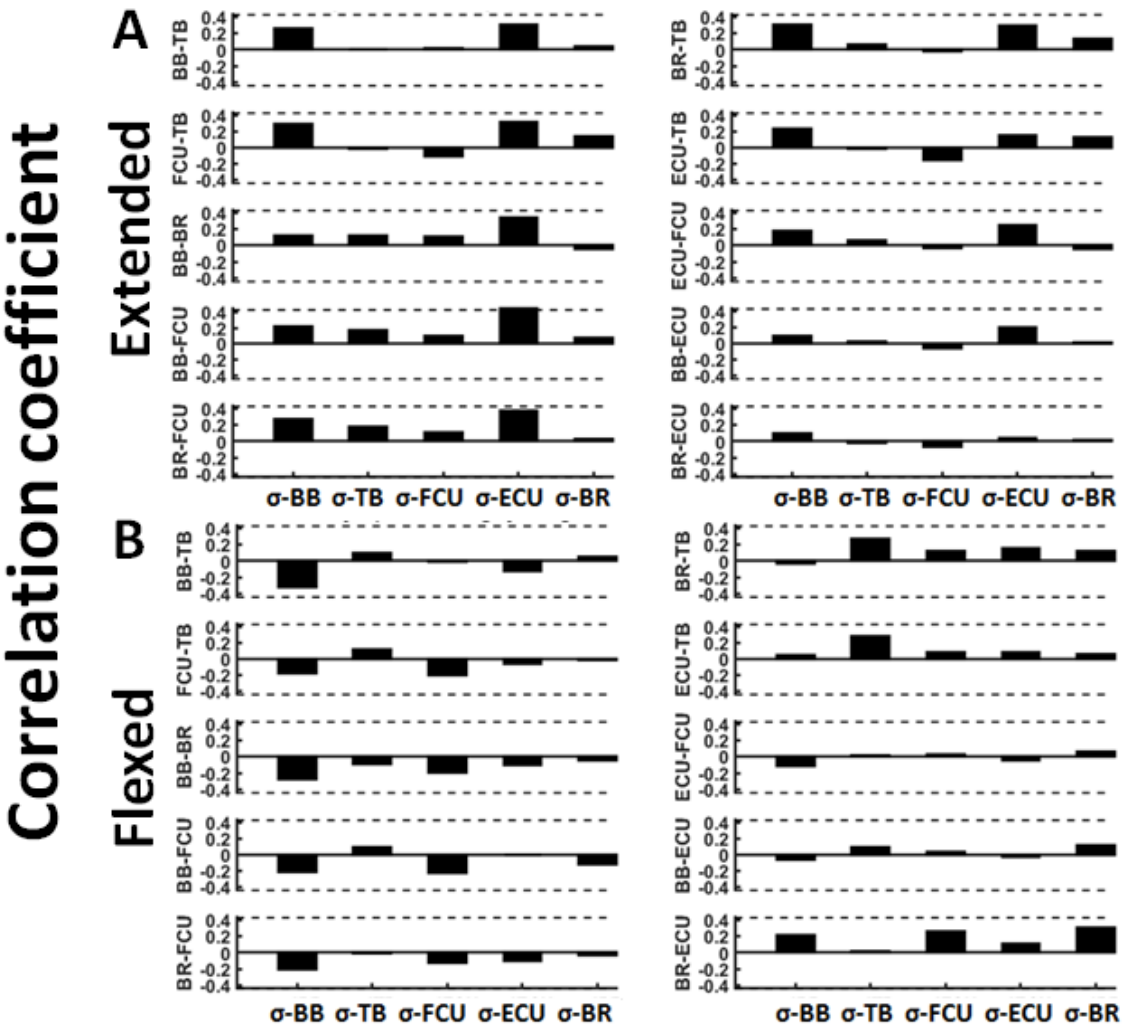

Figure 47 Correlation coefficients between σ-AEMG and coherence for all tested muscle pairs during steady coactivation at each end of the square-wave target: A, Extended arm, muscle pairs (BB-TB, FCU-TB, BB-BR, BB-FCU, BR-FCU, BR-TB, ECU-TB, ECU-FCU, BB-ECU, and BR-ECU); σ, standard deviation of AEMG (BB, TB, FCU, ECU, and BR); B, Flexed arm. Broken horizontal lines represent correlation coefficient at *P* = 0.05.

4.2.2 Correlation between oscillations and mechanical output

To address the second purpose of aim-III, and to extend the findings into mechanical motor output, amplitude and in-phase coherences were correlated for the ten pairs of

muscles with 8 different kinetic / kinematic variables for different trajectories (sine, square), different direction (pull, push), and different state (steady-state, transient). For instance, Figure 48 illustrates the negative correlation between RMSE of position and in-phase coherence for BB-BR pair in the slow quasi-constant velocity segment of the sine-wave trajectory, with a linear regression fit of all 20 subjects' data points. Figure 49 displays the correlation coefficient for five measures of mechanical output (rmsePOS, μ-FRC, σ-FRC, μ-STF, and σ-STF) and ten pairs of muscles in the slow push and pull directions in the slow quasi-constant velocity segment of sine-wave trajectory. Figure 50-A displays the correlation coefficient for the same five measures of mechanical output and six pairs of muscles that did not involve TB for amplitude coherences (BB-BR, BB-FCU, BR-FCU, ECU-FCU, BB-ECU, and BR-ECU). An in-phase coherence version of the same statistics is displayed in Figure 50-B. Subjects who achieved lower error (w.r.t. position, rmsePOS), lower mean stiffness and variability (μ-STF / σ-STF) and lower mean force (μ-FRC) tended to have greater coherence (amplitude or in-phase) in cases of statistical significance. Alternatively, subjects with lower force variability (σ-FRC) tended to have lower coherence in cases of statistical significances. Likewise, push target (Figure 49-A) had a similar relationship with lower correlation coefficients. There was no significant correlation between the coherence of other muscle pairs that involved (BB-TB, FCU-TB, BR-TB, and ECU-TB) and these mechanical variables. Note again that the correlation coefficients were below 0.5 even when significant due to the presence of multiple components and possible interference of action potentials. Such low correlation coefficients are common in physiological data.

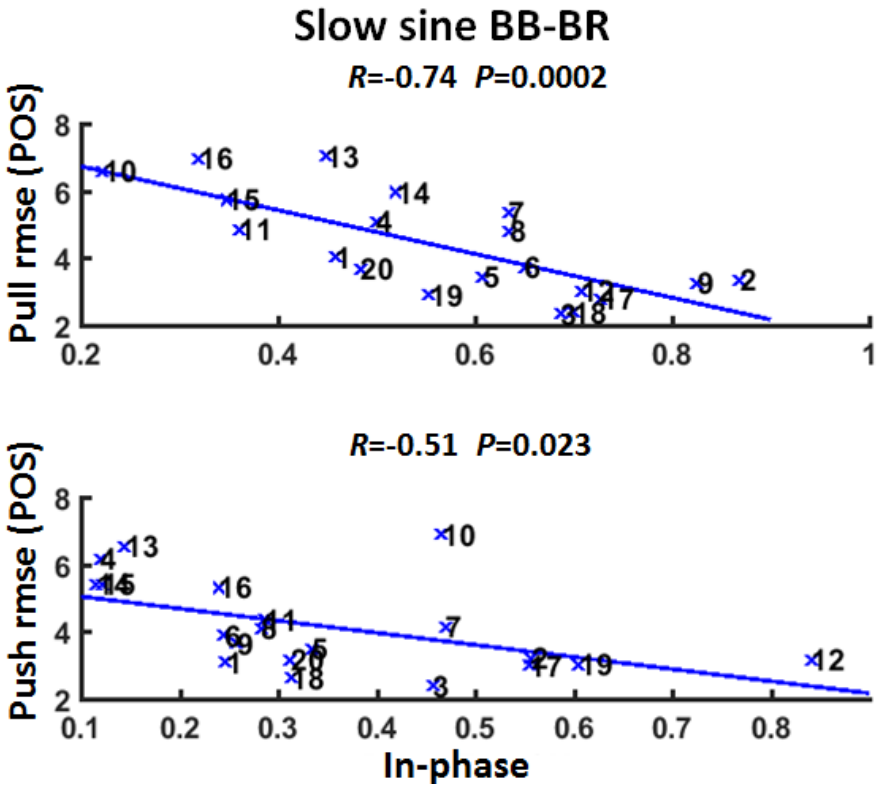

Figure 48 Correlation between RMSE of POS and in-phase coherence of BB-BR muscle pair during slow quasi-constant velocity in sine-wave trajectory across subjects: Top, pull (r = -0.74, P<0.001); Bottom, push (r = -0.51, P<0.05); Linear regression fit for twenty subjects' data points that are numbered and displayed.

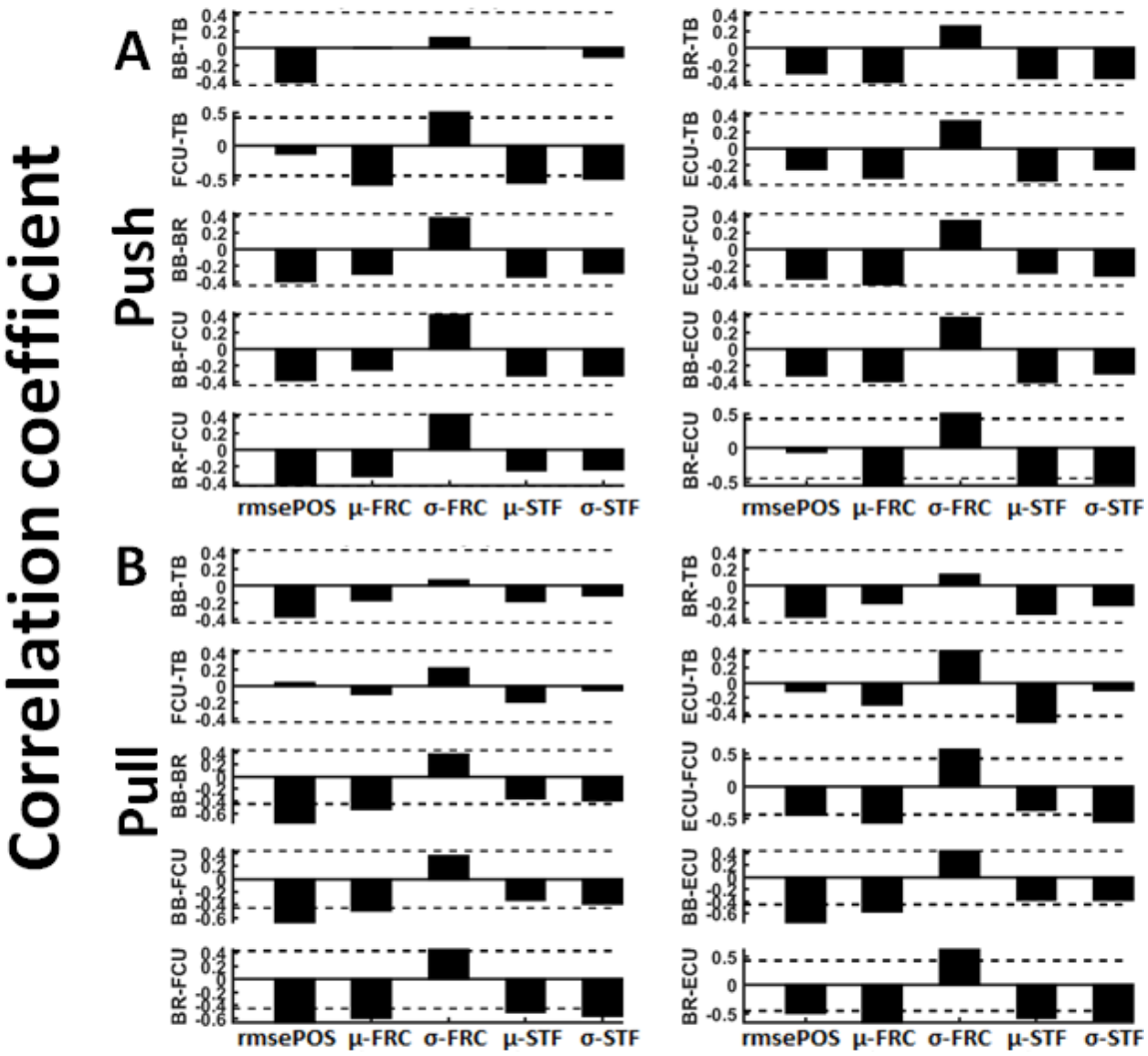

Figure 49 Correlation coefficients between amplitude coherence and measures of mechanical output during slow quasi-constant velocity in the sine wave trajectory in the push (A) and pull (B) directions. On the y-axis are coherences between muscle pairs (BB-TB, FCU-TB, BB-BR, BB-FCU, BR-FCU, BR-TB, ECU-TB, ECU-FCU, BB-ECU, and BR-ECU). Subjects with lower error (w.r.t. position, rmsePOS), lower stiffness mean / variability (μ-STF / σ-STF) and lower mean force (μ- FRC), are those who had a higher coupling of muscles. On the other hand, less force variability (σ-FRC) was associated with lower coherence. Broken horizontal lines represent correlation coefficient at *P* = 0.05.

Distribution of the correlation coefficient for the fast transient segment in the square-wave trajectory was similar to that of the sine wave trajectory preserving the relationship

between the coherence of some muscles and mechanical output (Figure 50-C). Likewise, transient sine trajectory (pull to push or push to pull) had a similar trend with different correlation coefficients.

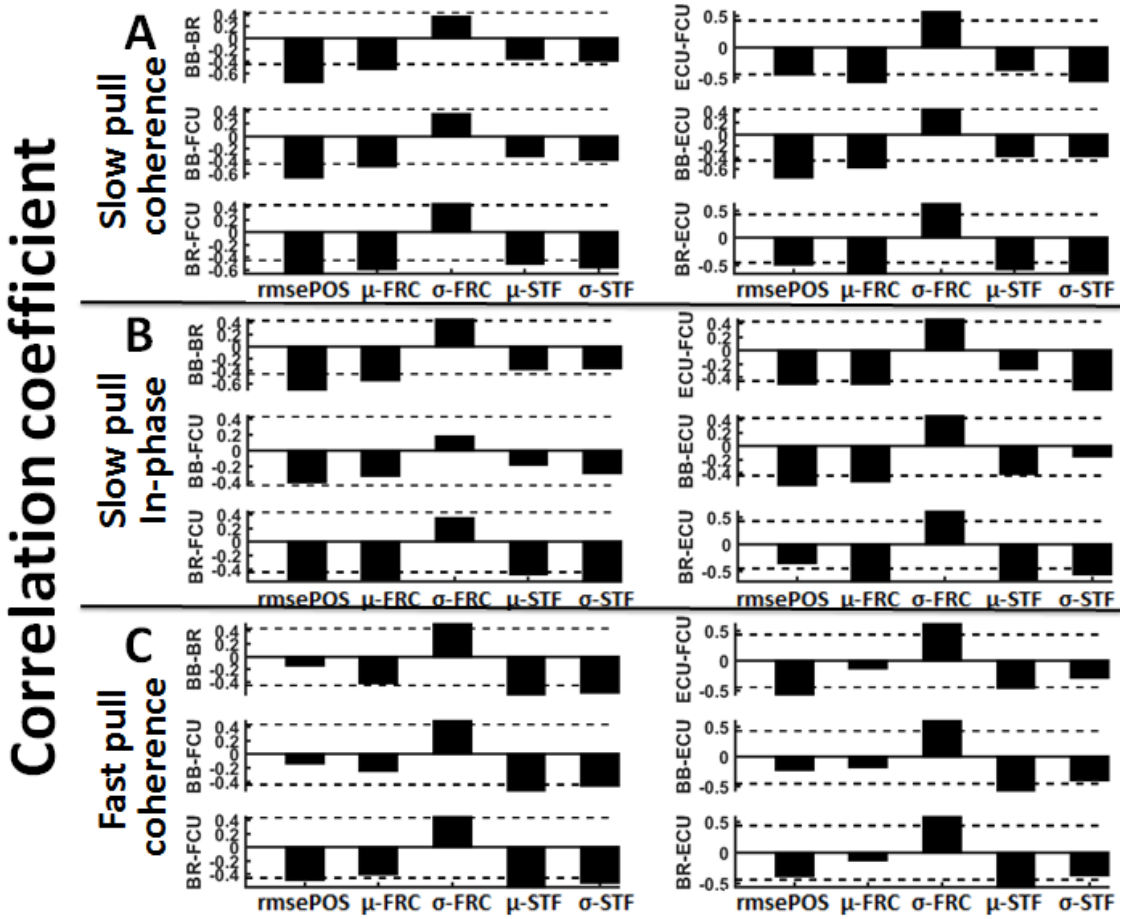

Figure 50 Correlation coefficients between muscle pairs that did not involve TB (BB-BR, BB-FCU, BR-FCU, ECU-FCU, BB-ECU, and BR-ECU) and measures of mechanical output in the pull direction: A, amplitude coherence during slow quasi-constant velocity in the sine wave trajectory; B, in-phase coherence during slow quasi-constant velocity in the sine-wave trajectory; C, amplitude coherence during the fast pull in the square-wave trajectory. Broken horizontal lines represent correlation coefficient at *P* = 0.05.

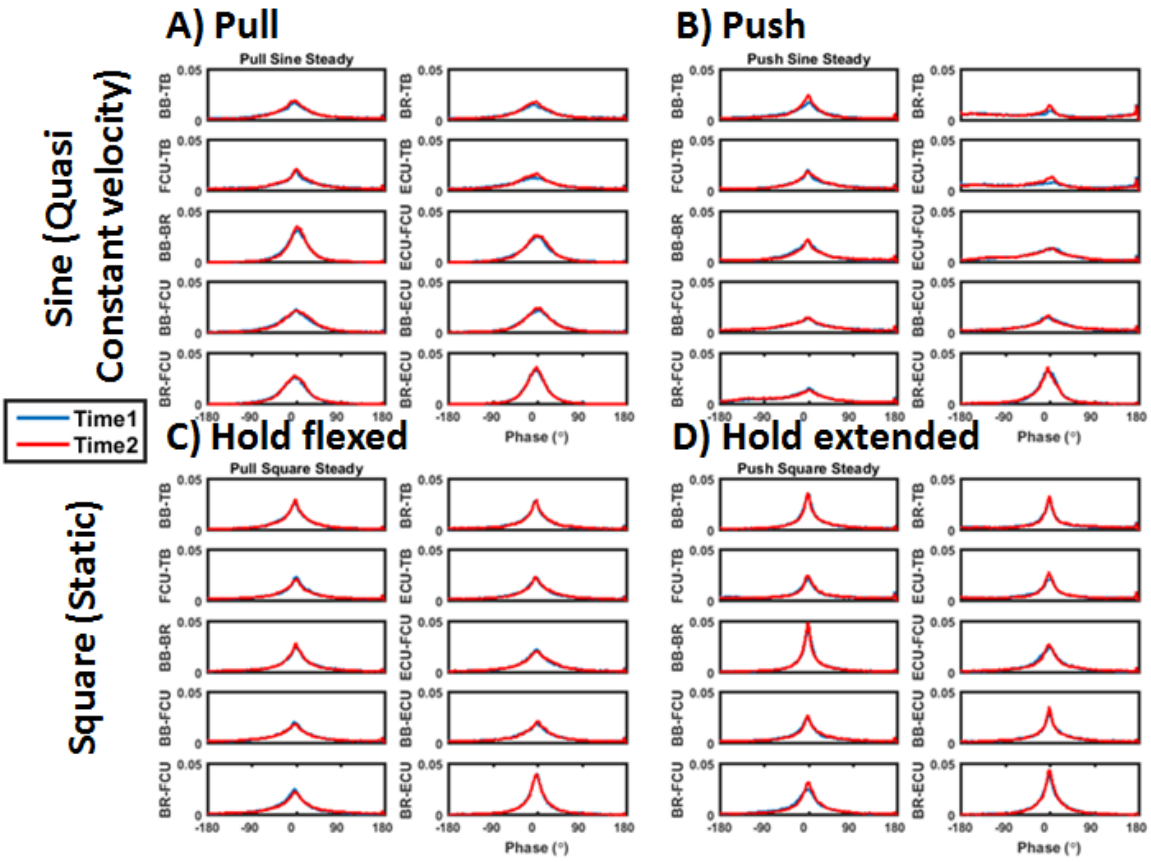

Figure 51 pdf of phase coherence during steady-state dynamic activation. Top, data during slow quasi-constant velocity in pull (A) and push (B) directions in the sine-wave trajectory. Bottom, data during static holding in flexed (C) and extended (D) position in the square wave trajectory. Ten pairs of muscles per each, averaged across subjects.

In-phase coherence during steady-state (Figure 51) or transient dynamic activation (Figure 52) did not change in either sine- or square-wave trajectory due to repetition. With visual inspection, subtle observational changes in the in-phase coherence appear to be in the direction of an increase in value (ex. push to pull for the sine-wave trajectory, Figure 52-B). There was no statistically significant effect of time, however.

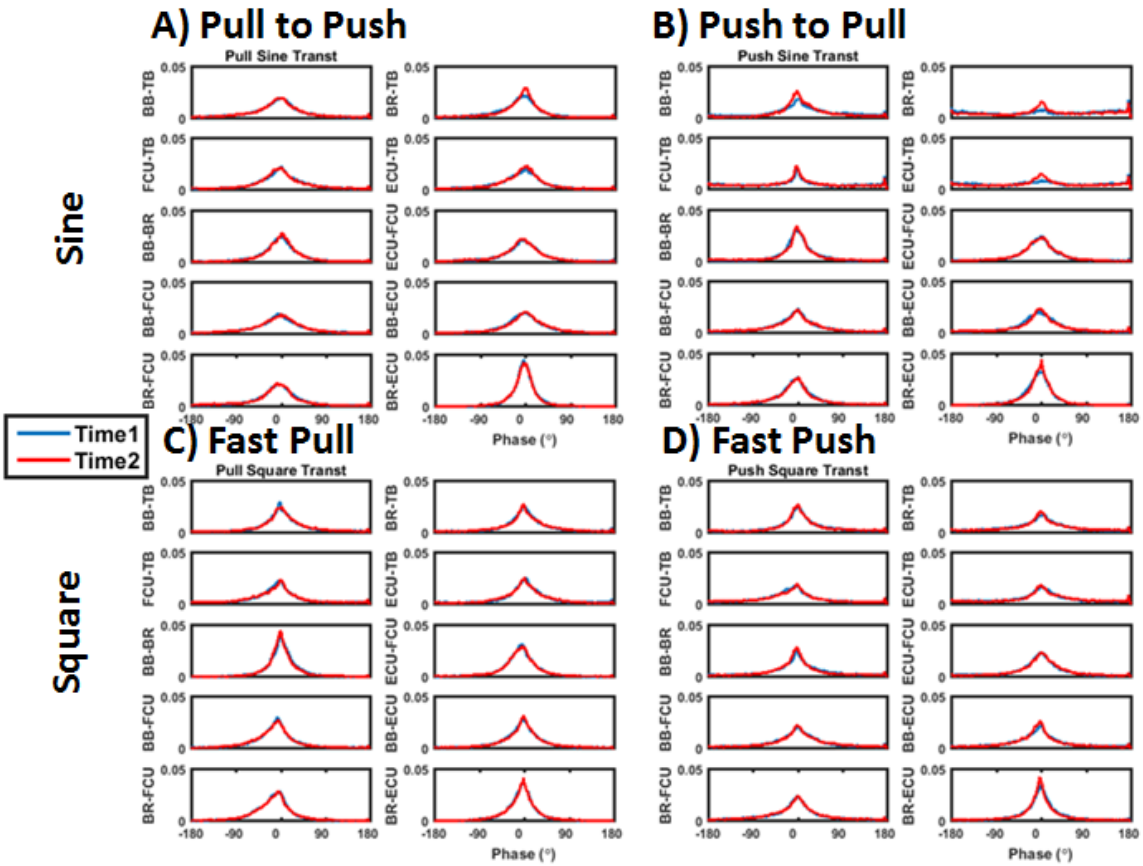

Figure 52 pdf of phase coherence during transient dynamic activation. Top, data during pull to push transition (A) and push to pull transition (B) in the sine-wave trajectory. Bottom, data during fast pull (C) and fast push (D) in the square-wave trajectory. Ten pairs of muscles per each averaged across subjects.

4.2.3 Correlated oscillations, neural and mechanical output effects

There was little to no statistically significant effect of time (apart from some minor changes in AEMG during sine trajectory). As a result, data from both times were combined in further analysis.

4.2.3.1 Measures of correlated oscillations

As for coherence, there was no significant main effect of time. It was non-significant for amplitude or in-phase metrics; push or pull; square or sine waves; steady-state or transient segments. Nevertheless, although not significant, coherences overall either increased or stayed the same after repetitions, but they rarely dropped (Table 13, and Table 14).

Table 13 Neural output and EMG oscillations during slow quasi-constant velocity coactivation and transient reverse direction coactivation in pull and push directions in the sine-wave trajectory, divided into 1st and 2nd half of trials.

	Slow coactivation (Quasi-constant velocity)				Reverse direction coactivation (Transient)			
	Pull		Push		Pull to Push		Push to Pull	
	Time 1	Time 2	Time 1	Time 2	Time 1	Time 2	Time 1	Time2
μ-% AEMG	60.5 (18.0)	55.3 (18.2)	41.6 (16.0)	36.7 (14.5)	52.0 (12.7)	45.9 (12.6)	54.3 (13.7)	48.3 (13.8)
σ-% AEMG	46.2 (20.6)	42.7 (18.8)	32.7 (18.5)	30.2 (18.1)	40.0 (20.3)	37.6 (20.3)	45.2 (21.8)	41.6 (21.2)
Coherence	0.576 (0.096)	0.592 (0.094)	0.533 (0.102)	0.535 (0.107)	0.588 (0.096)	0.596 (0.098)	0.558 (0.111)	0.578 (0.121)
In-phase %	13.2 (7.60)	14.4 (8.31)	9.8 (8.52)	10.7 (10.41)	13.8 (7.70)	14.4 (7.82)	12.3 (9.90)	14.1 (12.94)

Mean and standard deviation of AEMG (averaged across BB, TB, BR, FCU, ECU) after MVC normalization. Coherence, mean area of event-related amplitude coherence between muscles; In-phase, percentage of corresponding phase coherence between ±5 degrees; Time 1&2, averaged data across first and second sets of 5 trials each; MVC, maximal voluntary contraction.

There was, however, a main effect of target direction in amplitude coherence or in-phase coherence in a few segments. In the quasi-constant velocity segment of the sine-wave trajectory, amplitude coherence was not significantly different between direction

(pull, 0.584±0.095; push, 0.534±0.105), but in-phase coherence was higher in pull than push direction (pull, 14.1±7.8; push, 10.0±9.2, $P < 0.01$).

In the steady coactivation segment of the square-wave trajectory, amplitude coherence was not significantly different between arm positions (flexed, 0.611±0.118; extended, 0.614±0.147), but in-phase coherence was lower in the arm flexed than extended position (flexed, 14.2±10.5; extended, 17.0±15.4, $P < 0.05$). In the transient fast coactivation segment of the square-wave trajectory, higher values were found in fast pull than fast push for both amplitude coherence (fast pull, 0.650±0.094; fast push, 0.590±0.110, $P < 0.01$), and in-phase coherence (fast pull, 16.5±9.2; fast push, 13.5±10.4, $P < 0.05$).

Table 14 Neural output and EMG oscillations during steady coactivation while holding with arm flexed/extended and transient fast coactivation for pull/push in the square-wave trajectory, divided into 1st and 2nd half of trials.

	Steady coactivation (Static)				Fast coactivation (Transient)			
	Hold flexed		Hold extended		Fast Pull		Fast Push	
	Time 1	Time 2	Time 1	Time 2	Time 1	Time 2	Time 1	Time2
μ-% AEMG	32.9 (22.4)	30.6 (20.3)	38.7 (23.8)	39.0 (23.8)	52.0 (12.7)	45.9 (12.6)	54.3 (13.7)	48.3 (13.8)
σ-% AEMG	23.0 (20.7)	20.4 (18.9)	26.0 (22.8)	26.3 (23.7)	40.0 (20.3)	37.6 (20.3)	45.2 (21.8)	41.6 (21.2)
Coherence	0.612 (0.121)	0.611 (0.115)	0.615 (0.140)	0.613 (0.154)	0.648 (0.093)	0.652 (0.095)	0.583 (0.101)	0.597 (0.119)
In-phase %	14.3 (10.7)	14.2 (10.4)	16.3 (13.9)	17.8 (16.8)	16.4 (8.5)	16.6 (10.0)	12.9 (9.1)	14.0 (11.6)

Mean and standard deviation of AEMG (averaged across BB, TB, BR, FCU, ECU) after MVC normalization: Coherence, mean area of event-related amplitude coherence between muscles; In-phase, percentage of corresponding phase

coherence between 0 ± 5 degrees; Time 1&2, averaged data across first and second sets of 5 trials each; MVC, maximal voluntary contraction.

4.2.3.2 Neural output

Mean (activation level) and standard deviation (variability) of AEMG signals were assessed for all five muscles (BB, TB, BR, FCU, and ECU) after normalizing per each muscle (Table 13, and Table 14). There was no time effect on mean activation level or variability of AEMG in the sine- or square-wave trajectories.

There was, however, a main effect of target direction. In the steady-state quasi-constant velocity segment of the sine-wave trajectory, the values were higher in pull than push direction for both standard deviation of AEMG (pull, 44.46±19.67; push, 31.45±18.30, $P < 0.05$) and mean AEMG (pull, 57.91±18.08; push, 39.16±15.25, $P < 0.05$). In the transient fast coactivation segment of the square-wave trajectory, the values were greater in fast pull than fast push for both standard deviation of AEMG (fast pull, 49.77±21.21; fast push, 29.05±18.18, $P < 0.05$) and mean AEMG (fast pull, 56.18±17.62; fast push, 37.76±15.07, $P < 0.05$). No significant effect of target direction was found in the reverse direction coactivation segment of the sine-wave trajectory or the static steady coactivation segment of the square-wave trajectory.

Table 15 Mechanical output during slow quasi-constant velocity coactivation and transient reverse direction coactivation in pull and push directions in the sine-wave trajectory, divided into 1st and 2nd half of trials.

	Slow coactivation (Quasi-Constant velocity)		Reverse direction coactivation (Transient)	
	Pull	**Push**	**Pull to Push**	**Push to Pull**

	Time 1	Time 2	Time 1	Time 2	Time 1	Time 2	Time 1	Time2
RMSE POS	4.42 (2.51)	4.40 (2.45)	4.23 (2.10)	4.17 (2.15)	3.19 (1.78)	2.83 (1.30)	3.27 (1.91)	2.82 (1.34)
σ-POS	2.73 (1.71)	2.32* (0.97)	2.51 (0.97)	2.24* (0.86)	2.39 (1.31)	2.20 (1.16)	2.48 (1.45)	2.16 (1.12)
μ-ACC	2.45 (0.96)	2.69 (0.83)	2.51 (0.84)	2.63 (0.79)	3.19 (1.07)	3.00 (1.10)	3.25 (1.20)	2.93 (1.13)
σ-ACC	4.47 (0.89)	4.52 (0.88)	4.44 (0.94)	4.44 (0.89)	4.09 (1.08)	3.91 (1.09)	4.03 (1.12)	3.86 (1.11)
μ-FRC	28.16 (6.33)	27.44 (5.77)	31.82 (6.17)	32.16 (5.89)	24.60 (7.07)	21.99* (6.53)	28.82 (6.59)	27.74 (7.05)
σ-FRC	10.79 (3.16)	10.47 (3.02)	10.27 (3.02)	9.73 (2.99)	10.32 (3.05)	9.91 (2.8)	11.59 (3.04)	11.61 (3.18)
μ- STF	9.87 (4.43)	10.13 (4.40)	11.37 (4.43)	12.25 (4.67)	9.09 (3.40)	7.95* (3.38)	10.50 (3.77)	9.65 (3.83)
σ-STF	10.54 (1.78)	10.16 (1.76)	11.31 (2.03)	11.25 (1.91)	9.67 (2.54)	9.04 (2.59)	10.97 (2.56)	10.92 (2.85)

RMSE POS, root mean square error of position; σ-POS, standard deviation of position; μ-ACC, mean acceleration; σ-ACC, standard deviation of acceleration; μ-FRC, mean force; σ-FRC, standard deviation of force; μ-STF, mean stiffness; σ-STF, standard deviation of stiffness; Time 1&2, averaged data across first and second sets of 5 trials each; *, $P < 0.05$. Values are mean (standard deviation) across subjects.

Table 16 Mechanical output during steady coactivation while holding with arm flexed / extended and transient fast coactivation for pull / push in the square-wave trajectory divided into 1st and 2nd half trials.

	Steady coactivation (Static)				Fast coactivation (Transient)			
	Hold flexed		Hold extended		Fast Pull		Fast Push	
	Time 1	Time 2	Time 1	Time 2	Time 1	Time 2	Time 1	Time2
RMSE POS	1.39 (1.65)	1.07 (1.22)	1.22 (1.77)	1.01 (1.34)	18.76 (5.81)	18.62 (6.12)	18.34 (5.83)	17.86 (5.88)
σ-POS	0.79 (1.47)	0.55 (1.15)	0.74 (1.61)	0.59 (1.26)	14.27 (3.47)	14.21 (3.76)	14.33 (3.55)	14.15 (3.81)
μ-ACC	0.36	0.24	0.26	0.24	4.62	4.54	4.55	4.58

	(0.68)	(0.58)	(0.51)	(0.59)	(1.14)	(1.18)	(1.09)	(1.10)
σ-ACC	2.00	1.55*	1.76	1.71	6.55	6.67	6.34	6.66
	(1.43)	(1.32)	(1.29)	(1.24)	(2.13)	(1.72)	(1.53)	(1.58)
μ-FRC	8.41	7.26	9.93	7.95	28.78	27.45	30.45	29.46
	(6.62)	(5.88)	(8.39)	(7.96)	(6.64)	(6.92)	(6.47)	(6.30)
σ-FRC	6.25	5.23*	6.66	5.95	23.99	26.44	25.18	26.67
	(4.01)	(3.79)	(4.45)	(3.98)	(7.67)	(7.82)	(7.40)	(7.97)
μ-STF	0.43	0.19**	0.43	0.28	6.73	5.92	7.07	6.45
	(1.13)	(0.47)	(1.01)	(0.77)	(2.80)	(2.45)	(2.86)	(2.59)
σ-STF	4.00	3.04**	4.33	3.85	7.75	7.40	8.49	8.15
	(3.00)	(2.82)	(3.46)	(3.36)	(2.38)	(2.53)	(2.82)	(2.86)

RMSE POS, root mean square of position; σ-POS, standard deviation of position; μ-ACC, mean acceleration; σ-ACC, standard deviation of acceleration; μ-FRC, mean force; σ-FRC, standard deviation of force; μ-STF, mean stiffness; σ-STF, standard deviation of stiffness; Time 1&2, averaged data across first and second sets of 5 trials each; *, $P < 0.05$; **, $P < 0.01$. Values are mean (standard deviation) across subjects.

4.2.3.3 Mechanical motor output measurements

Mechanical output signals (Position, Velocity, Acceleration, Force, and Stiffness) were collected for both sine and square waveforms (Table 15 and Table 16) during a train of events (Figure 41, A&B). In the reverse direction coactivation segment of the sine-wave trajectory, mean force decreased in the second half trials for pull to push (by 10.6%, $P<0.05$), (Table 15). In this segment, mean stiffness also decreased in the second half trials for pull to push (by 12.5%, $P<0.05$). For the steady coactivation segment of the square-wave trajectory, mean STF in the flexed position was decreased in the second half trials (by 56%, $P < 0.05$), (Table 16). The standard deviation of STF in the second half trials was also reduced in the flexed position (by 24%, $P < 0.01$). For the slow

coactivation segment of the sine-wave trajectory, the standard deviation of POS was reduced in the second half trials (pull, by 15.1%, $P < 0.05$; push, by 10.8%, $P < 0.05$) (Table 15).

4.2.4 Task posture effect

The general behaviour of each muscle can be described qualitatively as below, based on the average signals in Figure 41. On average, in the sine-wave trajectory, TB was active as an agonist during slow coactivation in the push segment (antagonists: BB and BR muscles), whereas it was less active in the pull segment (Figure 41-C). When the activation of TB was at its peaks during the push segment, all other measured muscles were at their minimum amplitude. All four other muscles are similar to each other on average. BR AEMG average across subjects seems to alternate synchronization between BB (during push stage) and FCU / ECU (during pull stage). Maximum correlated coherence across all ten pairs is between BR-ECU ($r = 0.68$). There was a minor peak for TB as the target goes from pull to push. FCU and ECU muscles were mostly similar to each other throughout all tasks (except for a short period during pull action) on average across subjects. BR was similar to BB in the push segment and to FCU / ECU in the pull segment. Second highest correlated coherence across all ten pairs is between BB-BR ($r = 0.65$).

During steady coactivation segment in the square-wave trajectory (Figure 41-D), on the other hand, all five muscles are somehow similar toward each other on average. BR is similar to BB throughout the trajectory. While maximum correlated coherence across the ten muscle pairs is between BR-ECU ($r = 0.70$), second highest correlated coherence is between BB-BR ($r = 0.66$). FCU and ECU muscles were mostly alike during square

trajectory (except when they were in the extended position). During transient fast coactivation segment in the square-wave trajectory, TB was at its maximum during the fast push. During fast pull, all muscles except TB were at their maximum.

Table 17 summarizes average amplitude and in-phase coherence for each segment of sine- and square-wave trajectories divided into pulling and pushing directions. It highlights the level of coherence (amplitude and in-phase) across different tasks. Fast pull and steady extended coactivation had the highest coherences implying that muscles worked most in tandem in these cases.

Table 17 Average amplitude and in-phase coherences in each direction for each coactivation segment of sine- and square-wave trajectories.

	Segment	Coherence	In-phase %
Sine	Slow coactivation (pull / push)	0.580 / 0.530	14.0% / 10.0%
	Reverse direction coactivation (pull to push / push to pull)	0.592 / 0.568	14.1% / 13.2%
Square	Steady coactivation (flexed / extended)	0.611 / 0.614	14.2% / 17.0%
	Fast coactivation (pull / push)	0.650 / 0.590	16.5% / 13.5%

Data were averaged across muscle pairs and subjects

4.2.5 Higher-frequency oscillations

During dynamic coactivation task, correlated oscillations (coherence) were observed at 20 Hz (Figure 53), as well as its harmonics at lower amplitudes (i.e., 40, 60, and 80 Hz) in EMGs. These oscillations were frequent in all ten pairs of muscles, sine or square waves, although they were more prominent in the latter.

During steady or slow coactivation, these higher-frequency oscillations were consistent; however, it is weakened during transient fast pull / push or reverse direction pull to push tasks during sine trajectory. It is possible that these high-frequency oscillations are amplified by the mechanical behavior of the robotic system during steady or slow coactivation, however, a neural factor cannot be ruled out.

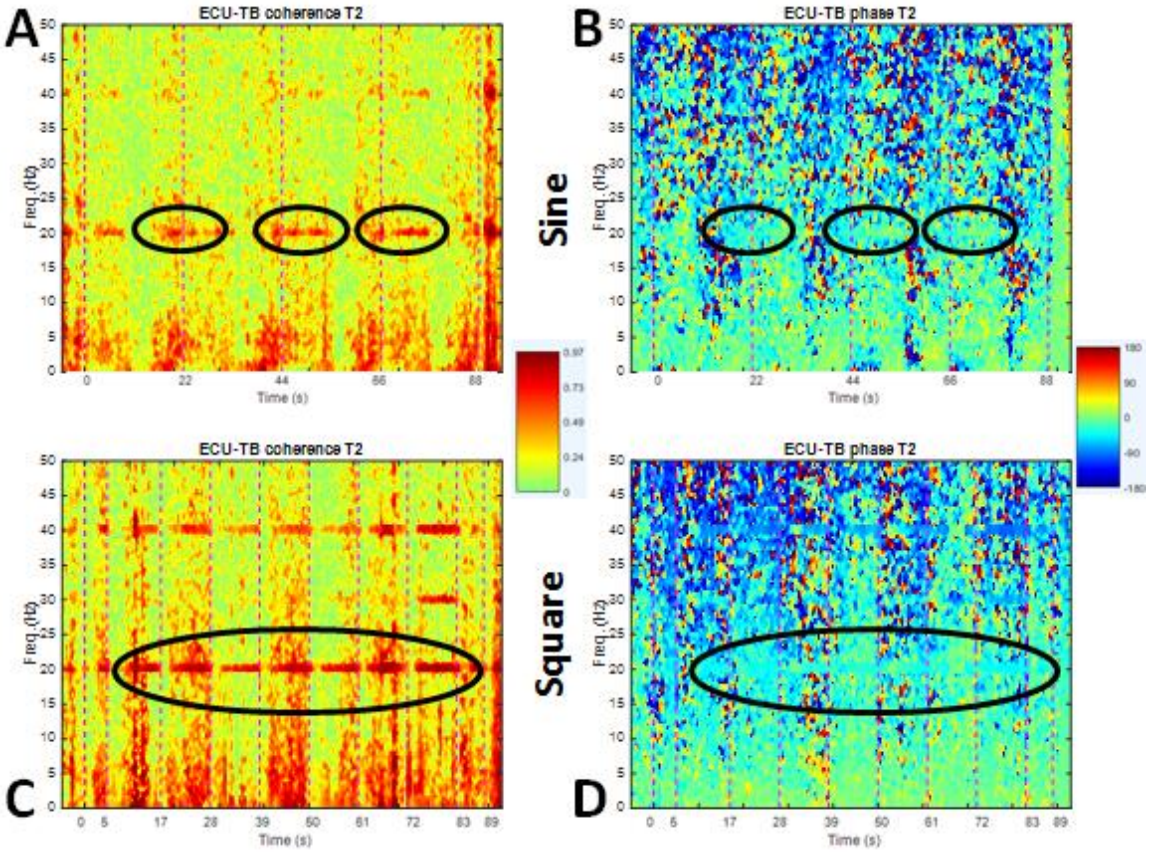

Figure 53 Higher-frequency coherence in EMG between a muscle pair (ECU-TB as an example), during the second set of trials (T2) for sine (A, B) and square-wave (C, D) trajectories. Amplitude coherence is shown in column 1, and phase coherence is shown in column 2. Average data across subjects.

4.2.5.1 FFT vs. Wavelet correlated oscillations

Correlated oscillations were computed using both FFT and sinusoidal Wavelet (Figure 54 as an example) methods. Although Wavelet had more potential advantages over FFT based methods overall, its strength was more present in higher frequencies. However, the main focus of this study is on low frequencies < 3 Hz.

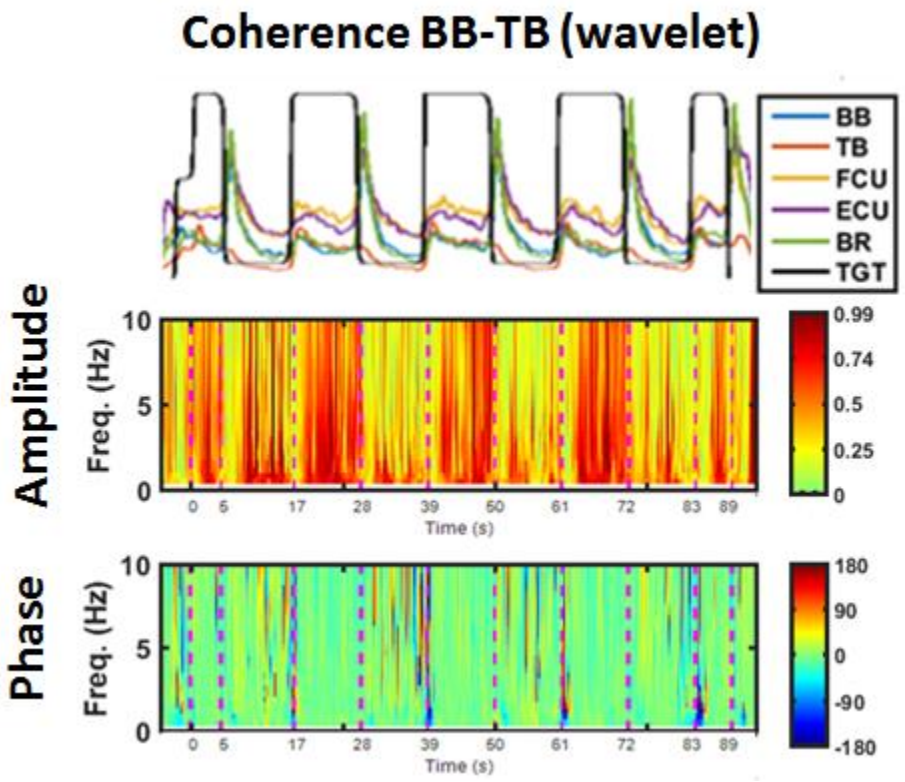

Figure 54 Event-related coherence amplitude and phase using sinusoidal Wavelet for BB-TB pair for the square-wave trajectory. Target trajectory and AEMG behaviors are shown on the top. Average data across subjects.

4.2.6 Discussion

The study aimed to 1) determine whether there is an underlying association between the low-frequency correlated neural oscillations between muscles and the mean activation level and variability of AEMG during steady coactivation task across individuals, 2) determine whether there is an underlying association between the low-frequency correlated neural oscillations between muscles and the mechanical output performance and characteristics (a- position accuracy, and b- endpoint stiffness) during slow coactivation task across individuals. The main findings are as follows: 1) Mean activation level of AEMG during the steady coactivation segment was negatively correlated to the amount of low-frequency correlated neural oscillations in some muscles across subjects when holding at each end of the square-wave trajectory, i.e., static contraction (Figure 46). However AEMG variability was not significantly correlated with slow oscillations (Figure 47); and 2) Some measures of mechanical output (a- position error, b- endpoint stiffness) during slow quasi-constant velocity coactivation segment in the pull direction were negatively correlated to the amount of low-frequency correlated neural oscillations in some muscle pairs that did not involve TB across subjects (Figure 49, Figure 50).

In this aim-III, it was anticipated that the role of in-phase low-frequency correlated neural oscillations found in the static cocontraction in aim-1 may still apply to non-static activations when moving the limb at least slowly during interaction with a robot. However, due the absence of intervention, the relatively high in-phase coherence observed in most of the cases, in addition to the vast differences between the two experiments, the results were not as straightforward.

The negative linear relationship between coherence and mean activation level of AEMG (i.e., higher coherence is associated with lower mean activation level of AEMG) for steady coactivation in the square-wave trajectory (Figure 46) does not have references to compare to in aim-I because this relationship was not examined, and mean activation level of AEMG was designed to be comparable across subjects in aim-I. The absence of a significant correlation between coherence and variability in AEMG for the corresponding segment (Figure 47) did not support the findings of aim-I: lower coherence is correlated with lower AEMG variability and error (higher mean activation level of AEMG is related to higher variability). The possible factor that may have influenced this discrepancy could be related to differences between experiment II / experiment I that includes presence / absence of vibration, unintentional / intentional coactivation, constant position / AEMG requirement and feedback. For example, it is possible that the open-ended instruction to hold the vibrating robotic arm steadily in place did not put any constraints on activating muscles systematically across subjects (i.e., subjects followed different strategies or activation levels to meet requirements).

Kinetic and kinematic sensors such as force, position, and acceleration measure physical properties that are stationary. On the other hand, a biological signal such as electromyogram is harder to measure and quantify for various reasons: Placement and preparation of electrodes, skin conductance properties, muscle properties, the strategy followed in conducting tasks during the experiment, repeatability of the task, the potential of fatigue (8) and many more. As a result, correlating mechanical and neural features is of high value. When two measures are highly correlated, if one is more readily available, it could help predict the other.

There was indeed a correlation between mechanical output and coherence (amplitude and in-phase) at least for some muscle pairs. Error, as measured by the root mean square of the difference between position and target during quasi-constant velocity contraction in the pull direction of the sine-wave trajectory, had a negative correlation with either type of coherence in some muscle pairs across subjects (Figure 49, Figure 50). In other words, subjects with less targeting error during the task tended to have higher coherence between those muscles. This was opposite to aim-I finding (less targeting error with lower coherence). Any of the following might have contributed to such discrepancy: Having a dynamic task, position based target and feedback or involuntary coactivation. Voluntary cocontractions based on AEMG feedback could induce different influence on correlated oscillations than involuntary coactivation such as position feedback. In the former, subjects are directly targeting activation of both muscles whereas, in the latter, activating muscles became secondary to matching the position to the target. Adding vibration to the task could be a possible cause for the reversal of such relationship as well. Isometric exercises were compared in the presence and absence of vibration for their effect on the activation and coactivation of BB and TB muscles (33). It has been found that devices vibration increased both activation and coactivation of muscles. These findings, together with the observation that many of the muscles in both transient and steady-state tasks behaved similarly to each other in experiment II could imply that vibration facilitated higher coherence. As such, an association between higher coherence and lower position error was observed.

Endpoint stiffness was negatively correlated to the coherence of some muscle pairs across subjects during slow quasi-constant velocity coactivation in the push / pull

direction of the sine-wave trajectory (Figure 49). It means that subjects with greater decoupling of those muscle pairs tended to have higher endpoint stiffness. To suppress the mechanical consequence of vibration, it is possible that subjects would coactivate their muscles more. Hence the association between higher coherence and lower endpoint stiffness was observed. A similar negative correlation existed for the transient stage as the fast pull in the square-wave trajectory in some muscle pairs (Figure 50-C). As for steady coactivation in the square-wave trajectory, it is meaningless to compute and correlate endpoint stiffness since there was no displacement.

Tonic vibration reflex is a persistent contraction of the muscle under the effect of pulsation. Such reflex is the result of vibratory activation of muscle spindles, those receptors sensitive to stretch. It is usually evoked by a vibrating electrical motor with an eccentric load on its shaft on a muscle's tendon between 20 and 100 Hz. Vibration activates muscle spindles in addition to receptors of the skin and tendons. Muscle spindle discharges are directed to the spinal cord via afferent nerve fibers activating synaptic reflex arcs and therefore prompting the muscle to contract. As an illustration and validation, vibration exercise at 28 Hz has been shown to have an increase in the activation and coactivation of BB and TB (33). Current findings deviated from the static experiment I likely due to the added vibration, at least partially, although other factors cannot be assessed until a future dynamic experiment is designed and tested to investigate similar hypotheses with the absence of vibration.

There was no main effect of time in correlated oscillations. The short duration of the task (13 mins per all ten repetitions) possibly was not enough to see desired differences.

However, there were also other important reasons for the absence of differences such as vibration, the absence of intervention, or indirect activation of muscles. Involuntary coactivation with position feedback is used that could be slower to respond to changes compared to voluntary cocontraction with AEMG feedback (aim-I). Alternatively, the absence of oscillations time effect implies that this study was not able to modulate coherence via repetition or other means.

Each muscle has different functions. For instance, BB is a tonic (5) muscle (flexor, slow twitch, balance posture, prone to tightness or shortness), while TB is a phasic (5) muscle (extensor, flaccid, fast twitch, movement, prone to weakness and inhibition). During the dynamic task, the posture of the required experiment would influence the role of agonist and antagonist muscles in a fundamental way that needs to be taken into consideration for understanding coactivation. This is different from aim-I because the task objective is to minimize position error irrespective of any constraints on muscles during the current task. In other words, subjects could adopt other strategies that do not rely much on muscle coactivation to achieve the required results introducing a challenging real-world scenario that was not present in experiment I. As a result, for dynamic coactivation, posture and other potential strategies effects need to be accounted for in experimental design and analysis.

Other notable observations during aim-III included the comparison between slow and fast coactivation. Similar to aim-II conclusion, there was some resemblance between transient and steady-state coactivation. Measured characteristics of mechanical output

during the transient fast coactivation segment in pull or push direction turned out to be similar (with different intensities) to those in slow quasi-constant velocity coactivation segment in pull or push direction in the sine-wave trajectory (Figure 50). More, the large measures of in-phase coherence statistics gave a clear reason why no change was present in the main effect due to repetition. In-phase statistics, again, confirmed its usability as a tool in the study of correlated oscillations.

The physiological requirement of experiment II is far different from experiment I. Accordingly, it appears experiment II has conflicting results from experiment I. Subjects with higher coherence between some of the measured muscle pairs tended to have lower position error, lower endpoint stiffness, and lower mean activation level of AEMG in some muscles depending on the details of the task (Figure 46, Figure 49, Figure 50). Although other influences are not ruled out, indication points to the conventional controller vibration that was added to the robotic arm to induce muscle coactivation. This vibration may have influenced the subjects' strategies in the control of the robotic arm so that the association between high muscle coherence in conjunction with reduced endpoint stiffness and reduced error was observed. Although the primary focus is on antagonist muscles, subjects exercised the majority of their muscles in a similar fashion toward each other in completing the task. Such findings confirm that physiological neural system is not hard-wired, but it adapts to the requirements to complete the task, and thus cannot be studied in isolation of the properties of the robotic system. Integration into a real-world application could be hardware and task-specific.

4.2.7 Conclusions

The significant findings were: 1) Mean activation level of AEMG during steady coactivation segment at each end of the square-wave trajectory was negatively correlated to the amount of low-frequency correlated neural oscillations in some muscles across subjects. However AEMG variability was not significantly correlated with low-frequency oscillations; and 2) some measures of mechanical output (a- position error, and b- endpoint stiffness) during slow quasi-constant velocity coactivation segment in the pull direction are negatively correlated to the amount of low-frequency correlated neural oscillations in some muscle pairs that did not involve TB. These findings were in conflict with aim-I likely because of differences in the task, including added vibration that was supposed to increase coactivation between muscles leading to an increase in coherence. There was no main effect of time (repetition) on coherence (amplitude or in-phase). However, with repetition, position error decreased during the slow coactivation segment of the sine-wave trajectory, and mean value and variability of endpoint stiffness decreased during the static steady coactivation segment of the square-wave trajectory. These results reaffirm that a generalized model does not exist; instead, any possible HRI integration needs to take into consideration both hardware and task dependencies.

CHAPTER 5. OVERVIEW

5.1 Putting it all together

Two experiments, 80 subjects, and three specific aims were concluded. Specific or generalized patterns, processes, models, and classes were explored. In other words, a framework based on the previous findings was built in order to infer the most reliable information. For instance, one would assess and communicate expertise level to an impedance controller for HRI application; or in clinical settings, one would identify a set of tasks to intervene with motor neuron tremor induced processes in Parkinson's disease through repetition or intervention. A fundamental neural process typical to some tasks in hand (steady-state or transient, static or dynamic, and many others summarized in Table 18) did not emerge, but there were instead multiple task-specific processes. There were many relationships between oscillations and system output that could be taken advantage of for better HRI; however, these are limited in scope. A closing summary follows.

Table 18 Summary of the three aims and their components

Aim-I	Aim-II	Aim-III
1. Steady-state	1. Transient / Intervention	1. Steady-state / Transient
2. Static	2. Static	2. Static / Dynamic
3. Cocontraction (intentional)	3. Cocontraction (intentional)	3. Coactivation (unintentional)
4. Steady	4. Steady	4. Steady / slow / fast
5. Test & Repetition	5. Practice & Repetition	5. Repetition
6. Performance vs. Oscillations	6. Performance vs. Oscillations	6. Neural / Mech. Out vs. Oscillations
7. Match High / Low AEMG target	7. Match High / Low AEMG target	7. Match position

8. BB / TB / BR	8. BB / TB / BR	8. BB / TB / BR / FCU / ECU
9. BB HIGH/TB LOW and vice versa	9. Rise / Fall / alternate level	9. Push / Pull / Hold
10. Cocontraction / Contraction / Control groups	10. Cocontraction / Contraction groups	10. Square / Sine trajectories
11. Stationary	11. Almost-stationary	11. Non-stationary
12. MECH: ACC	12. MECH: ACC	12. MECH: POS, VEL, ACC, FRC, STF
13. No object / no vibration	13. No object / no vibration	13. With object / with vibration

5.1.1 Neural and mechanical output and their physiological significance

Here is an attempt to make a connection between observed features (neural, mechanical, and spectro-temporal) and their possible physiological meaning and underlying neural processes. Such associations can lead to better design of an impedance controller or more generally, better use of the tools being developed in the diagnosis and various applications for the clinical population. Some features and their possible neural significance are outlined in Table 19.

Table 19 EMG features and their possible neural factors

	Feature	Neural significance
AEMG	• Speed of switching between % MVC	• Neural efficiency
	• Mean square error	• Accuracy
	• Standard deviation	• Variability
	• Cross-Correlation	• Oscillations
	• Autoregression coefficients	• Performance
	• Maximum rate of	• Initiation, neural

	latency change from rest • Overshoot peak	efficiency • Neural control deficiency
Spectro-temporal	• Median Frequency • Event-related amplitude coherence • Event-related phase coherence • Spectral power • Low-frequency rectified coherence • In-phase synchrony	• Measure of fatigue • Intermuscular amplitude oscillations • Intermuscular phase oscillations • Neural activation • Common drive • In-phase common drive
Mechanical	• Endpoint stiffness • Acceleration rate of change (Jolt) • Position error • Force variability	• Neural efficiency • Neural overshoot • Accuracy • Neural control

5.1.2 Modulating or influencing intermuscular correlated oscillations

Once relationships between system performance and correlated oscillations were clarified, the objective was to uncover possible modulation schemes for intervening with intermuscular synchrony. Four possible methods were identified:

- Repetition: Familiarity with the task reduced correlated oscillation for steady and alternating static cocontractions.
- Prior contraction habituation: Although there was no time x group interaction for performance measures, the association between performance and coherence stood out for Contraction group. Muscle habituation of single muscle activation conditioning resulted in an apparent strategy across subjects that uncovered or

enhanced the association between performance and correlated oscillations in Contraction group: significant associations were 3/24 before practice vs. 15/24 after practice (Figure 31). Significant associations for Cocontraction group (3/24 before practice vs. 2/24 after practice) and Control group (3/24 before practice vs. 4/24 after intervention break) did not change through time.

- Out-of-phase cocontraction practice: The Cocontraction group had a series of alternating out-of-phase cocontraction trials during practice for 52 min (including 37 min of rest). The same group also had a significant reduction of in-phase correlated oscillations during the steady cocontraction test (24%, Table 4, Figure 17), during VL1 (26%, Table 8, Figure 25), and during VL2 (29%, Table 9, Figure 26) (i.e., possible transfer of skills from practice to test) with no significant in-phase coherence decrease in the Control group for all three cases. However, there was no clear evidence that out-of-phase practice did influence performance measures.
- The added perturbation to robotic arm: During static or quasi-constant velocity coactivation in the presence of vibration, a negative linear association was revealed between correlated oscillations and neural or mechanical performance output. Subjects who had higher intermuscular coherence also had lower mean AEMG, lower position error, and lower endpoint stiffness. Although there was no significant main effect of time, it is possible that vibration changed the association observed in the static condition of aim-I and II. Nevertheless, a separate future experiment needs to be conducted that compare these associations in the presence and absence of vibration in order to confirm the possible role of vibration.

5.1.3 Relevant questions for developing an HRI algorithm and a practical example

This study had concluded that there was some possible generalization like when the task became familiar, subjects who decoupled their muscles tended to have better performance (uncovered in both test and practice of cocontraction experiment). However, neural strategies for controlling muscles may change with details of the task. One's body develops a preferred strategy to achieve an outcome to the problem in hand by taking into consideration phenomenon like stiffness, force level, energy consumption optimization, and many more. Using the uncovered knowledge to improve HRI setting involves classifying the type of task by asking the following questions,

- What type of muscle activation is involved? Is it voluntary cocontraction, involuntary coactivation, or single muscle contraction?
- What muscles are involved, and what are their orientations? Note those that are agonist to each other vs. antagonist depending on the direction of the joint torque which may change with the posture of the operator.
- Are muscles contribution equal or unequal and who has the higher involvement if unequal?
- Does it involve visual feedback? If so, is it based on the mechanical output (ex. steady velocity) or neural output (ex. AEMG activation)?
- What are the properties of the external device? Ex. does it vibrate?
- Is the task repetitive, is it periodic? If so, is it local (cycles), or global (trials)?
- Does it involve some intervention (ex. habituation or interference of synchrony)?

- Is the task static or dynamic? Steady-state or transient? Slow or fast?
- What type of trajectory or motion? For instance, sine, square, pull, push, reach, alternate, hold, ...

Once these questions are clarified, measures of EMG coherences (amplitude and in-phase) could be acquired, assessed, and then sent to a high level controller that can make some predictions on the outcome of the task and adjust the difficulty as needed.

For example, in HRI applications, various measures of correlated oscillations including amplitude and in-phase information could be quantified using the novel presented tools to assess synchrony between muscles. This information is then sent to a stochastic impedance controller. The controller will adjust the smoothness and other characteristics of the system based on the new real time data and its prior knowledge of the closed loop system between the human and robot for better interaction.

5.2 Other applications

The current findings on the association between the low-frequency correlated neural oscillations and coactivation output performance (mechanical and neural) in addition to the tools developed to modulate such relationship is not limited to HRI. It is not field-specific. It could have a functional significance in the majority of settings where stabilizing an object is required. Such discoveries and tested methods to modulate such correlated oscillations could be considered as a proof of concept to be exploited in sports, rehabilitation, elderly studies, and many others. For instance, some of the strategies to

control cocontraction studied could be applied to Parkinson's disease patients. More generally, individuals could be tested and categorized based on their potential ability for stabilization by analyzing their EMG features during coactivation. Those who may have compromised capability for steadiness can be identified and trained.

5.3 Future direction

Some questions were answered, but many more remains. For instance, investigation was limited to common drive frequency (< 5 Hz). Higher frequencies can reveal interesting insights; however such discoveries necessitate the analysis of raw EMG rather than its rectified version due to the effect of cancellation (39). Other exciting oscillations identified at 20 Hz can also be investigated; their neural origin and implication, once confirmed, could be valuable to understand and utilize for current HRI as well as for medical applications such as Parkinson disease tremor effect. More work can be done to test whether the linear relationship between performance and neural oscillations for static target level cases replicates under dynamic tasks in the absence of vibration and with or without intervention. Finally, posture is known to play an essential role in contact sports and other activities; both experiments (static and dynamic) attempted to limit its effects for the purpose of this study. Studying the role of posture in similar tasks might shed light on some of the results.

5.4 Contribution

Some of the contributions are listed below:

- Uncovered a linear association between correlated neuromuscular oscillations and performance measures during static steady-state tasks that emerged in some muscles after repetition across individuals.

- Revealed a linear association between correlated neuromuscular oscillations and performance measures across individuals during cocontraction practice. Error in performance decreased and a positive association between the error or variability in some muscles and coherence in some muscle pairs did emerge after subjects became familiar with alternating trials through repetition.

- Exposed a negative linear association between correlated oscillations in some muscle pairs and mechanical output (position error and endpoint stiffness) through dynamic repetitions of tracking trajectories in the presence of vibration across individuals.

- Discovered a practical method to lead subjects stealthily into using what could be a common strategy during test by having them practice single muscle activation beforehand. This prior muscle habituation uncovered or enhanced the association between performance and correlated oscillations after practice in Contraction group that was not evident in either Cocontraction or Control groups. This could have far-reaching clinical applications.

- Uncovered a significant decrease of in-phase correlated oscillations after intervention present in Cocontraction group but not in Control group during steady

and varying levels (VL1 and VL2) of the cocontraction test. Cocontraction group, that practiced out-of-phase bout of cocontraction trials, achieved more than 24% in-phase coherence reduction. This is significant because the interaction was found during the test while the out-of-phase brief intervention was during practice. I.e., there could be transfer of skills from a task to another.

- Devised a new method to quantify in-phase coherence based on pdf distribution that was successful in revealing the effect of the intervention. This metric sometimes correlates with amplitude coherence; however, it captures different intermuscular correlated oscillations features.

- Used FFT and Wavelet-based transforms to assess event-related coherence (amplitude and in-phase) for steady and transient coactivation correlated oscillations.

- Identified higher frequencies of tremor oscillations in the two completely different experiments (static and dynamic). Once their neural source is identified, they can play a role as a vehicle for testing neuromuscular properties for clinical as well as normal population.

- Adopted a holistic approach to the problem addressing many aspects: Static / dynamic, intentional / unintentional, steady-state / transient, AEMG / position feedback, and many more.

- Designed two novel, well controlled, neuromuscular physiology experiments with potential functional applications outside laboratories.

- Developed signal processing algorithms to assess features, and statistical tools for establishing significance to the large multi-dimensional (11D) nature of the data set collected.

- Excluded common algorithms and techniques in the analysis of correlated neural oscillations. Cross-correlation, for example, had some limitations in preserving and conveying phase information at low frequencies in the application to the current problem; Simulation revealed that they introduce artifacts.

- Uncovered role of posture and varying unintentional inhibition level across subjects and tasks for idle muscle during contraction that has various implications during cocontraction. For example, BB-HIGH/TB-LOW task is easier than BB-LOW/TB-HIGH in experiment I setup.

5.5 Originality and broader impact

The presented work is original and significant in many ways,

- The novel signal processing techniques and algorithms applied to the field of neuromuscular physiology not exploited before will assess, quantify, and relate neural oscillations and performance, and elucidate basic patterns and functions not available otherwise.
- The identification of new methods and techniques to modulate or influence intermuscular correlated oscillations will equip clinical practitioners, trainers, and others with the necessary tools to intervene when necessary, treat patients and turn novices into experts. Intervention with agonist or antagonist muscle activity will also increase knowledge of neural control of the musculoskeletal system and might lead to advances in the rehabilitation practices for patients suffering neuro-motor impairment.
- The uncovered associations between correlated oscillations and performance (neural and mechanical) under various conditions (static, dynamic, and transient) could lead to the establishment of sophisticated methodologies that enable human-robot coupled systems to cope with failures, interference, unexpected changes to the environment and its constituent.
- Findings will shed a light on some of the fundamental physiological mechanisms of common drive, stiffness control, and coactivation with many applications including but not limited to human-robot interaction, providing insights into physiological triggers for adaptive automation.

5.6 Conclusions

So how would one tango with a robot? To tango with a robot in synchrony, one's muscles need to learn how to oscillate in disharmony more skillfully! That was one of the main findings of this thesis; however, this is not a panacea for all scenarios, but rather a starting framework.

The primary objective was to facilitate the interaction between a human operator and a robot. This is possible when the message is clear and has a well-defined correlated representation. In other words, it is about uncovering signal from noise, then comparing and relating it to one's internal physiological dictionary. For example, one would uncover significant output measures (neural or mechanical) then relate them to internal processes such as correlated oscillations. Some associations were uncovered between correlated oscillations and performance under various scenarios. Then an attempt was made to modulate and tune such association via multiple mechanisms with various successes having the objective of turning a novice into an expert in mind. Correlated neural oscillations were modulated through repetition; in-phase coherence through out-of-phase intervention. Muscle habituation was also identified as a tool that clarified associations. However, this study was short in uncovering whether vibration could be a potential tool for increasing correlated oscillations.

It has been shown that uncovering a general coactivation theory seemed to be ambiguous or ill-defined. The data do not support it. Subject's performance is rather task-specific where they alter their strategies to meet specific objectives under certain

constraints. Many of the variables and controls that influence given strategies were identified that could lead to an outcome; however, this is far from a complete list.

On the other hand, new engineering tools were tested and applied to the assessment of intermuscular correlated oscillations. Event related coherence methods were introduced to the analysis of EMG signals while a novel technique was devised to quantify the in-phase coherence that captures characteristics not found in other measures such as amplitude coherence. The in-phase coherence method already found its way to being utilized directly in some HRI applications in other lab.

REFERENCES

1. Ahmar NE. da Vinci's Encephalogram: In search of significant brain signals. University of Maryland College Park; 2005.

2. Ahmar NE, Shinohara M. Slow Intermuscular Oscillations are Associated with Cocontraction Steadiness. *Med Sci Sports Exerc*. 2017; 49 (9):1955-64.

3. Barbero M, Merletti R, Rainoldi A. Generation, propagation, and extinction of single-fiber and motor unit action potentials. In. *Atlas of Muscle Innervation Zones*: Springer; 2012, pp. 21-38.

4. Beck TW, DeFreitas JM, Stock MS, Dillon MA. Effects of Resistance Training on Force Steadiness and Common Drive. *Muscle & nerve*. 2011;43(2):245-50.

5. Bergmark A. Stability of the lumbar spine. A study in mechanical engineering. *Acta Orthop Scand Suppl*. 1989;230:1-54.

6. Cui J, Wong W. Visual Evoked Potential Analysis Using Adaptive Chirplet Transform. In: A Naït-Ali editor. *Advanced Biosignal Processing*: Springer Berlin Heidelberg; 2009, pp. 221-44.

7. Cui J, Wong W, Mann S. Time-frequency analysis of visual evoked potentials using chirplet transform. *Electron Lett*. 2005;41(4):217-8.

8. De Luca CJ. The use of surface electromyography in biomechanics. *J Appl Biomech*. 1997;13(2):135-63.

9. De Luca CJ, Erim Z. Common drive in motor units of a synergistic muscle pair. *J neurophysiol*. 2002;87(4):2200-4.

10. De Luca CJ, LeFever RS, McCue MP, Xenakis AP. Control scheme governing concurrently active human motor units during voluntary contractions. *J Physiol*. 1982;329:129-42.

11. De Luca CJ, Mambrito B. Voluntary control of motor units in human antagonist muscles: coactivation and reciprocal activation. *J neurophysiol*. 1987;58(3):525-42.

12. Delorme A, Makeig S. EEGLAB: an open source toolbox for analysis of single-trial EEG dynamics including independent component analysis. *J neurosci methods*. 2004;134(1):9-21.

13. Dideriksen JL, Negro F, Enoka RM, Farina D. Motor unit recruitment strategies and muscle properties determine the influence of synaptic noise on force steadiness. *J neurophysiol*. 2012;107(12):3357-69.

14. Duda RO, Hart PE, Stork DG. *Pattern classification*. John Wiley & Sons; 2012.

15. Englehart K, Hudgins B, Parker PA, Stevenson M. Classification of the myoelectric signal using time-frequency based representations. *Med Eng Phys*. 1999;21(6-7):431-8.

16. Farina D, Févotte C, Doncarli C, Merletti R. Blind separation of linear instantaneous mixtures of nonstationary surface myoelectric signals. *IEEE trans on bio-medical eng*. 2004;51(9):1555-67.

17. Farina D, Merletti R, Enoka RM. The extraction of neural strategies from the surface EMG. *J appl physiol*. 2004;96(4):1486-95.

18. Farina D, Negro F. Common synaptic input to motor neurons, motor unit synchronization, and force control. *Exerc Sport Sci Rev*. 2015;43(1):23-33.

19. Farina D, Negro F, Jiang N. Identification of common synaptic inputs to motor neurons from the rectified electromyogram. *J Physiol (London)*. 2013;591(10):2403-18.

20. Gallagher W. Modeling of operator action for intelligent control of haptic human-robot interfaces. 2013.

21. Glendinning DS, Enoka RM. Motor unit behavior in Parkinson's disease. *Phys Ther*. 1994;74(1):61-70.

22. Halliday DM, Farmer SF. On the need for rectification of surface EMG. *J neurophysiol*. 2010;103(6):3547; author reply 8-9.

23. Hogan N. The mechanics of multi-joint posture and movement control. *Biol cybern*. 1985;52(5):315-31.

24. Holmes MR, Gould JR, Pena-Gonzalez I, Enoka RM. Force steadiness during a co-contraction task can be improved with practice, but only by young adults and not by middle-aged or old adults. *Exp Physiol*. 2015;100(2):182-92.

25. Karlsson S, Yu J, Akay M. Time-frequency analysis of myoelectric signals during dynamic contractions: a comparative study. *IEEE trans on bio-med eng*. 2000;47(2):228-38.

26. Le Van Quyen M, Foucher J, Lachaux J et al. Comparison of Hilbert transform and wavelet methods for the analysis of neuronal synchrony. *J neurosci methods*. 2001;111(2):83-98.

27. Mann S, Haykin S. Chirplets and Warblets - Novel Time-Frequency Methods. *Electron Lett*. 1992;28(2):114-6.

28. McAuley JH, Marsden CD. Physiological and pathological tremors and rhythmic central motor control. *Brain : a journal of neurology*. 2000;123 (Pt 8):1545-67.

29. McAuley JH, Rothwell JC, Marsden CD. Frequency peaks of tremor, muscle vibration and electromyographic activity at 10 Hz, 20 Hz and 40 Hz during human finger muscle contraction may reflect rhythmicities of central neural firing. *Exper brain res*. 1997;114(3):525-41.

30. McClelland VM, Cvetkovic Z, Mills KR. Rectification of the EMG is an unnecessary and inappropriate step in the calculation of Corticomuscular coherence. *J neurosci methods*. 2012;205(1):190-201.

31. McClelland VM, Cvetkovic Z, Mills KR. Inconsistent effects of EMG rectification on coherence analysis. *J Physiol (London)*. 2014;592(1):249-50.

32. Merletti R, Parker P. *Electromyography : physiology, engineering, and noninvasive applications*. Hoboken, NJ: IEEE/John Wiley & Sons; 2004, xxii, 494 p. p.

33. Mischi M, Cardinale M. The effects of a 28-Hz vibration on arm muscle activity during isometric exercise. *Med Sci Sports Exerc*. 2009;41(3):645-53.

34. Moon H, Kim C, Kwon M et al. Force control is related to low-frequency oscillations in force and surface EMG. *PloS one*. 2014;9(11):e109202.

35. Murray WM, Buchanan TS, Delp SL. The isometric functional capacity of muscles that cross the elbow. *J biomechanics*. 2000;33(8):943-52.

36. Myers LJ, Lowery M, O'Malley M et al. Rectification and non-linear pre-processing of EMG signals for cortico-muscular analysis. *J neurosci method*. 2003;124(2):157-65.

37. Nait-Ali A. *Advanced Biosignal Processing*. Springer Publishing Company, Incorporated; 2009, 374 p.

38. Negro F, Holobar A, Farina D. Fluctuations in isometric muscle force can be described by one linear projection of low-frequency components of motor unit discharge rates. *J Physiol*. 2009;587(Pt 24):5925-38.

39. Negro F, Keenan K, Farina D. Power spectrum of the rectified EMG: when and why is rectification beneficial for identifying neural connectivity? *J neural eng*. 2015;12(3):036008.

40. Nielsen J, Kagamihara Y. The regulation of disynaptic reciprocal Ia inhibition during co-contraction of antagonistic muscles in man. *J Physiol*. 1992;456:373-91.

41. Oldfield RC. The assessment and analysis of handedness: the Edinburgh inventory. *Neuropsychologia*. 1971;9(1):97-113.

42. Perez MA, Lundbye-Jensen J, Nielsen JB. Task-specific depression of the soleus H-reflex after cocontraction training of antagonistic ankle muscles. *J neurophysiol*. 2007;98(6):3677-87.

43. Reaz MB, Hussain M, Mohd-Yasin F. Techniques of EMG signal analysis: detection, processing, classification and applications. *Biol Proced Online*. 2006;8(1):11-35.

44. Sanei S, Chambers JA. *EEG signal processing*. John Wiley & Sons; 2008.

45. Sörnmo L, Laguna P. Bioelectrical Signal Processing in Cardiac and Neurological Applications. In: Elsevier.

46. Taylor AM, Christou EA, Enoka RM. Multiple features of motor-unit activity influence force fluctuations during isometric contractions. *J neurophysiol*. 2003;90(2):1350-61.

47. Trumbower RD, Krutky MA, Yang B-S, Perreault EJ. Use of self-selected postures to regulate multi-joint stiffness during unconstrained tasks. *PloS one*. 2009;4(5):e5411.

48. Unnithan VB, Dowling JJ, Frost G, Bar-Or O. Role of cocontraction in the O2 cost of walking in children with cerebral palsy. *Med Sci Sports Exerc*. 1996;28(12):1498-504.

49. Vaillancourt DE, Newell KM. Amplitude changes in the 8-12, 20-25, and 40 Hz oscillations in finger tremor. *Clinical neurophysiology : J Clin Neurophysiol*. 2000;111(10):1792-801.

50. Van Ham R, Sugar TG, Vanderborght B, Hollander KW, Lefeber D. Compliant actuator designs. *IEEE Trans Robot Autom*. 2009;16(3).

51. Yoshitake Y, Kanehisa H, Shinohara M. Correlated EMG Oscillations between Antagonists during Co-contraction in Men. *Med Sci Sports Exerc*. 2016.

52. Yoshitake Y, Shinohara M. Oscillations in motor unit discharge are reflected in the low-frequency component of rectified surface EMG and the rate of change in force. *Exp brain res*. 2013;231(3):267-76.

VITA

Nayef Elian Ahmar is a brain - body research and development engineer with more than a decade experience in bio signal processing and pattern recognition. He published or researched in cognitive neuro/science, behavioral analysis, motor control, artifact removal, adaptive signal processing, and many more. He specializes in the processing of electric and magnetic cortical time series (EEG / MEG), muscular (EMG), cardiac (EKG) and other physiological signals. Nayef was born in Beirut, Levant. He earned his BS and MS in Electrical and Computer Engineering from University of Maryland College Park in 1999 and 2005 respectively. Before coming to Georgia Institute of Technology to pursue his doctoral degree researching Bio-signal processing, physiology, and human robot interaction, he worked in various capacities. He participated in the expansion of neuroscience department at Ohio State University by directing multiple EEG labs while researching memory, multisensory processing, learning, cognitive development and autism; He worked and consulted for many R&D startups in bio-data analysis including neuro-marketing, fetal heart rate detection and estimation and various EEG applications. He also motivated, founded and developed Olphas, a bold idea to reinvent human online communication system. Ahmar lives day to day by the motto - enjoy life independent of time, place, action, and form.